MHD in Plasma Astrophysics: Introduction & Highlights

Prof. Kanaris Tsinganos, Dept. of Physics, University of Athens

Lecture at 5th Hel.A.S Summer School "MHD in Astrophysics", 16/09/2024

Department of Physics, University of Ioannina

https://helas.gr/school/2024/

The Flammarion engraving

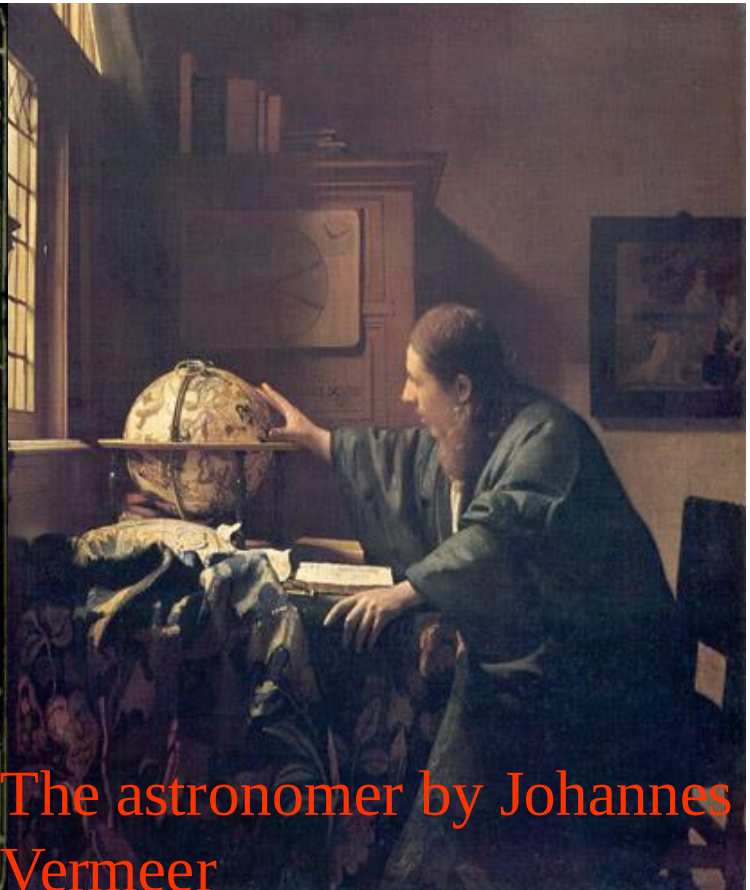

The astronomer by Johannes Vermeer

Plasma is the ***fourth*** *- or -* ***first*** *state of matter*

Human experience

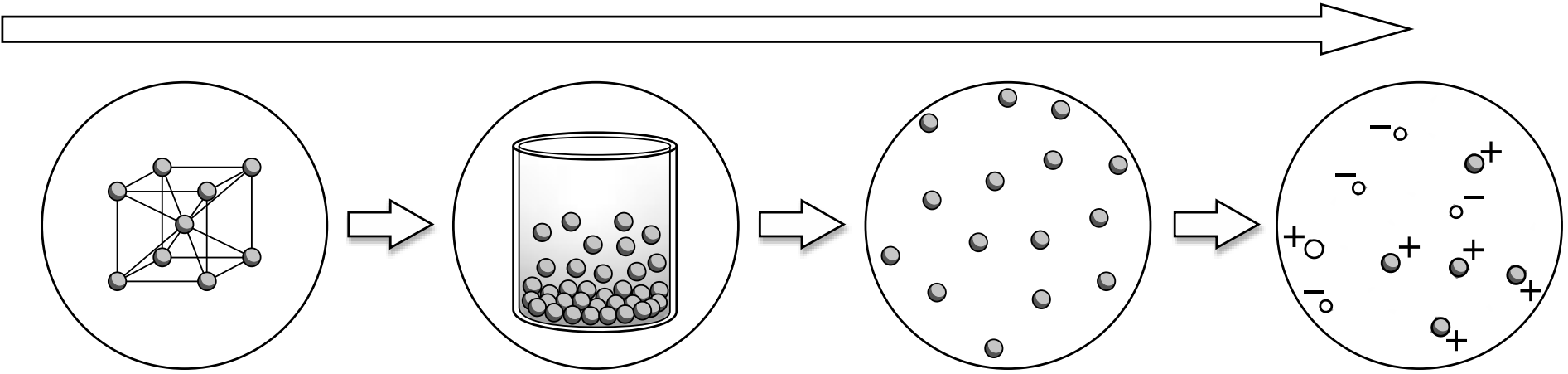

Cold: Solid/Ice Warm: Liquid/Water Hot: Gas/Vapor **Very hot**: Plasma

Matter in the Universe

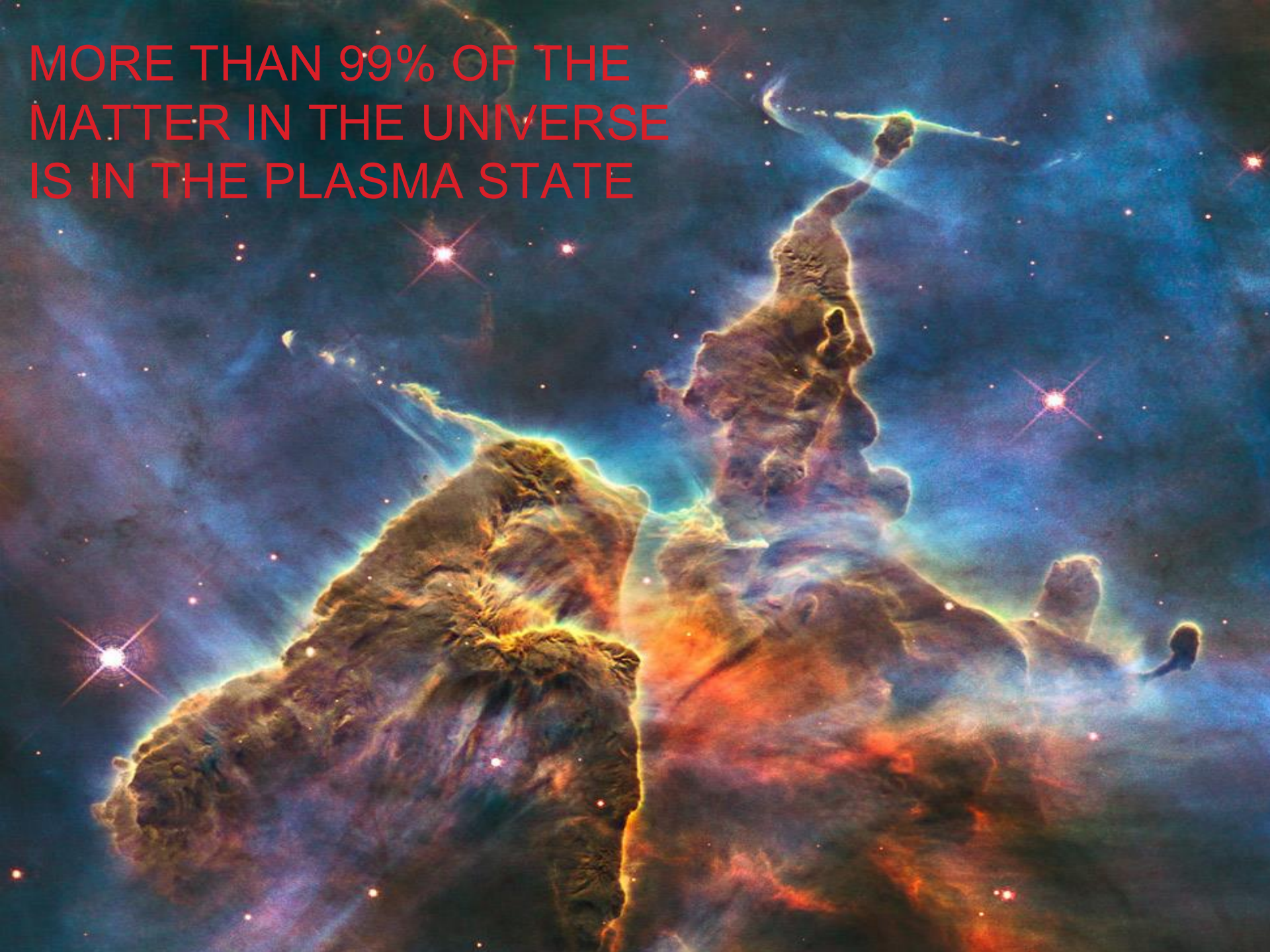
MORE THAN 99% OF THE
MATTER IN THE UNIVERSE
IS IN THE PLASMA STATE

PLASMAS IN A DIAGRAM OF DENSITY + TEMPERATURE (moldable substances)

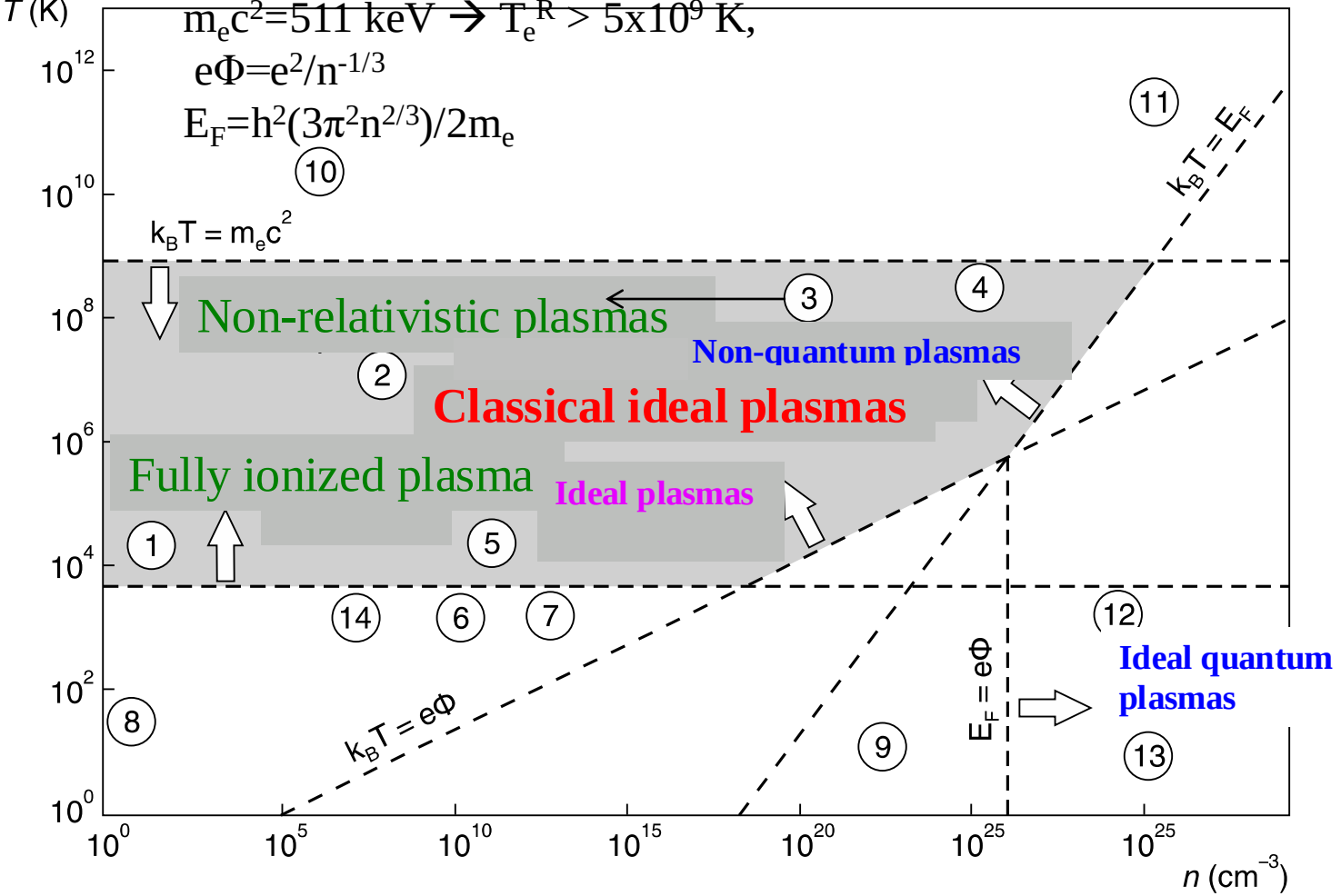

1. Solar Wind
2. Solar Corona
3. Tokamak experiments (ITER)
4. Solar core
5. Plasma in electrical tubes
6. Chromosphere
7. Photosphere
8. Interstellar Space
9. Electron Gas in Metals
10. Pulsar Magnetospheres
11. Hydrogen Bomb
12. Jupiter's Interior
13. White Dwarfs
14. Ionosphere

The plasma microscopically:
basic parameters for lengths and frequencies

1) The Plasma frequency

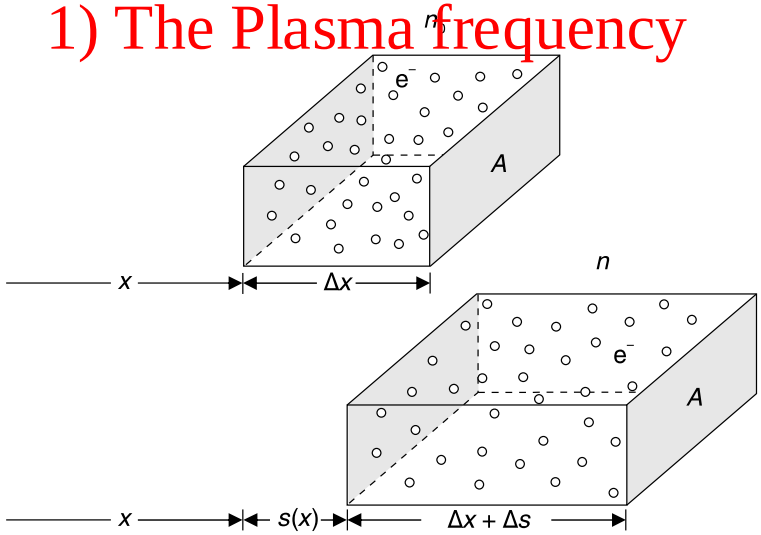

Suppose that the number of electrons between two surfaces of area A is $N = n_0 \Delta x A$, where n_0 is the undisturbed density of the plasma. After the disturbance, the number of electrons between the two surfaces is $N' = n(\Delta x + \Delta s)$. Since the total number of electrons remains the same, $N = N'$ and we have,

$$n = \frac{n_0 \Delta x}{\Delta x + \Delta s} = \frac{n_o}{1 + \frac{\Delta s}{\Delta x}} \simeq n_0 \left(1 - \frac{\Delta s}{\Delta x}\right).$$

We assume that the heavy ions do not move at all, so that their density remains constant and equal to no. Since the total charge density at each point in space is $\rho = (n_o - n)e$,

$$\rho = n_o e \frac{\mathrm{d}s}{\mathrm{d}x}.$$

The density ρ is related to **E** via Gauss law,

$$\vec{\nabla} \cdot \vec{E} = 4\pi\rho.$$

$$\frac{\partial E_x}{\partial x} = 4\pi n_0 e \frac{\partial s}{\partial x} \Rightarrow E_x = 4\pi n_o \, e \, s + C \,,$$

The Coulomb force on an electron is,

$$F_x = -eE_x = -4\pi n_o e^2 s = -ks \,,$$

And the restoring force is,

$$m_e \frac{d^2 s}{dt^2} = -4\pi n_o e^2 s \,.$$

By substituting in this differential equatiom s~ $e^{i\omega pt}$,

$$\omega_p^2 = \frac{4\pi n_o e^2}{m_e} \,. \tag{1.12}$$

μπορούμε να έχουμε αποκλίσεις από την ουδετερότητα μέσα σε μία διάσταση της τάξεως του λ_D. Επομένως μπορούμε να έχουμε ταλαντωτική μεταφορά ενέργειας από τη θερμική ($kT/2$) σε κινητική ενέργεια ($m_e v_e^2/2$). Τα φορτία για την ταχύτητα των ηλεκτρονίων $v_e \simeq \omega_{p_e} \lambda_D$, μπορούμε να υπολογίσουμε αμέσως την συχνότητα πλάσματος ω_p,

$$\omega_p = \left(\frac{4\pi n \times (4.8 \times 10^{-10})^2}{9.1 \times 10^{-28}} \right)^{1/2} \simeq 56400 \sqrt{n} \, \text{Hz}; \tag{1.13}$$

$$\frac{1}{2} \mathrm{k}T = \frac{1}{2} m_e \omega_p^2 \lambda_D^2 \Rightarrow \omega_p = \left(\frac{\mathrm{k}T}{m_e \lambda_D^2} \right)^{1/2} = \left(\frac{4\pi n \, e^2}{m_e} \right)^{1/2} .$$

$\omega_p = 2\pi f_p,$

$$f_p \simeq 9 \sqrt{n} \, \text{kHz} \,. \tag{1.14}$$

→ oscillates with rather large frequencies ..

2) Debye length

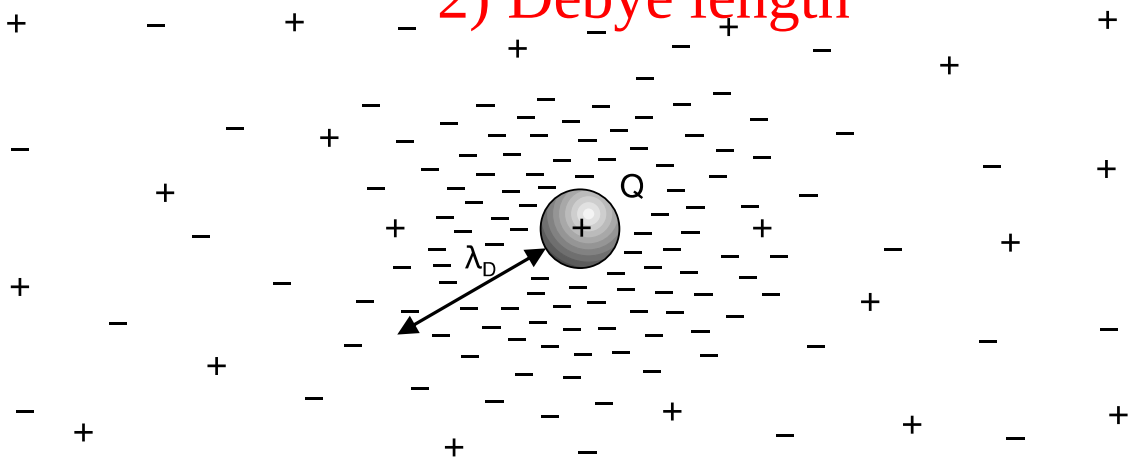

$$n_e = n_0 \exp\left(-\frac{e\,V}{\mathrm{k}T_e}\right), \qquad n_i = n_0 \exp\left(-\frac{e\,V}{\mathrm{k}T_i}\right),$$

$$\nabla^2 V(r) = -4\pi\rho(r)\,,$$

$$\rho(r) = Q\delta(r) + e\,n_o\left[\exp\left(-\frac{eV(r)}{\mathrm{k}T_i}\right) - \exp\left(\frac{eV(r)}{\mathrm{k}T_e}\right)\right].$$

Assume that within the plasma e V $\ll$ (kT_e, kT_i), so thermal motion prevents complete ion-electron recombination. Then we can expand the Taylor exponentials, exp x $\simeq$ 1 + x. The Laplacian is,

$$\nabla^2 V(r) = \frac{1}{r^2}\frac{\mathrm{d}}{\mathrm{d}r}\left(r^2\frac{\mathrm{d}V(r)}{\mathrm{d}r}\right).$$

$$\frac{1}{r^2}\frac{\mathrm{d}}{\mathrm{d}r}\left(r^2\frac{dV(r)}{dr}\right) = -4\pi Q\delta(r) + \left(\frac{1}{\lambda_{D_e}^2} + \frac{1}{\lambda_{D_i}^2}\right)V(r)\,,$$

$$\frac{1}{\lambda_{D_i}^2} = \frac{4\pi e^2 n_o}{\mathrm{k}T_i}\,, \qquad \frac{1}{\lambda_{D_e}^2} = \frac{4\pi e^2 n_o}{\mathrm{k}T_e}\,,$$

where λ_{De}, λ_{Di} are the Debye lengths for electrons and ions, resspectively. Similarly, we can define the plasma Debye length λ_D,

$$\frac{1}{\lambda_D^2} = \frac{4\pi n_o e^2}{k}\left(\frac{1}{T_e} + \frac{1}{T_i}\right).$$

It is easily verified that the solution of the previous differential equation satisfies the requirements

$$V \to \frac{Q}{r} \quad \text{when} \quad r \to 0\,,$$
$$V \to 0 \quad \text{when} \quad r \to \infty$$

is

$$\boxed{V = \frac{Q}{r}\exp\left(-\frac{r}{\lambda_D}\right).}$$

$$\lambda_D = 6.9 \left(\frac{T}{n_o} \right)^{1/2} \text{ cm}$$ with the T in K, and the n_o in cm^{-3}

In fusion experiments $(T \sim 10^6\,\text{K},\ n \sim 10^{14}\,\text{cm}^{-3})$:

$\lambda_D \sim 7 \times 10^{-4}\,\text{cm} \ll L \sim 1\,\text{m}\,.$

In electrical discharges $(T \sim 10^4\,\text{K},\ n \sim 10^{10}\,\text{cm}^{-3})$:

$\lambda_D \sim 7 \times 10^{-3}\,\text{cm} \ll L \simeq 1\,\text{m}\,.$

In the ionosphere $(T \sim 10^3\,\text{K},\ n \sim 10^5\ \text{cm}^{-3})$:

$\lambda_D \sim 0.7\,\text{cm} \ll L \simeq 300\,\text{km}.$

In the solar corona $(T \sim 10^6\,\text{K},\ n \sim 10^8\text{cm}^{-3})$:

$\lambda_D \sim 0.7\,\text{cm} \ll L \sim 100.000\,\text{km}\,.$

In the solar wind $(T \sim 10^5\,\text{K},\ n \sim 7\,\text{cm}^{-3})$:

$\lambda_D \sim 10\,\text{m} \ll L \simeq 1\,\text{AU} \sim 10^8\,\text{km}\,.$

Quasi-neutrality!!

→ deviations from neutrality are in rather small scales ..

3) Larmor radius r_L:

In astrophysical conditions we usually have very high temperatures and very low densities (relative to those of the Earth's atmosphere), while we also have the presence of strong magnetic fields. In the solar corona, $T \sim 10^6$ K, $n \sim 10^8$ cm^{-3}, B ~ 1 Gauss, so,

$$\lambda_D = \left(\frac{kT}{4\pi n e^2}\right)^{1/2} = 7\left(\frac{T}{n}\right)^{1/2} \simeq 7\left(\frac{10^6}{10^8}\right)^{1/2} \simeq 0.7\,\mathrm{cm}\,.$$

The Larmor radius r_L for speeds of the order of $v \sim 200\,\mathrm{km/sec}$ is,

$$r_L = \frac{mvc}{qB} = \frac{(1.6\times10^{-24})\times(2\times10^{7})\times(3\times10^{10})}{4.8\times10^{-10}\times 1} \simeq 20\,\mathrm{m}\,.$$

→ rather small Larmor radii for astrophysical scales ..

The Larmor frequency, ω_L

$$\omega_L = eB/mc$$

4) The mean free path of electrons due to Coulomb scatterings:

The mean free path λ of electrons due to Coulomb scattering, is

$$\lambda = \frac{m_e^2 v_o^4}{2\pi e^4 n \ell \mathrm{n}\Lambda} = \frac{9(\mathrm{k}T)^2}{2\pi e^4 n \ell \mathrm{n}\Lambda} \simeq 0.257 \frac{T^2}{n} \ \mathrm{km}\,.$$

In the solar Corona we have T ~ 10^6 K, n ~ 10^8 cm^{-3} and hence λ ~ 2500 km.
Also, regarding the plasma and Larmor frequencies we have,

→ rather small mean free paths for astrophysical scales ..

$$\omega_p = \sqrt{\frac{4\pi n e^2}{m_e}}, \ f_p = 9\sqrt{n} \simeq 10^5 \ \mathrm{Hz} \qquad \omega_L = \frac{qB}{mc} \sim 10^6 \ \mathrm{Hz}$$

For magnetic fields of 100 Gauss.

In such cases wherein, $[(L \gg \lambda \gg r_L \gg \lambda_D)$ και $(\omega \ll \omega_p \ll \omega_L)]$ we can take average values and treat the plasma as a common fluid.

→ Take mean values of the plasma variables:

Flow speed: $\vec{V} = \dfrac{n^+ m^+ V^+ + n^- m^- V^-}{n^+ m^+ + n^- m^-} = \dfrac{m^+ V^+ + m^- V^-}{m^+ + m^-} \simeq V^+ ,$

Density: $\rho = n^+ m^+ + n^- m^- = n^+ \left(m^+ + m^-\right) \simeq n^+ m^+ = nm$

Pressure $P = P^+ + P^- = 2n\mathrm{k}T$ Temperature: $T = \dfrac{T^+ + T^-}{2} .$

:

(2)

MHD equations are derived from Boltzmann's kinetic theory.

The distribution function: In 6-D phase space,

$$(\vec{r},\ \vec{v}) = (x,\ y,\ z,\ v_x,\ v_y,\ v_z) \tag{3.1}$$

The motion of each charge corresponds to the trajectory:

$$\big[x(t),\ y(t),\ z(t),\ v_x(t),\ v_y(t),\ v_z(t)\big] = \big[\vec{r}(t),\ \vec{v}(t)\big]. \tag{3.2}$$

For each type of charged particle there is a function, the distribution function, f_α (**r,v,t**), α=e,i, which gives the density of charged particles in the 6-dimensional phase space, so that their number dN in the unit cell of the phase space d**r**d**v** to be at any time is,

$$\mathrm{d}N = f_\alpha(\vec{r},\ \vec{v},\ t)\ \mathrm{d}^3\vec{r}\,\mathrm{d}^3\vec{v},$$

where d**r** = dx dy dz and d**v** = $dv_x dv_y dv_z$. The number of particles n_α(r, t) per unit volume of 3-dimensional space is for each species a,

$$n_\alpha(\vec{r},t) = \iiint_{-\infty}^{+\infty} f_\alpha(\vec{r},\ \vec{v},\ t)\mathrm{d}v_x\mathrm{d}v_y\mathrm{d}v_z\ .$$

where T is the temperature of the gas and $v_\theta = \sqrt{2kT/m}$ is the thermal velocity. The isotropic Maxwell-Boltzmann (1860) velocity distribution f_o(r, v) gives us the number of particles with velocity between $\vec{v}$, $\vec{v}$ + d$\vec{v}$ per unit volume $d^3\vec{r}$,

$$f_o(\vec{r},\vec{v}) = n(\vec{r})\left[\frac{m}{2\pi kT}\right]^{3/2}\exp\left[-\frac{v^2}{v_\theta^2}\right]. \tag{3.3}$$

This is the famous Maxwell-Boltzmann distribution, when the gas is in thermodynamic equilibrium.

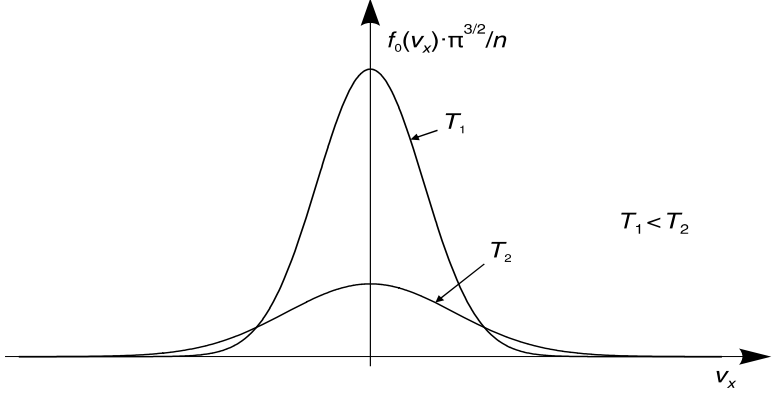

(above) The Maxwell-Boltzmann distribution for the velocities v_x of the atoms of a gas, for two different values of its temperature, T_1 and T_2, with $T_1 < T_2$.

Since the Maxwell-Boltzmann distribution is isotropic, we may introduce the distribution $F_o(v)$ instead of the distribution $f_o(\vec{v})$ so that $F_o(v)dv$ gives us the number of atoms with velocity magnitude between v, v + dv, per unit volume $d^3\vec{r}$, $F_o(v)dv = f_o(\vec{v})d^3\vec{v} = f_o 4\pi v^2 dv$,

$$F_o(v) = 4\pi n\left[\frac{m}{2\pi kT}\right]^{3/2} v^2 \exp\left[-\frac{mv^2}{2kT}\right]. \qquad (3.5)$$

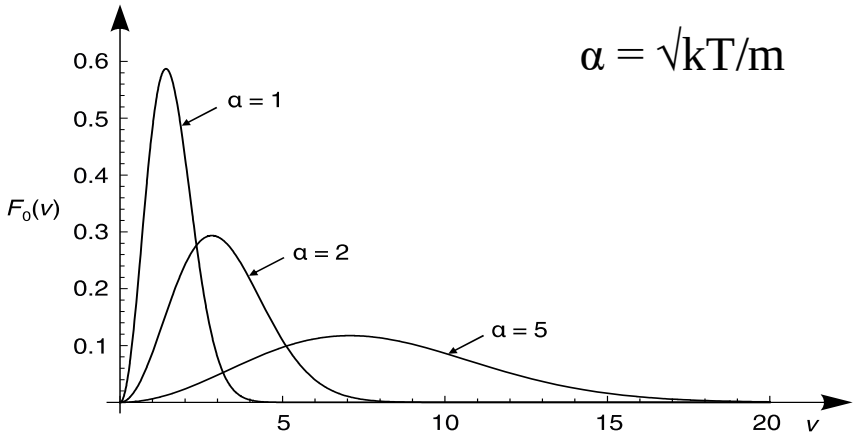

$\alpha = \sqrt{kT/m}$

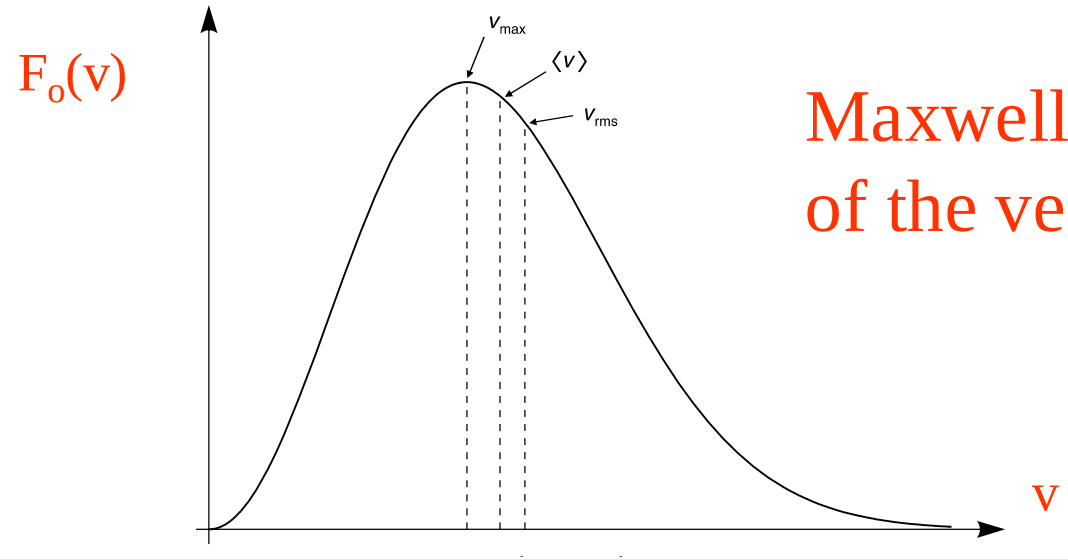

Maxwellian distribution of the velocities v

$$\langle v_x \rangle = \langle v_y \rangle = \langle v_z \rangle = 0, \tag{3.6}$$

$$\langle v_x^2 \rangle = \frac{1}{n} \iiint_{-\infty}^{+\infty} f_o(\vec{v}) v_x^2 \mathrm{d}^3\vec{v} = \frac{1}{n} \int_{-\infty}^{+\infty} F_o(v) v_x^2 \mathrm{d}v = \frac{\mathrm{k}T}{m} = \langle v_y^2 \rangle = \langle v_z^2 \rangle, \tag{3.7}$$

$$\langle v^2 \rangle = 3\langle v_x^2 \rangle = 3\frac{\mathrm{k}T}{m} \equiv v_{\mathrm{rms}}^2, \tag{3.8}$$

$$\langle v \rangle = \frac{1}{n} \int_0^{+\infty} F_o(v) v \mathrm{d}v = \sqrt{\frac{8}{\pi}} \frac{\mathrm{k}T}{m}, \tag{3.9}$$

$$v_{\max} = v_\theta = \sqrt{\frac{2\mathrm{k}T}{m}}, \text{ όπου } \; F_o(v_{\max}) = \max\{F_o(v)\}. \tag{3.10}$$

The Boltzmann and Vlasov transport equations

Because the distribution function $f_\alpha = f_\alpha(x,\ y,\ z,\ v_x,\ v_y,\ v_z,\ t)$
is a function of 7 variables, its total time derivative is,

$$\frac{\mathrm{d}f_\alpha}{\mathrm{d}t} = \frac{\partial f_\alpha}{\partial t} + v_x\frac{\partial f_\alpha}{\partial x} + v_y\frac{\partial f_\alpha}{\partial y} + v_z\frac{\partial f_\alpha}{\partial z} + a_x\frac{\partial f_\alpha}{\partial v_x} + a_y\frac{\partial f_\alpha}{\partial v_y} + a_z\frac{\partial f_\alpha}{\partial z},$$

where $\vec{a} = \mathrm{d}\vec{v}/\mathrm{d}t$ is the acceleration $\vec{F}/m$ or,

$$\frac{\mathrm{d}f_\alpha}{\mathrm{d}t} = \frac{\partial f_\alpha}{\partial t} + (\vec{v}\cdot\vec{\nabla})f_\alpha + \left[\frac{\vec{F}}{m}\cdot\vec{\nabla}_{\vec{v}}\right]f_\alpha .$$

The change with time t of the function f_α may be due to collisions (e.g., Coulomb scatterings). This changes the number dN of some type α of particles in the unit of phase volume. Therefore, we have for the time change of the function f_α because of such collisions,

$$\left[\frac{\partial f_\alpha}{\partial t}\right]_{\text{coll.}} = \frac{\partial f_\alpha}{\partial t} + (\vec{v}\cdot\vec{\nabla})f_\alpha + \left[\frac{\vec{F}}{m}\cdot\vec{\nabla}_{\vec{v}}\right]f_\alpha , \qquad (3.11)$$

which is called the Boltzmann equation. In the absence of collisions, the kinetic equation for the distribution function f_α is called the **Vlasov** equation (1947),

$$\frac{\partial f_\alpha}{\partial t} + (\vec{v}\cdot\vec{\nabla})f_\alpha + \left[\frac{\vec{F}}{m}\cdot\vec{\nabla}_{\vec{v}}\right]f_\alpha = 0 , \qquad (3.12)$$

which should be solved in combination with Maxwell's equations and the expression of the Lorenz force **F**=q(**E**+**v**x**B**/c).

The Maxwell- Boltzmann equations

The Maxwell-Boltzmann equations are the complete system of Maxwell's equations describing the interaction of charged particles with electric (**E**) and magnetic (**B**) fields AND the Boltzmann transport equation, which describes the evolution of the distribution function f_α for each component α=i,e of the plasma,

$$\frac{\partial f_\alpha}{\partial t} + (\vec{v}\cdot\vec{\nabla}) f_\alpha + \left[\frac{q_\alpha}{m_\alpha}\left(\vec{E} + \frac{\vec{v}\times\vec{B}}{c}\right)\cdot\vec{\nabla}_v\right] f_\alpha = \left[\frac{\partial f_\alpha}{\partial t}\right]_{\text{coll.}},$$

$$\vec{\nabla}\times\vec{E} = -\frac{1}{c}\frac{\partial\vec{B}}{\partial t}, \qquad \vec{\nabla}\times\vec{B} = 4\pi c\vec{J} + \frac{1}{c}\frac{\partial\vec{E}}{\partial t},$$

$$\vec{\nabla}\cdot\vec{E} = 4\pi\delta, \qquad \vec{\nabla}\cdot\vec{B} = 0,$$

where, $\delta = \sum_\alpha q_\alpha \iiint_{\vec{v}} f_\alpha(\vec{r},\vec{v},t)\, \mathrm{d}^3\vec{v},$

$$\vec{J} = \sum_\alpha q_\alpha \iiint_{\vec{v}} f_\alpha(\vec{r},\ \vec{v},\ t)\, \vec{v}\, \mathrm{d}^3\vec{v}, \quad \mu\varepsilon\ \alpha = e, i.$$

The system of these equations must be solved for **E**, **B** and f_α self-consistently, i.e. the correct distributions f_α should be found such that they give the right expression of (δ, **J**) which then give **(E , B)** that determine the motion of the components of the plasma.

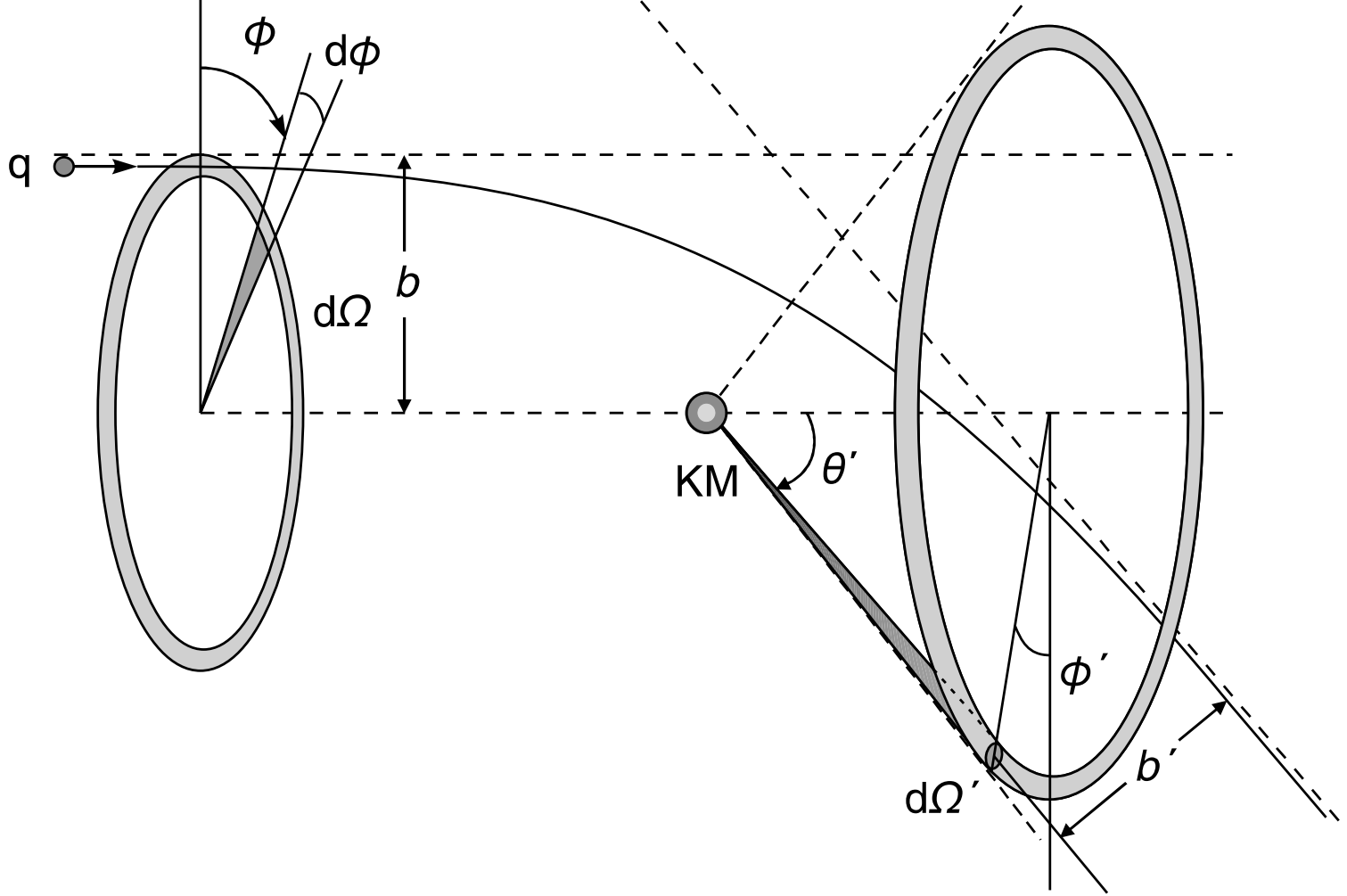

Scattering of a charge q (an electron) by a heavier (positive) proton, with parameter b, at an angle θ'.

Gauss' law

$$\vec{\nabla} \cdot \vec{E} = 4\pi\delta \simeq 0$$

No magnetic monopoles

$$\vec{\nabla} \cdot \vec{B} = 0$$

Faraday's law

$$\vec{\nabla} \times \vec{E} = -\frac{1}{c}\frac{\partial \vec{B}}{\partial t}$$

Ampere's law

$$\vec{\nabla} \times \vec{B} = \frac{4\pi}{c}\vec{J} + \frac{1}{c}\frac{\partial \vec{E}}{\partial t} \simeq \frac{4\pi}{c}\vec{J}$$

Ohm's law

$$\vec{J} = \underbrace{\sigma}_{\infty}\underbrace{\left(\vec{E} + \frac{\vec{V} \times \vec{B}}{c}\right)}_{0}$$

Newton's law

$$\rho\frac{\mathrm{d}\vec{V}}{\mathrm{d}t} = -\vec{\nabla}P + \frac{\vec{J} \times \vec{B}}{c} + \rho\vec{g}$$

With the notation:

- $\vec{E}(\vec{r},t)$: Electric field in plasma
- $\vec{B}(\vec{r},t)$ Magnetic field in plasma
- $\rho(\vec{r},t)$: Mass density field in plasma
- $\delta(\vec{r},t)$: Electric current density in plasma
- $\vec{J}(\vec{r},t)$: Electric current density in plasma
- $\vec{V}(\vec{r},t)$: Bulk flow speed in plasma
- σ: Electrical conductivity in plasma
- $\vec{P}(\vec{r},t)$: Pressure
- $\vec{g}$: Acceleration of gravity in plasma

MHD : basic interaction of magnetized plasmas
[As the Standard Model in Particle Physics]

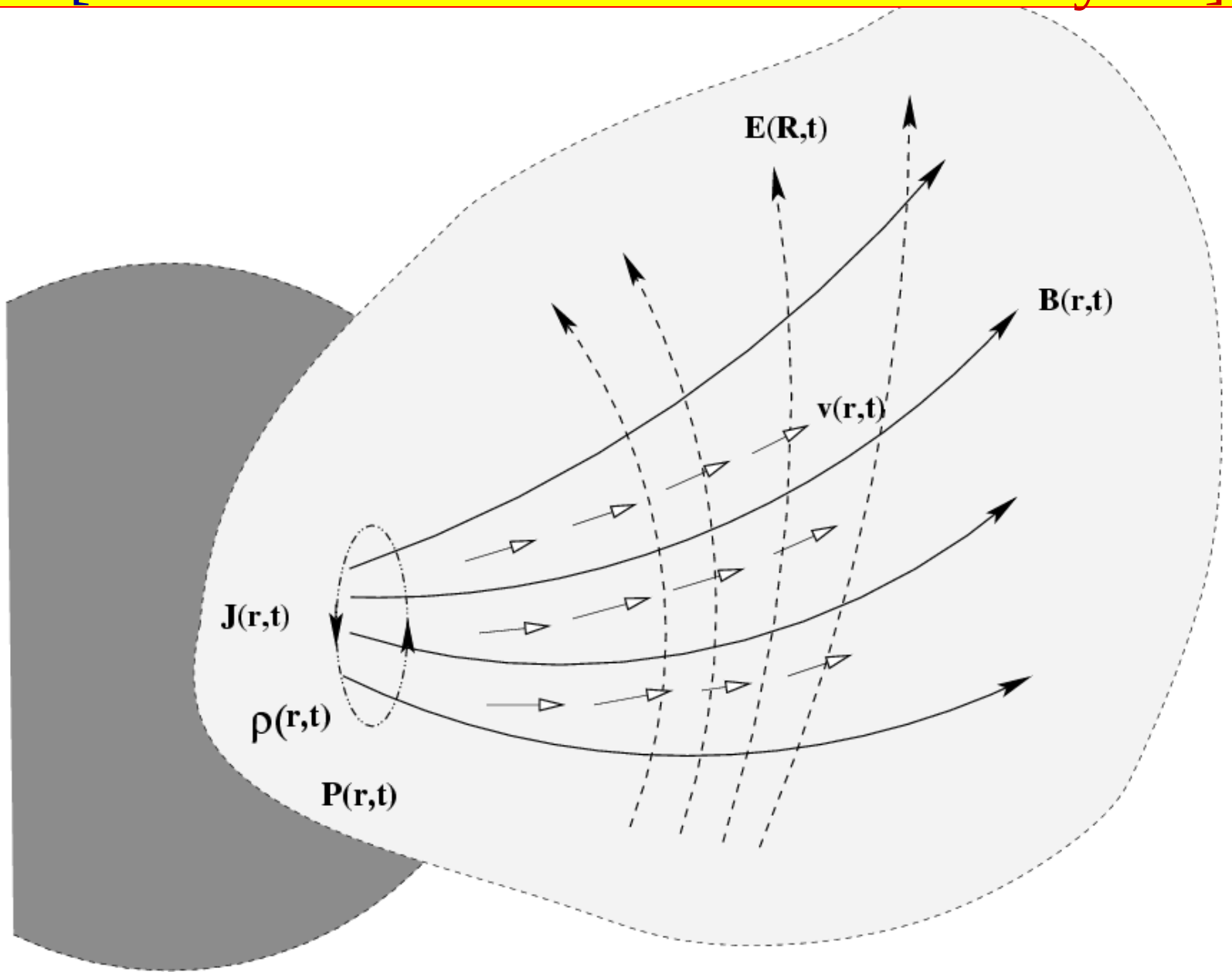

Illustration of the HD and MHD plasma interaction

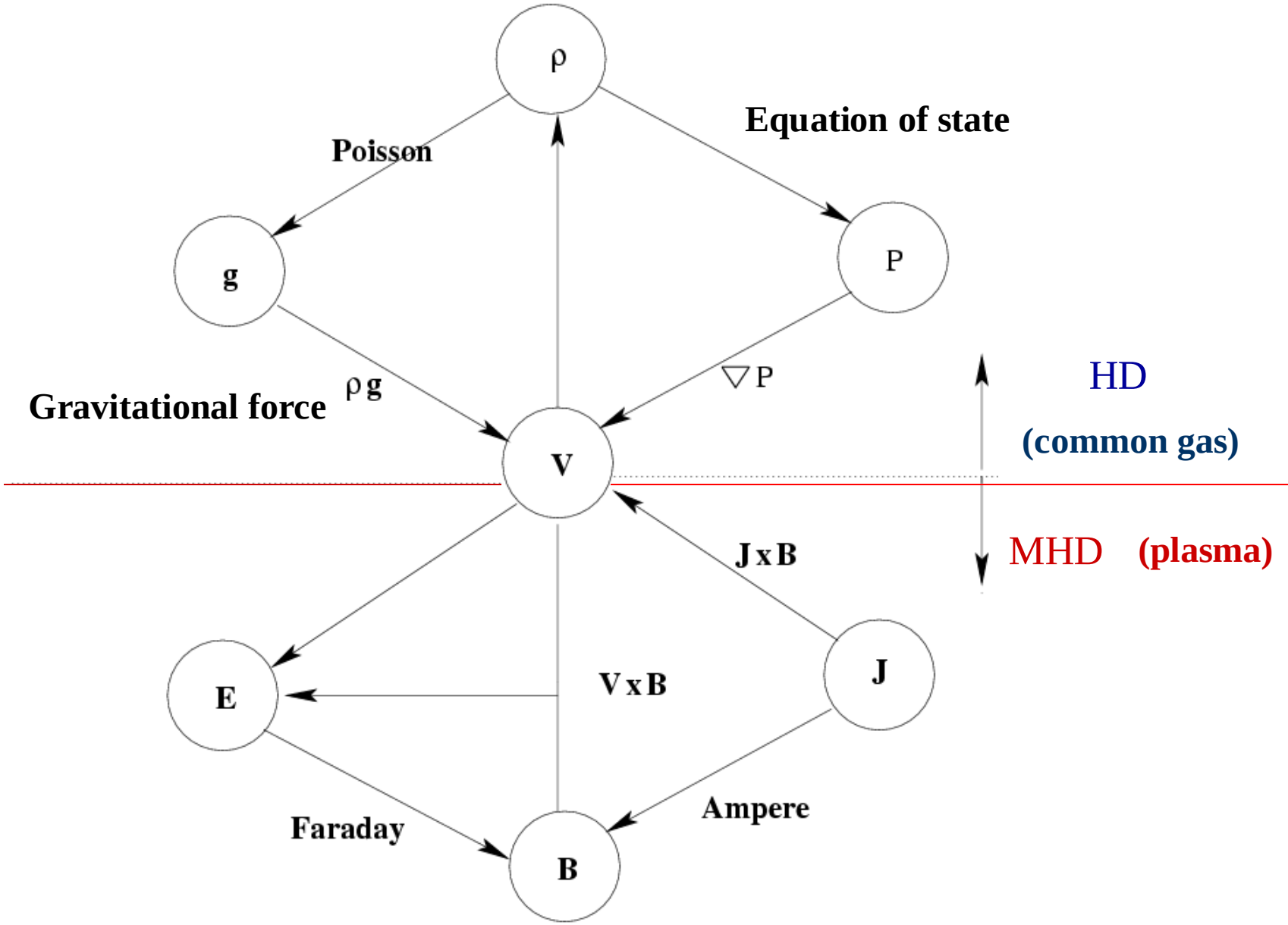

MHD approximations :

In astrophysical plasmas, the following approximations usually hold :

- nonrelativistic motion: $V/c \ll 1$.
- negligible displacement current in Ampere's law, $c\vec{\nabla} \times \vec{B} = 4\pi\vec{J} + \partial\vec{E}/\partial t$
  Let $(\ell - \tau)$ the characteristic spatial-temporal scales :
  $c|\vec{\nabla} \times \vec{B}| \simeq \frac{cB}{\ell} = \bigcirc(1)\ \tau \simeq \frac{\ell}{V}, E \sim \frac{V}{c}B \Rightarrow$
  $\frac{\partial E}{\partial t} \simeq \frac{VB}{c\tau} = \underset{\text{L}}{\frac{V^2}{\ell}}\underset{\text{L}}{\frac{B}{\tau}} \simeq \underset{\text{L}}{\frac{cB}{\ell}}\left(\frac{V}{c}\right)^2 = \bigcirc\left(\frac{V^2}{c^2}\right)$
- negligible polarization current:
  $\vec{\nabla} \cdot \vec{E} = 4\pi\delta\,;\ J_\delta = V\delta = \underset{\text{L}}{\frac{VE}{\ell}} = \underset{\text{L}}{\frac{cB}{\ell}}\left(\frac{V^2}{c^2}\right) = \bigcirc\left(\frac{V^2}{c^2}\right)$
- High electrical conductivity: $\sigma \simeq 6 \times 10^6 T^{3/2}/sec$
  $\vec{J} = \sigma\left[\vec{E} + \frac{\vec{V}}{c} \times \vec{B}\right],\ \sigma \to \infty \ \Rightarrow \vec{E} + \frac{\vec{V}}{c} \times \vec{B} \simeq 0$
  $\Longrightarrow \vec{E} = -\frac{\vec{V}}{c} \times \vec{B} \Longrightarrow \vec{\nabla} \times \vec{E} = -\frac{1}{c}\frac{\partial\vec{B}}{\partial t} \Rightarrow \vec{\nabla} \times (\vec{V} \times \vec{B}) = \frac{\partial\vec{B}}{\partial t}$
- High thermal conductivity: $\kappa \simeq 6 \times 10^{-6} T^{5/2}$
  (the solar corona extends to the interplanetary space)
- Negligible viscosity (mainly from the ions) : $\mu \simeq 10^{-16} T^{5/2}\, g/cm\, sec.$

For example, in plasma of temperature $T \sim 10^6 K$, density $N \sim 10^8\, cm^{-3}$ we have:
electrical conductivity: $\sigma \simeq 10^{16}/sec$ (for Cupper, $\sigma \simeq 10^{17}/sec$)
thermal conductivity: $\chi = \frac{\kappa}{c_p} \simeq \frac{6 \times 10^8}{10^9} \sim 0.6\ (g/cm sec)$
viscosity coefficient : $\mu \simeq 0.1 (g/cm\, sec)$.

Large magnetic Reynold's numbers :

Combining Faraday, Ohm and Ampere's equations,

$\vec{\nabla}\times\vec{E}=-\frac{1}{c}\frac{\partial\vec{B}}{\partial t}$ $\quad \frac{\vec{J}}{\sigma}-\frac{\vec{V}}{c}\times\vec{B}=\vec{E}$, $\quad \vec{\nabla}\times\vec{B}=\frac{4\pi}{c}\vec{J}$, we have

$$\Rightarrow \vec{\nabla}\times\left[\frac{c}{4\pi\sigma}(\vec{\nabla}\times\vec{B})-\frac{\vec{V}}{c}\times\vec{B}\right]=-\frac{1}{c}\frac{\partial\vec{B}}{\partial t} \Rightarrow \frac{\partial\vec{B}}{\partial t}=\vec{\nabla}\times(\vec{V}\times\vec{B})-\frac{c^2}{4\pi\sigma}\vec{\nabla}\times(\vec{\nabla}\ \text{xB})$$

Assuming a constant resistivity, $\eta=\frac{c^2}{4\pi\sigma}=\text{const.}$,

$$\frac{\partial\vec{B}}{\partial t}=\vec{\nabla}\times(\vec{V}\times\vec{B})+\eta\nabla^2\vec{B},\ |\vec{\nabla}\times(\vec{V}\times\vec{B})|\simeq\frac{VB}{L}\ ,\ \ |\eta\vec{\nabla}^2\vec{B}|\sim\frac{c^2B}{4\pi\sigma L^2}\ ,$$

Introducing Reynold's number $R_m=\frac{VL}{\eta}=\frac{4\pi\sigma VL}{c^2}$.

if $R_m\gg 1$ $\quad \frac{\partial\vec{B}}{\partial t}\simeq\vec{\nabla}\times(\vec{V}\times\vec{B})$,

and if , $R_m\leq 1$ $\quad \frac{\partial\vec{B}}{\partial t}\simeq\eta\nabla^2B$.

The electric field in the frame of the moving plasma is: $\vec{E}'=\vec{E}+\frac{\vec{V}\times\vec{B}}{c}=\frac{\vec{J}}{\sigma}$.

With $\frac{J}{\sigma}\simeq\frac{c}{4\pi\sigma}\frac{B}{L}=\eta\frac{B}{cL}$, and $R_m=\frac{\text{VL}}{\eta}\Rightarrow\frac{J}{\sigma}\simeq\frac{1}{R_m}\left(\frac{V}{c}B\right)$,

we have that E' is weaker than the induced electric field $(\frac{V}{c}B)$ by the factor $\frac{1}{R_m}$.

Examples of Reynold's number:

- Solar wind:
  $V\sim 400\ km/s,\ L\sim 1\ AU\sim 10^{13}\ cm,\ \sigma\simeq 10^{14}\ s^{-1}\Rightarrow R_m\simeq 10^{14}$.
- Galactic disk:
  $V\sim 10\ km/s,\ L\sim 100\ pc\sim 10^{20}\ cm,\ \sigma\simeq 10^{11}-10^{9}\ s^{-1}\Rightarrow R_m\simeq 10^{17}-10^{15}$
- Solar photosphere:
  $V\sim 1\ km/s,\ L\sim 10^{8}\ cm,\ \sigma\simeq 10^{11}-10^{9}s^{-1}\Rightarrow R_m\simeq 10^{4}-10^{2}$.

Flux freezing

Initial flux from S is: $\Phi = \iint_S \vec{B} \cdot d\vec{S}$,

Change in flux is : $\delta\Phi = \underbrace{\iint_S \frac{\partial \vec{B}}{\partial t} \cdot d\vec{S} \cdot \delta t}_{\delta\Phi_1} + \underbrace{\int_C (\vec{V}\,\delta t) \times d\vec{\ell} \cdot \vec{B}}_{\delta\Phi_2}$,

$$(\vec{V} \times d\vec{\ell}) \cdot \vec{B}\,\delta t = (\vec{B} \times \vec{V}) \cdot d\vec{\ell}\,\delta t = -(\vec{V} \times \vec{B}) \cdot d\vec{\ell}\,\delta t\,,$$

Therefore,

$$\delta\Phi_2 = -\int_C (\vec{V} \times \vec{B}) \cdot d\vec{\ell}\,\delta t \overset{Stokes}{=} -\iint_S \vec{\nabla} \times (\vec{V} \times \vec{B}) \cdot d\vec{S}\,\delta t\,,$$

and

$$\frac{\delta\Phi}{\delta t} = \iint_S \left[\frac{\partial \vec{B}}{\partial t} - \vec{\nabla} \times (\vec{V} \times \vec{B})\right] \cdot d\vec{S} = 0\,,$$

since,

$$\boxed{\frac{\partial \vec{B}}{\partial t} = \vec{\nabla} \times (\vec{V} \times \vec{B})\,.}$$

- **a marked proton**

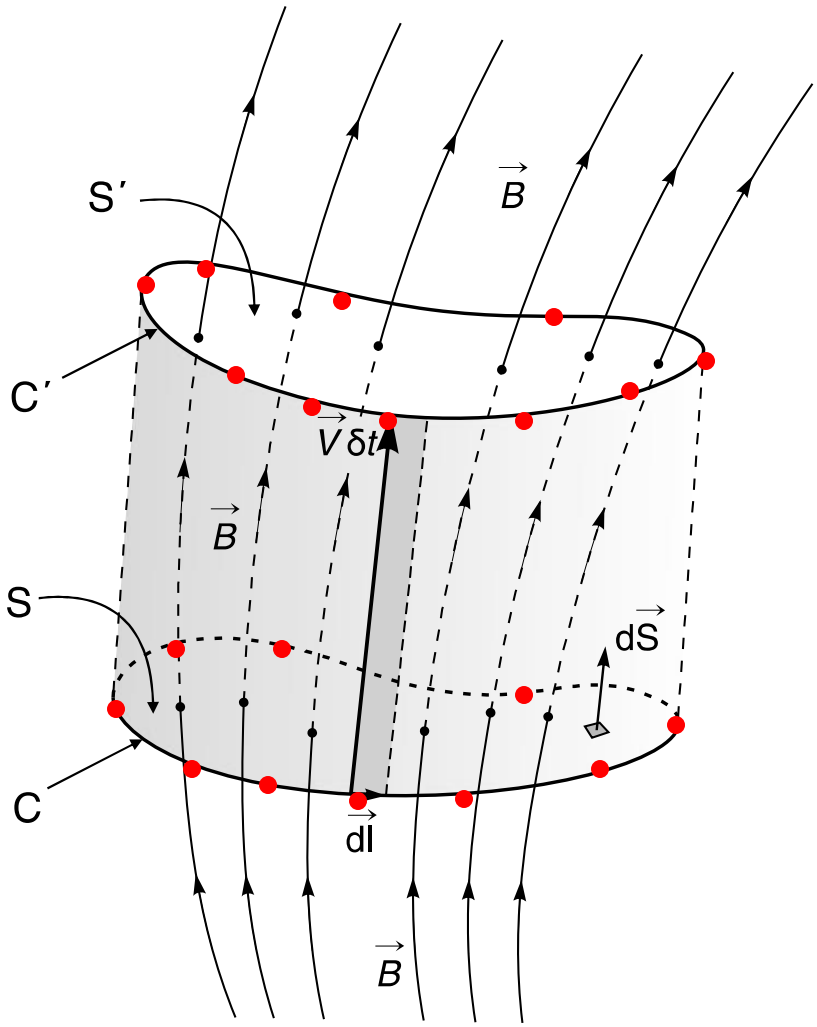

Magnetic flux tubes

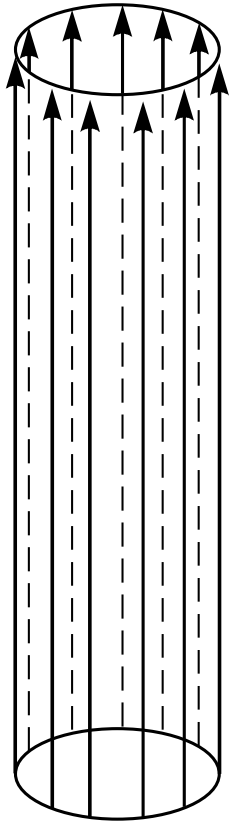

(α)

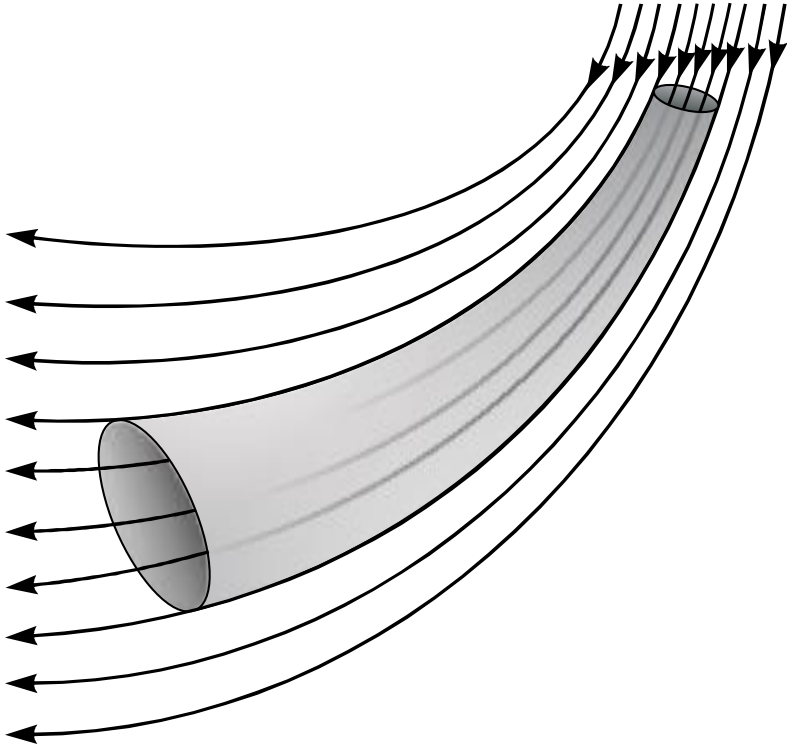

(β)

The **physics of magnetic flux tubes** (1979-1980)

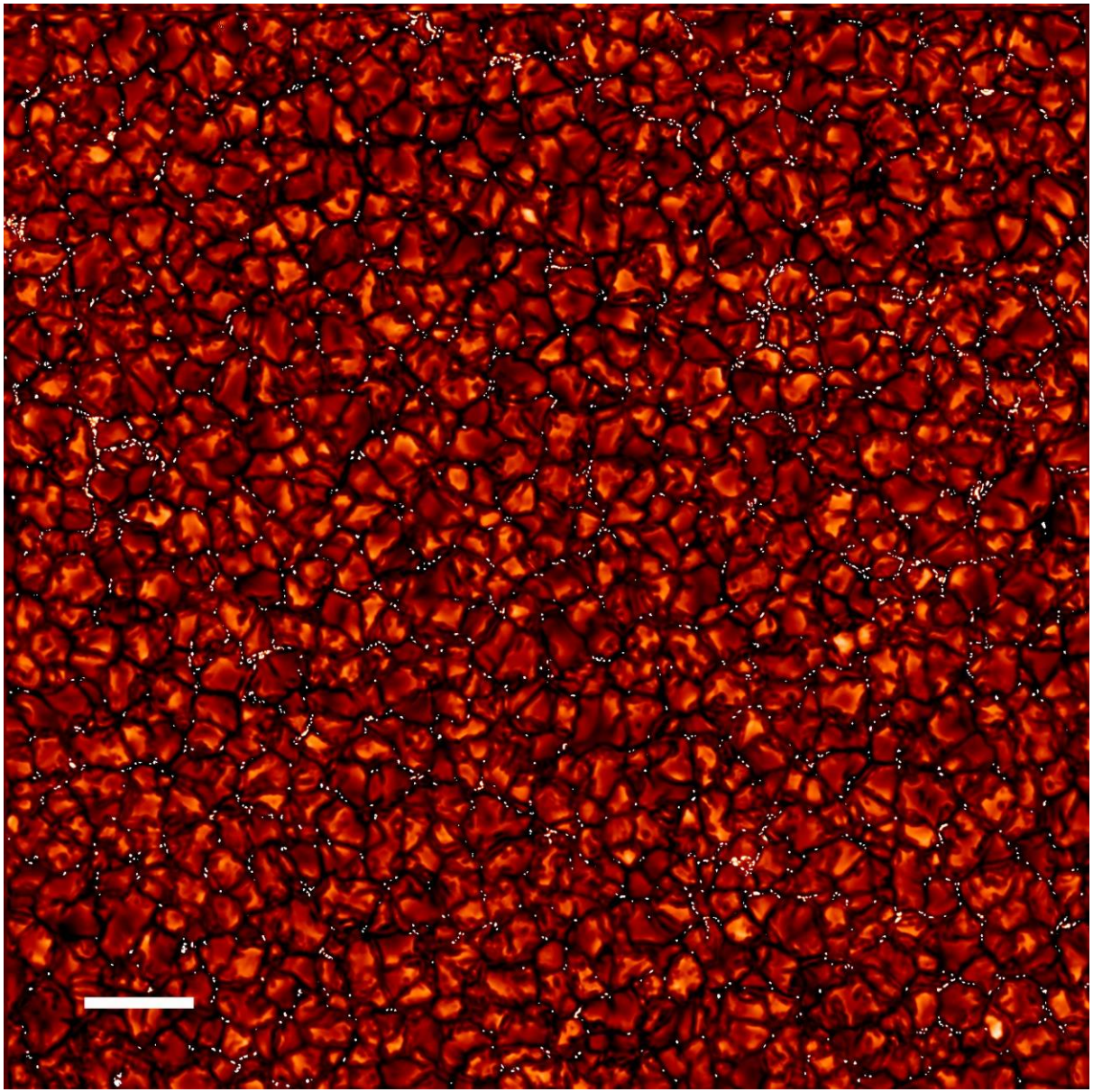

5000 km at photosphere, ➔

[Credit: Institute for Solar Physics, Sweden, Swedish 1-m Solar Telescope, September 2007, La Palma, Spain].

1 ☐ 1979ApJ...231..260T 1979/07 cited: 20

Sunspots and the physics of magnetic flux tubes. IV. Aerodynamic lift on a thin cylinder in convective flows.

Tsinganos, K. C.

2 ☐ 1979PhFl...22.1847P 1979/10 cited: 7

Bernoulli forces on an elliptical cylinder by a nonuniform flow

Parker, E. N.; Tsinganos, K. C.

3 ☐ 1980ApJ...239..746T 1980/07 cited: 43

Sunspots and the physics of magnetic flux tubes. X - On the hydrodynamic instability of buoyant fields

Tsinganos, K. C.

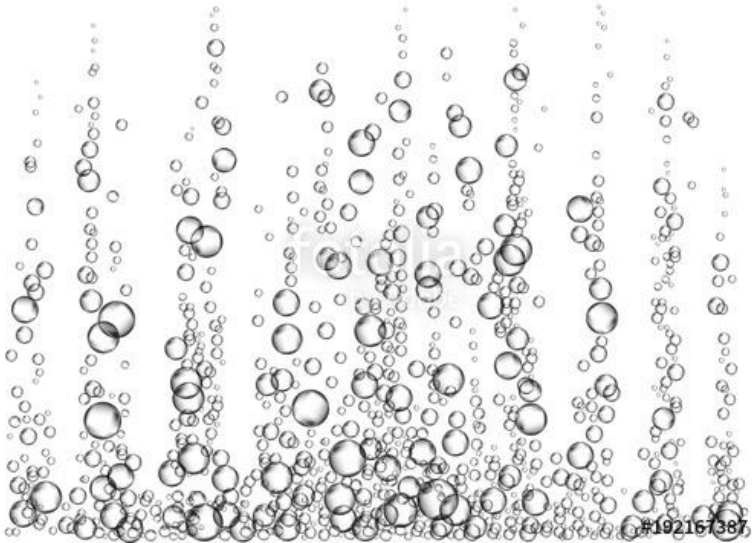

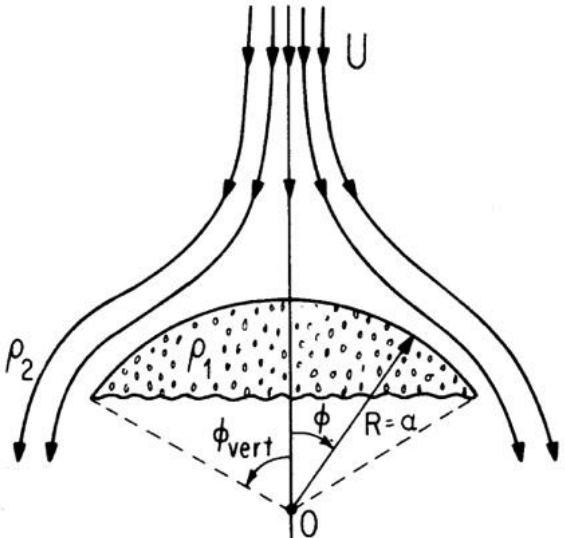

The two components of the Lorenz force:

$$\vec{F}_L = \frac{(\nabla \times B) \times B}{4\pi} = -\vec{\nabla}\left(\frac{B^2}{8\pi}\right) + \frac{(B \cdot \nabla)B}{4\pi},$$

The first corresponds to the magnetic pressure:

$$P_M = \frac{B^2}{8\pi}.$$

The ratio of the gass to the magnetic pressure defines the plasma β:

$$\beta = \frac{P}{B^2/8\pi}\,. \tag{4.1}$$

The plasma is cold if β <<1 while when β >> 1 is regarded as hot. The second term can be split in two components, by defining the unit vector T tangent to the magnetic line:

$$\frac{(\vec{B}\cdot\vec{\nabla})\vec{B}}{4\pi} = \frac{B}{4\pi}\frac{\mathrm{d}(B\hat{T})}{\mathrm{d}s} = \frac{B\hat{T}}{4\pi}\frac{\mathrm{d}B}{\mathrm{d}s} + \frac{B^2}{4\pi}\frac{\mathrm{d}\hat{T}}{\mathrm{d}s}$$

$$= \hat{T}\frac{\mathrm{d}}{\mathrm{d}s}\frac{B^2}{8\pi} + \frac{B^2}{4\pi}\kappa\hat{N} = \hat{T}\frac{\mathrm{d}}{\mathrm{d}s}\frac{B^2}{8\pi} + \frac{B^2}{4\pi R}\hat{N}\,, \qquad \frac{\mathrm{d}\hat{T}}{\mathrm{d}s} = \kappa\hat{N} = \frac{\hat{N}}{R},$$

where κ is the curvature equal to 1/R, with R the radius of curvature of the magnetic line and N the first nomal vector. The first term neutralizes the force of the magnetic pressure gradient along the magnetic field, so that only remains the magnetic pressure gradient perpendicular. The second term appears only for curved magnetic lines and is directed towards the local center of curvature. Because it is similar to the tension in a bent string, or to the tension in a stretched rubber band, it is called magnetic tension.

The magnetic tension creates the Alfvén waves, which propagate in a magnetized plasma at the Alfvén speed and are the main mode of propagation of disturbances in a magnetized plasma,

$$V_A = \frac{B_o}{\sqrt{4\pi\rho_o}}\,, \tag{4.2}$$

where V_A defines the Alfvén velocity. Thus, these waves propagate with the Alfvén speed along the dynamic lines of the magnetic field B_o, which depends on the intensity of this magnetic field and the density of the plasma. When the waves propagate at an angle θ to the field B_o, their speed $V_\varphi = \omega/k$ is less, reduced by the $\cos\theta$. Obviously in a directi perpendicular to the magnetic field B_o, $\theta = 90^o$, the waves do not propagate. In Alfvén waves the ions move under the influence of the restoring force of the magnetic tension of the curved magnetic lines.

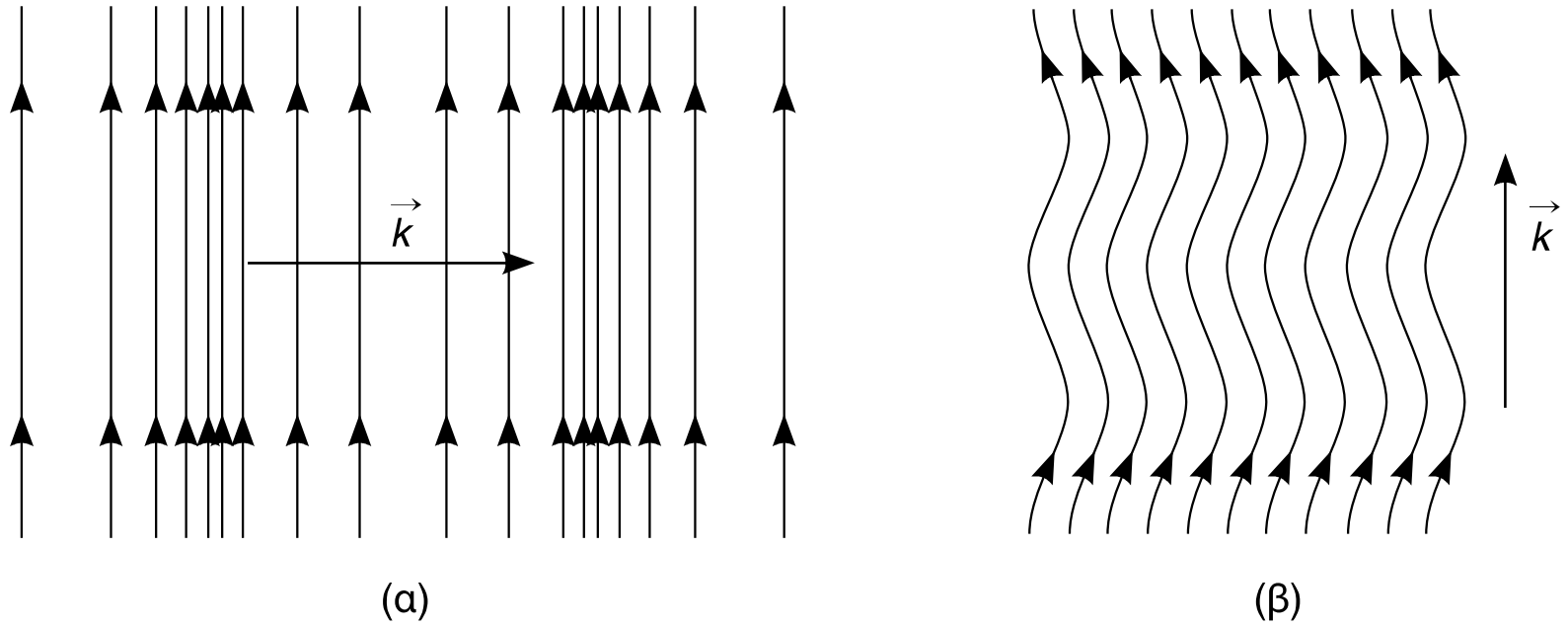

Magnetohydrodynamic waves in the plasma:

(a) Perpendicular to a magnetic field, longitudinal sound waves propagate with speed $\sqrt{V_A^2 + C_s^2}$.

(b) Transverse Alfvén waves with speed V_A and longitudinal sound waves with speed C_s propagate parallel to the magnetic field.

At a random angle to the direction of a magnetic field, three MHD waves propagate: Alfvén waves, slow and fast MHD waves.

Diagram of **phase** velocities for the three characteristic MHD waves: Fast (external) Alfvén and slow (internal), when $V_A = 0.5 > C_s = 0.4$. In the direction of the x-axis, the phase velocity of the fast wave is $V_+ = \sqrt{V_A^2 + C_s^2} = 0.64$.

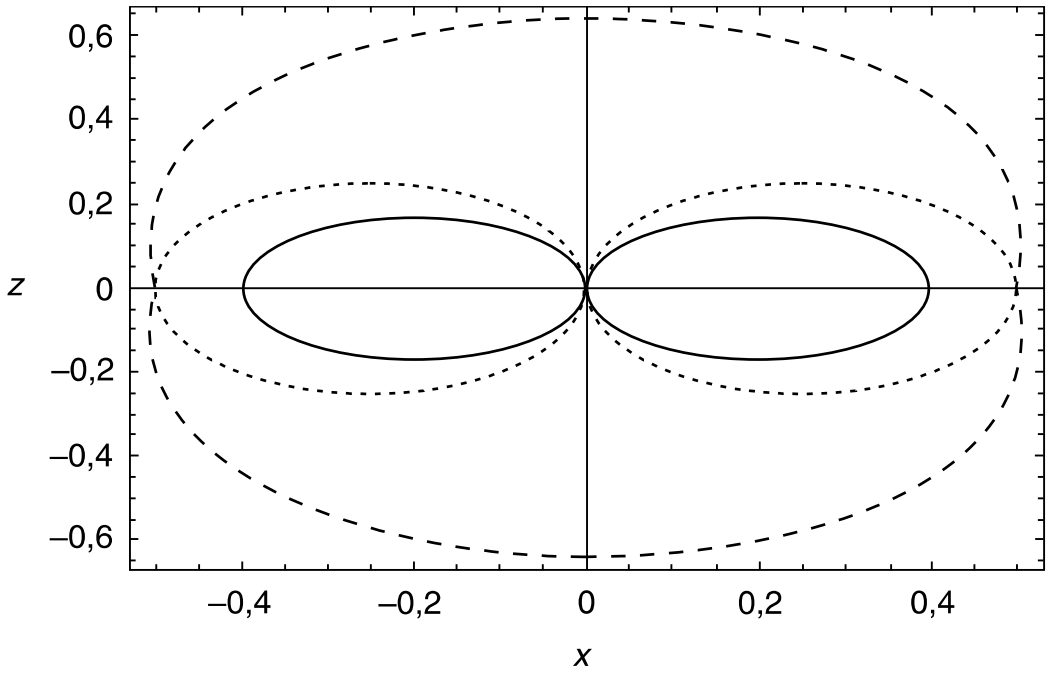

Group velocity diagram for the three characteristic MHD waves: Alfvén (black marks), slow (inner curve) and fast (outer curve) when $V_A = 0.5 > C_s = 0.4$. The two spherical triangles are internally terminated with characteristic velocity $C_T = (V_A C_s)/\sqrt{V_A^2 + C_s^2} = 0.31$.

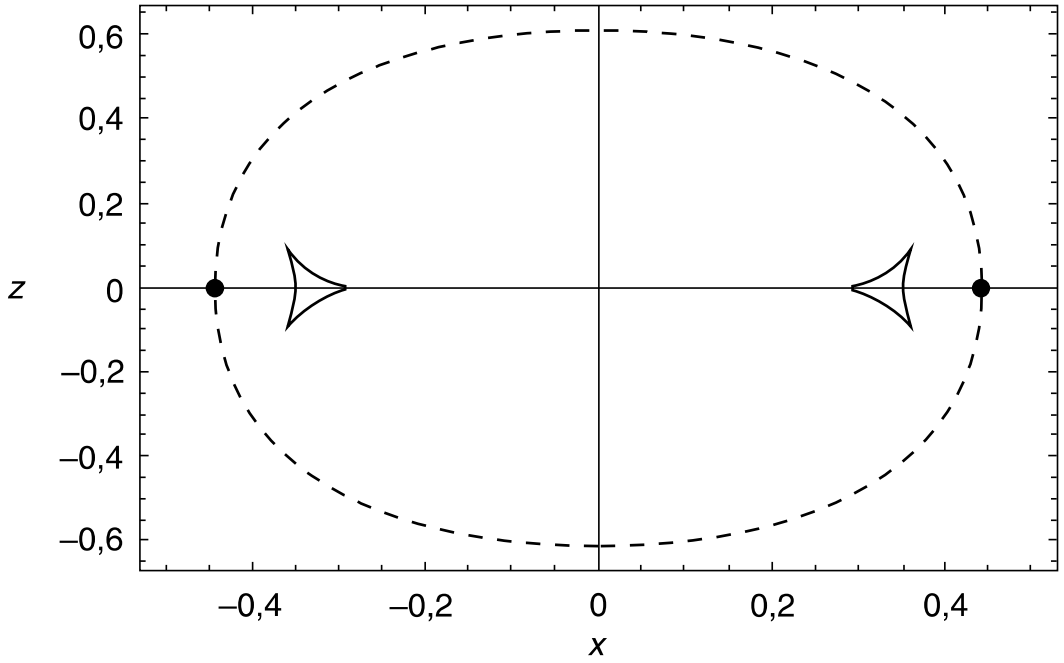

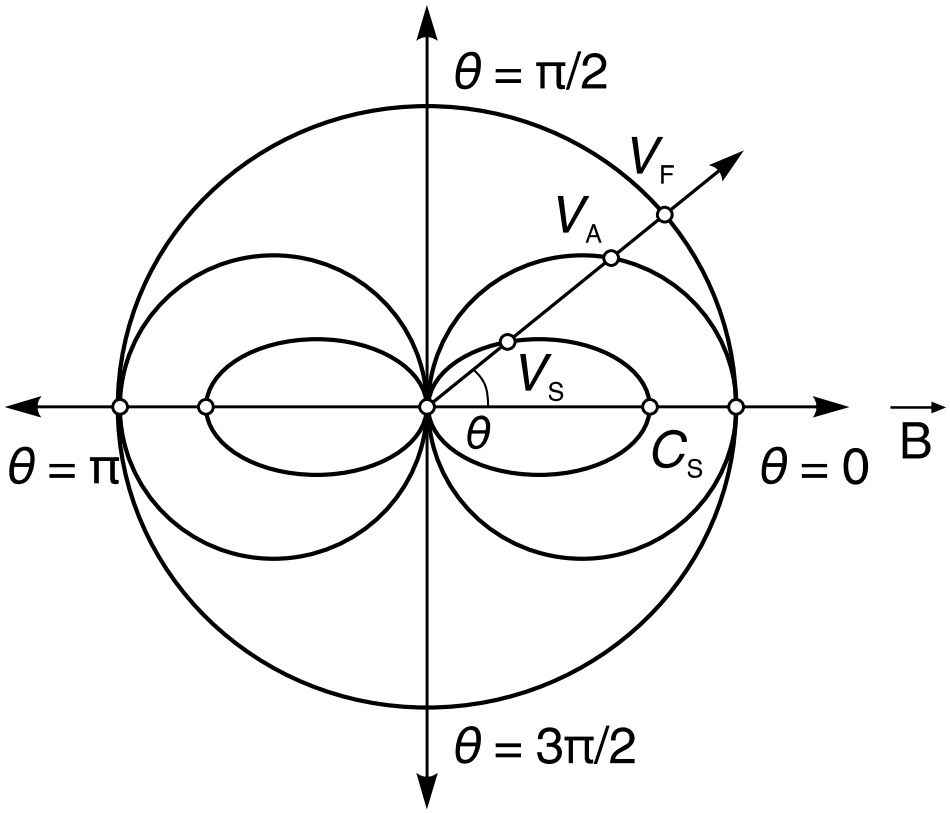

(α)

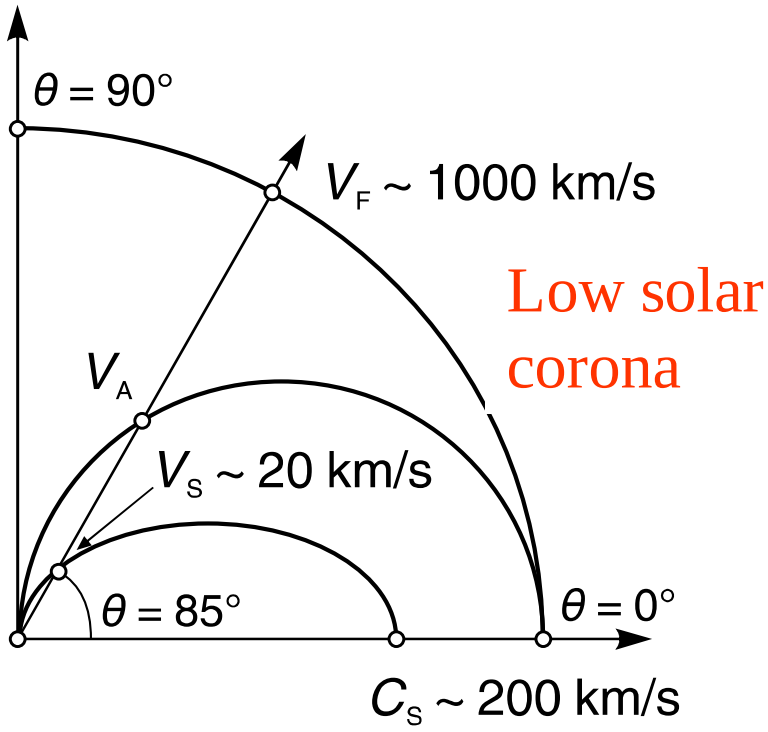

Low solar corona

(β)

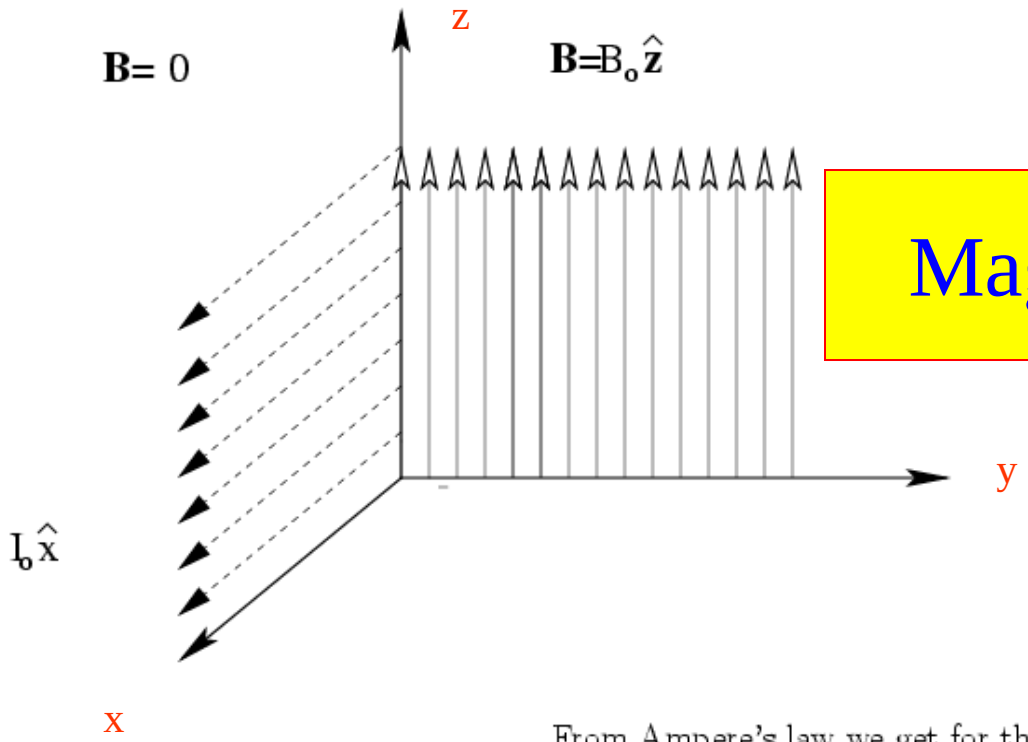

Magnetic pressure

From Ampere's law we get for the current that creates this field :

$$\vec{\nabla}\times\vec{B}=\frac{4\pi}{c}\vec{J}\Rightarrow\frac{4\pi}{c}J_x=\frac{\partial B_z}{\partial y}\Rightarrow\frac{4\pi}{c}\frac{I_x}{\Delta y\Delta z}=\frac{\Delta B_z}{\Delta y}\Rightarrow\frac{4\pi}{c}\frac{I_x}{\Delta z}=\Delta B_z=B_0\,.$$

From Laplace we get the force on the plasma :

$$\vec{F}=\frac{\ell\vec{I}\times\vec{B}}{c}\Rightarrow F_y=-\frac{\Delta x I_x B_z}{c}\Rightarrow-\frac{F_y}{\Delta x\Delta z}=\frac{I_x B_z}{c\Delta z}=\frac{B_0^2}{8\pi}\,,$$

where we substituted the mean value of B_z on theplane $y=0$, $B_z=B_o/2$. Hence, the force per unit area (pressure) is :

$$P_M=\frac{B_0^2}{8\pi}\,,$$

Magnetic tension

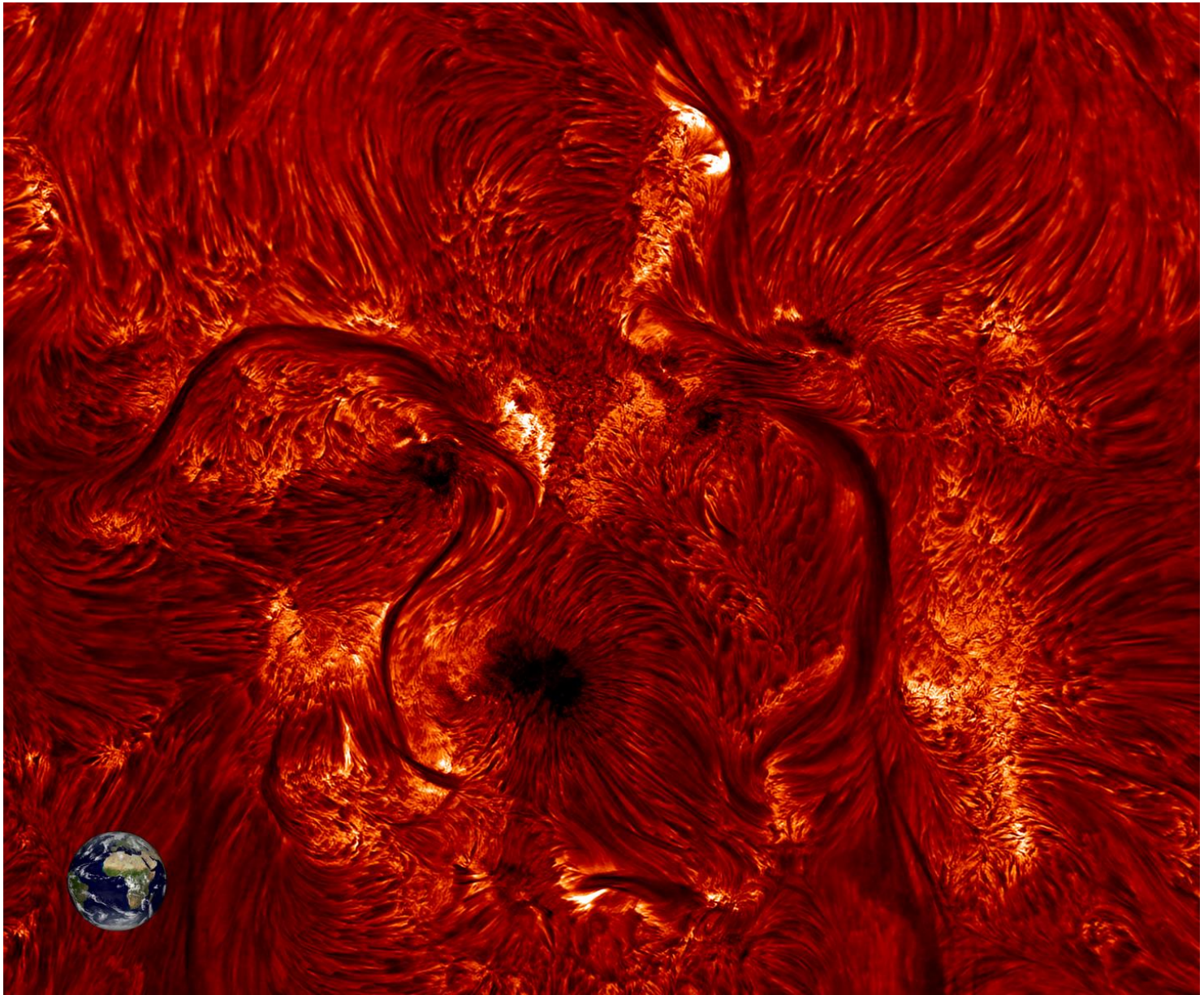

Magnetic support of prominences

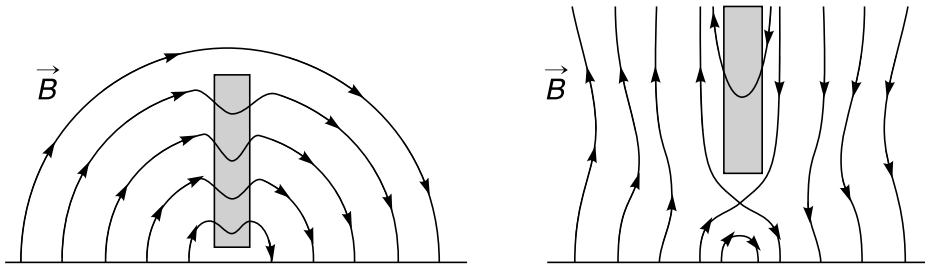

(α)

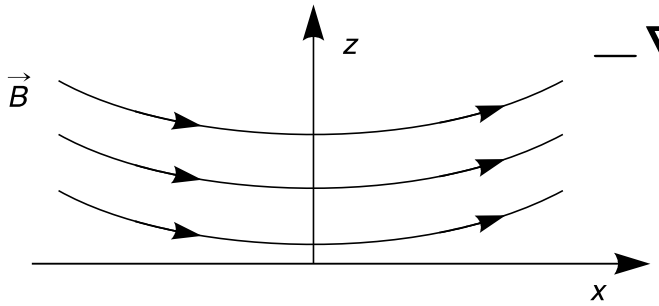

(β)

$$-\vec{\nabla}P - \rho g\hat{z} + \left(\vec{\nabla}\times\vec{B}\right)\times\vec{B}/4\pi = 0$$

(Equation of force balance)

Assume:

1. Constant horizontal field B_o
2. Constant temperature T_o
3. $P=P(x)$, $\rho = \rho(x)$, $B_z = B_z(x)$
4. $\Lambda=2kT_o/mg$, the scale height
5. $P=2k\rho T/m$, equation of state
6. Force balance in x-direction:

$$-\rho g+(B_o/4\pi)(dBx/dx) = 0,$$

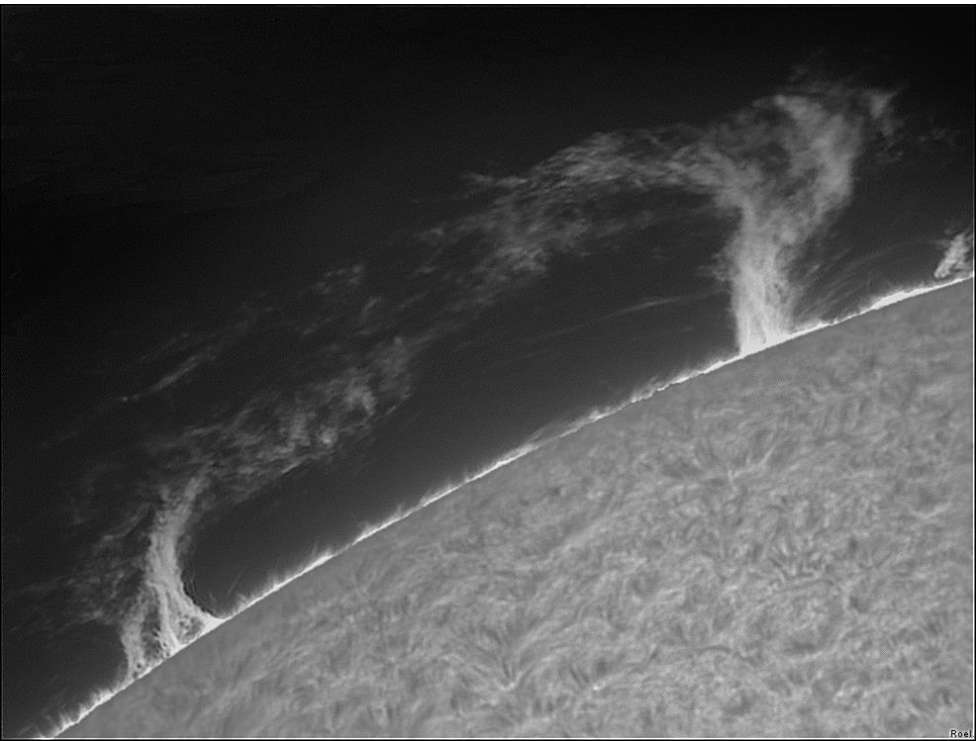

$$\frac{\mathrm{d}}{\mathrm{d}x}\left(P+\frac{B_z^2}{8\pi}\right)=0 \quad \Rightarrow \quad P+\frac{B_z^2}{8\pi}=\frac{B_{z\infty}^2}{8\pi}\,,$$

$\hat{x}$. Για τις διάστατες ποσότητες, b_z, b_o και X,

In terms of $b_z \equiv \dfrac{B_z}{B_{z\infty}}\,, \quad b_o \equiv \dfrac{B_o}{B_{z\infty}}\,, \quad X \equiv \dfrac{x}{2\Lambda}\,,$

We take the following differential equation for b_x

$$1-b_z^2=b_o\frac{\mathrm{d}b_z}{\mathrm{d}X}\,.$$

With solution,

$$b_z=\tanh\frac{X}{b_o}, \quad \frac{B_z(x)}{B_{z\infty}}=\tanh\frac{B_{z\infty}}{B_o}\frac{x}{2\Lambda}\,, \quad P(x)=\frac{B_{z\infty}^2}{8\pi}\mathrm{sech}^2\frac{B_{z\infty}}{B_o}\frac{x}{2\Lambda}\,.$$

In this solution it is worth noting the following. First, the plasma pressure at the center of the prominence equals to the magnetic pressure of the vertical magnetic field at infinity. Second, the width of the prominence is $\Delta x \approx 4\Lambda(B_o/B_{z\infty})$. Third, with the observational fact that the observed width of prominences is $\Delta x \approx 8000$ km, and that $\Lambda \approx 200$ km, we must have $B_{z\infty} \approx 0.1\ B_o$. That is, the magnetic support of the prominences requires only a small perturbation (B_z) in the external field (B_o).

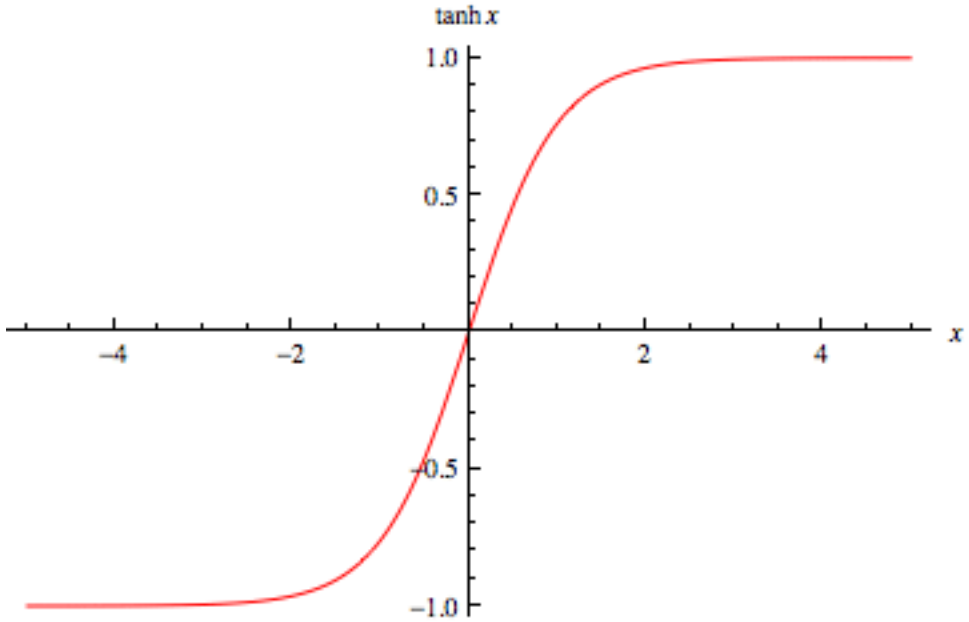
tanh x
1.0
0.5
−0.5
−1.0
−4
−2
2
4
x

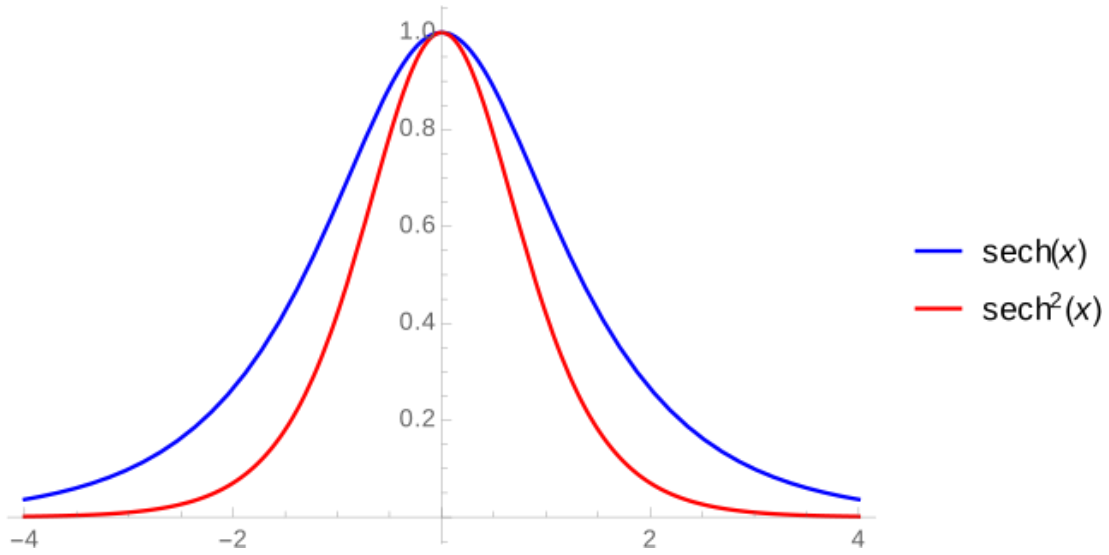
1.0
0.8
0.6
0.4
0.2
−4
−2
2
4
sech(x)
sech²(x)

Erupting prominence, March 30, 2010, SDO

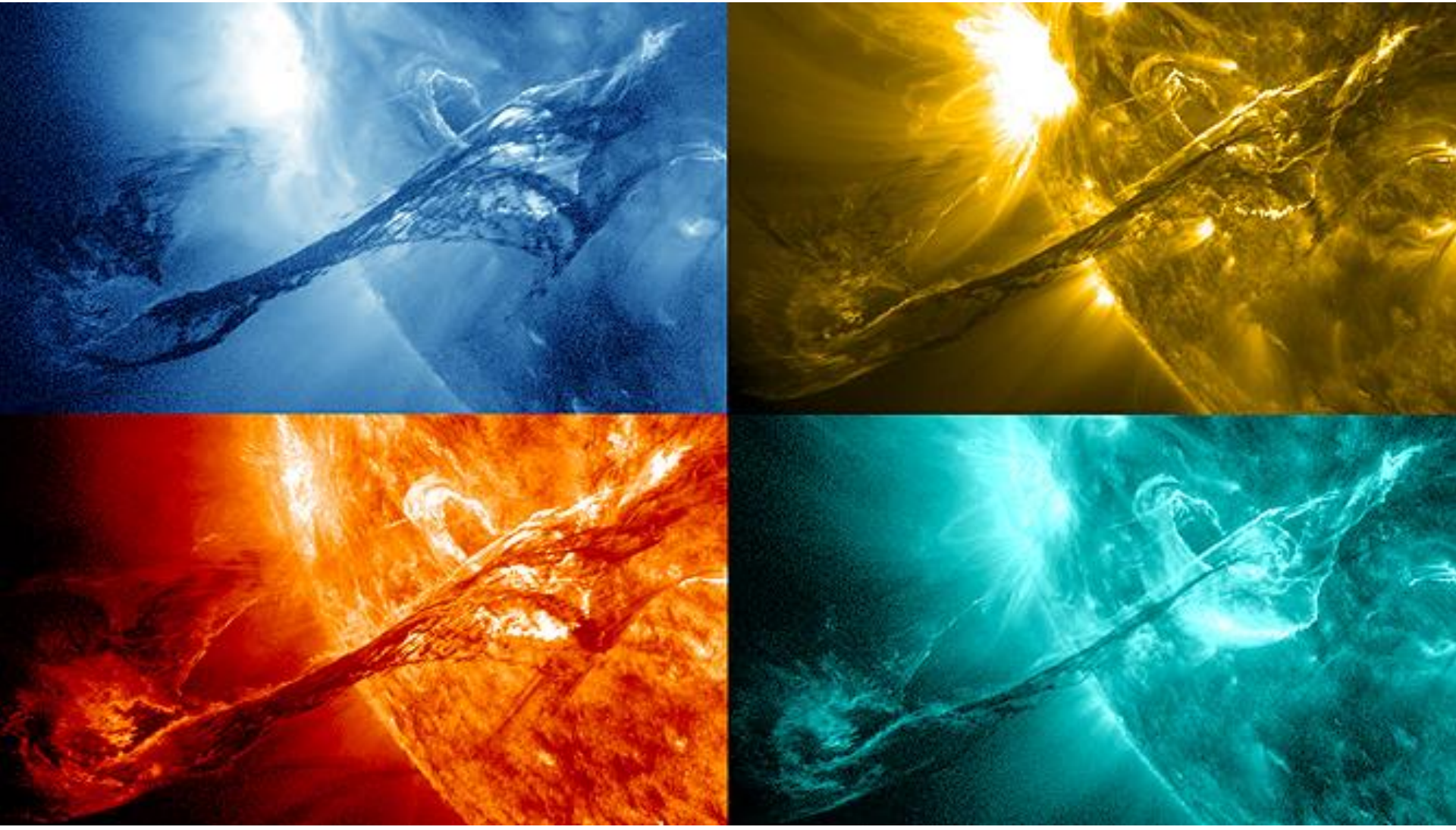

Magnetic buoyancy

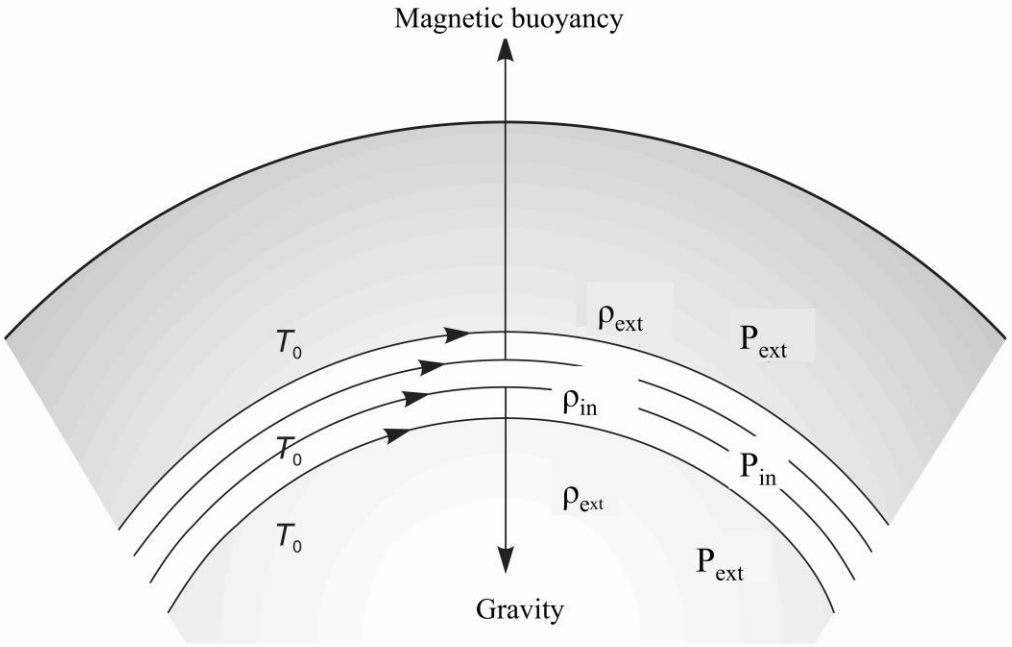

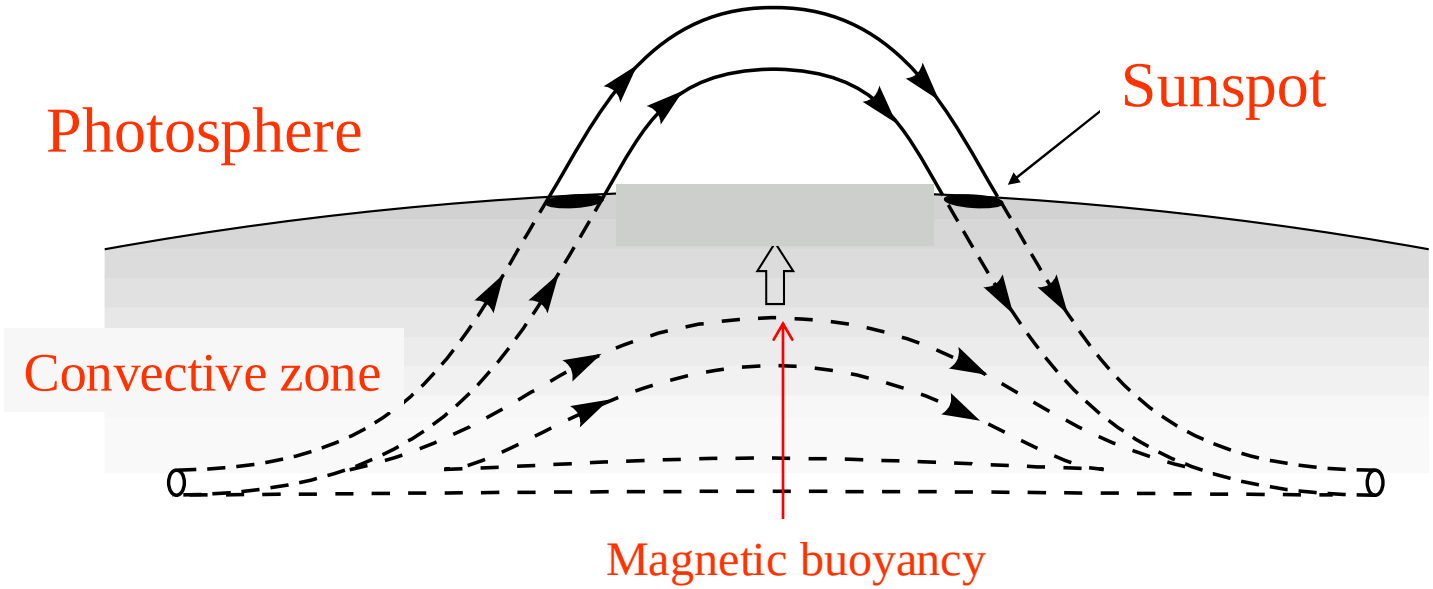

Magnetic Buoyancy and the Formation of Sunspots

1955, ApJ **121**, 491

THE FORMATION OF SUNSPOTS FROM THE SOLAR TOROIDAL FIELD*

EUGENE N. PARKER
Department of Physics, University of Utah, Salt Lake City, Utah
Received October 18, 1954

ABSTRACT

It is shown that a horizontal magnetic flux tube in an electrically conducting atmosphere is buoyant and will tend to rise. This magnetic buoyancy is large enough to bring an occasional strand of flux from the general solar toroidal field up into the photosphere, if we assume general field densities of a few hundred gauss farther down. Identifying the intersection of such ropes with the photosphere as the source of sunspots, we may deduce several general characteristics of the spots, e.g., east-west orientation, bipolarity, appearance only in low latitudes, migration, reversal of polarity, etc. The linearized static equilibrium equations for a flux tube are developed. With a cooling mechanism, such as that suggested by Biermann (1941), we find from the equilibrium equations that a sunspot group should consist of a diffuse flux tube of 10–100 gauss and 10^5 km extent in the photosphere, forming eventually a number of cool intense cores of several thousand gauss.

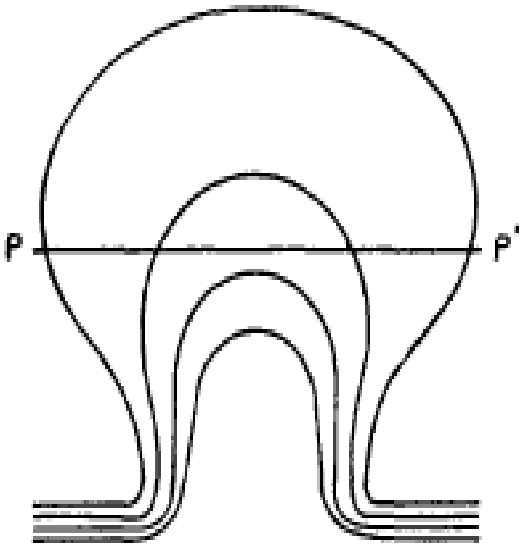

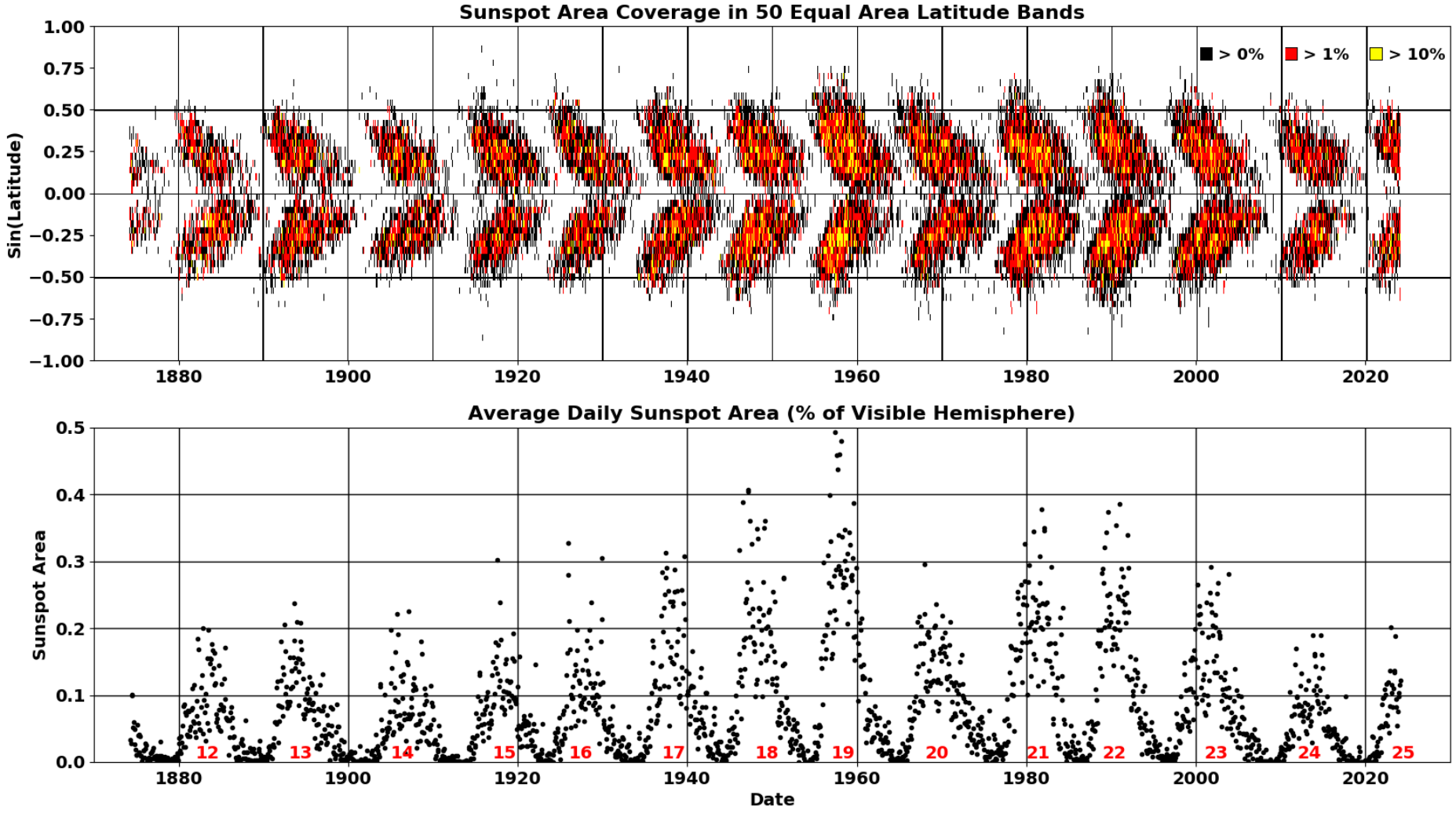
Sunspot Area Coverage in 50 Equal Area Latitude Bands
Sin(Latitude)
1.00
0.75
0.50
0.25
0.00
−0.25
−0.50
−0.75
−1.00
1880
1900
1920
1940
1960
1980
2000
2020
> 0%
> 1%
> 10%
Average Daily Sunspot Area (% of Visible Hemisphere)
Sunspot Area
0.5
0.4
0.3
0.2
0.1
0.0
12
13
14
15
16
17
18
19
20
21
22
23
24
25
Date
http://SolarCycleScience.com
2024/04 Hathaway

The **Parker dynamo** (1955)

HYDROMAGNETIC DYNAMO MODELS

EUGENE N. PARKER
Department of Physics, University of Utah, Salt Lake City, Utah
Received October 18, 1954; revised May 11, 1955

ABSTRACT

The purpose of this paper is to investigate the steady-state amplification of magnetic fields in a fluid It is shown that a rotating sphere of conducting fluid can regenerate a dipole magnetic field. It is sufficient for the angular velocity of rotation to vary with distance from the axis of rotation and for cyclonic fluid motions to be present The nonuniform rotation generates a toroidal field from the dipole field; the cyclones generate, from the toroidal field, loops of flux in the meridional plane which coalesce to amplify the dipole field The rotating sphere is discussed in relation to the liquid core of the earth and the geomagnetic dipole field. If, instead of a rotating sphere, one has a prismatic volume of fluid, it is possible to construct migratory dynamo waves The dynamo waves are discussed in relation to the solar convective zone; it is shown that such waves can account for many of the principal features of the observed solar magnetic activity

1955, ApJ **122**, 293

The Ω - effect and the α - effect. (Image by E. F. Dajka).

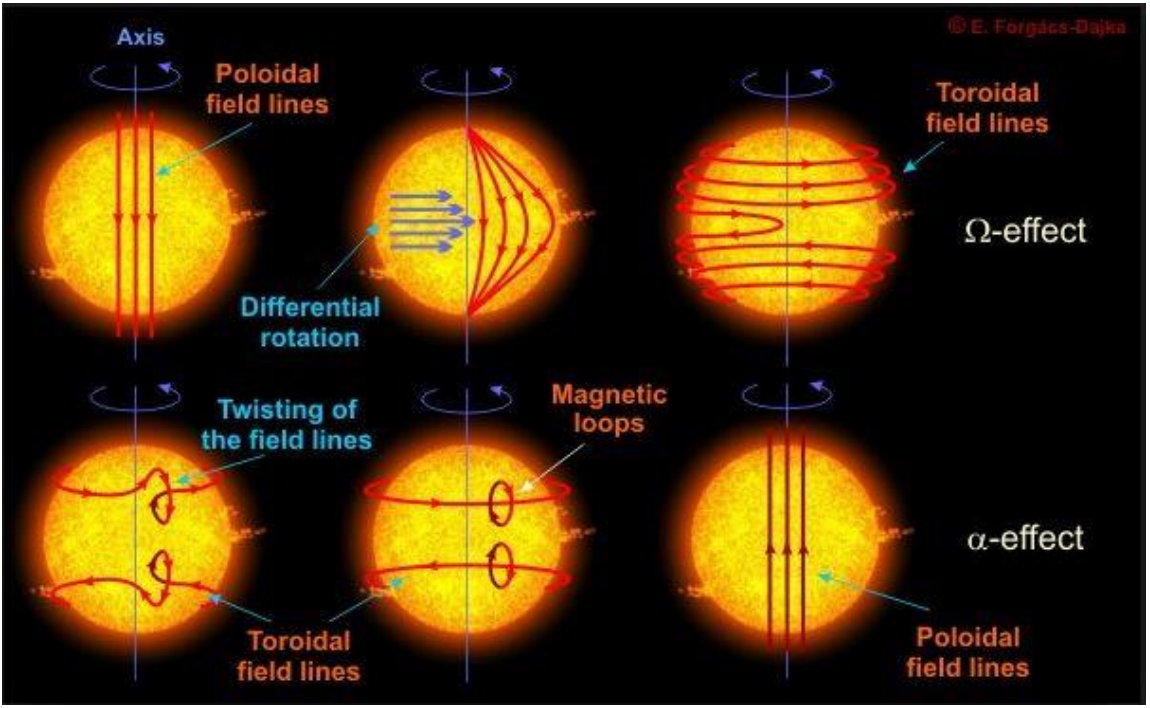

predicts that sunspots (star spots) appear periodically and within a period - for the sun it is the 11-year **Schwabe cycle** - of a higher heliographic latitude, about 30 ° -35 ° , walk to the equator (**Spörer's law**). The sunspots initiated by strong magnetic fields have a p-main spot (p = preceeding) and an f-main spot (f = following), the p-spot is somewhat closer to the solar equator, the two main spots form a bipolar group in which magnetic field linesexit from or enter the sun. Furthermore, bipolar groups correspond on the northern and southern hemisphere of the sun, whereby the magnetic orientation of the groups is opposite.

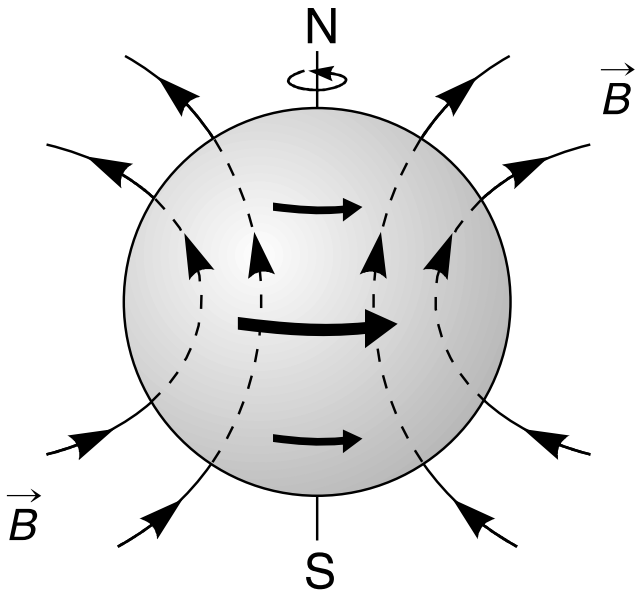

(α)

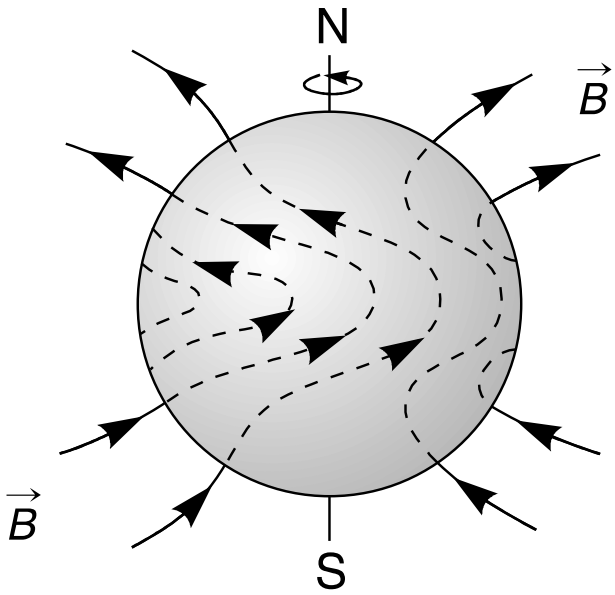

(β)

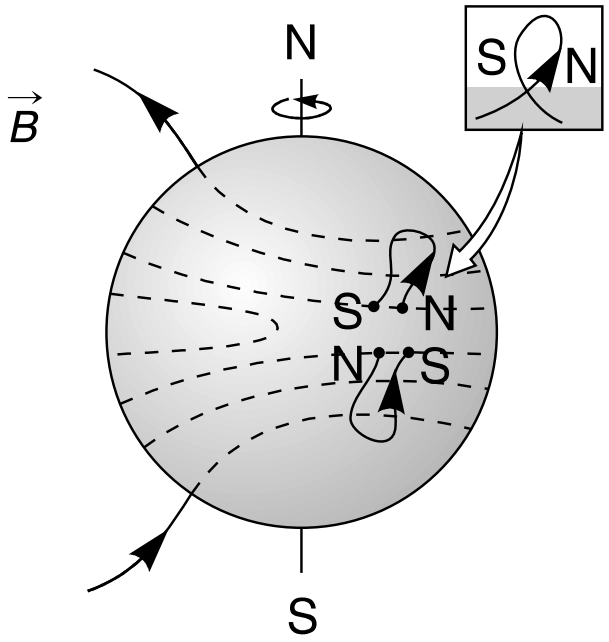

(γ)

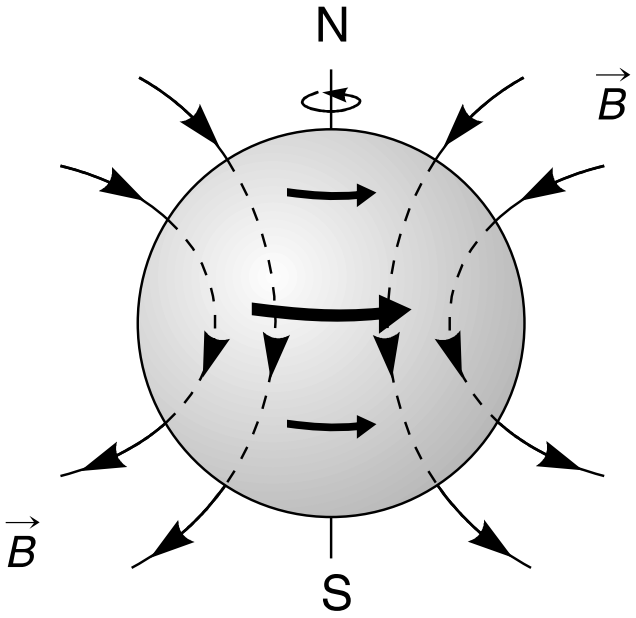

(δ)

Dynamo: a simple example

Suppose that we have a weak initial magnetic field **B** = $B_o y$ in a plasma of infinite electrical conductivity σ. Also suppose that we also impose a velocity field which acts from time t = 0 onwards,

$$\vec{V} = V_o \, e^{-\frac{y^2}{y_o^2}} \, \hat{x} \, .$$

Then, from the dynamo equation we have,

$$\vec{\nabla} \times (\vec{V} \times \vec{B}) = \hat{x} V_o B_o \frac{\partial}{\partial y} \left[e^{-\frac{y^2}{y_o^2}} \right] = -\hat{x} V_o B_o \frac{2y}{y_o^2} e^{-\frac{y^2}{y_o^2}} = \frac{\partial \vec{B}}{\partial t} \, .$$

Therefore, a new magnetic field is created in the x- direction with magnitude that increases linearly with time,

$$B_x = -\frac{2 V_o B_o y t}{y_o^2} e^{-\frac{y^2}{y_o^2}} \, .$$

Thus, from an initial weak magnetic field in the y-direction, a strong magnetic field in the orthogonal x-direction is produced - mainly near the y- axis.

The **Parker instability** in the ISM (1957)

THE DYNAMICAL STATE OF THE INTERSTELLAR GAS AND FIELD*

E. N. PARKER
Enrico Fermi Institute for Nuclear Studies and Department of Physics, University of Chicago
Received January 3, 1966; revised March 10, 1966

The Rayleigh-Taylor instability of magnetized gas supported by gravity.

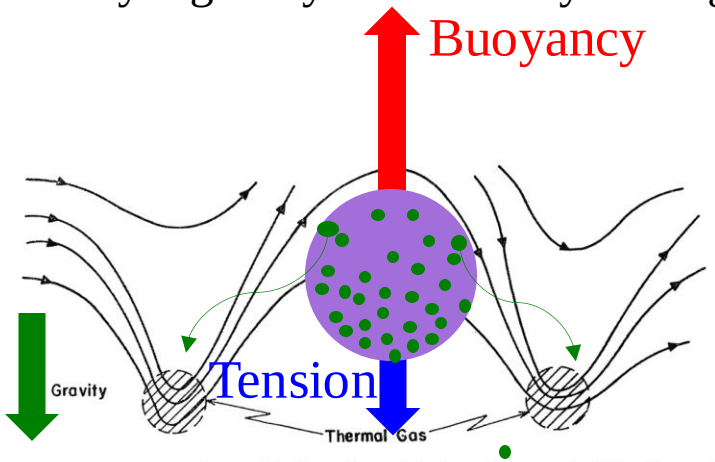

FIG. 2.—Sketch of the local state of the lines of force of the interstellar magnetic field and interstellar gas-cloud configuration resulting from the intrinsic instability of a large-scale field along the galactic disk or arm when confined by the weight of the gas.

Parker, 1966, ApJ,145, 811

Tarantula Nebula,
J. Webb telescope

NIRspec

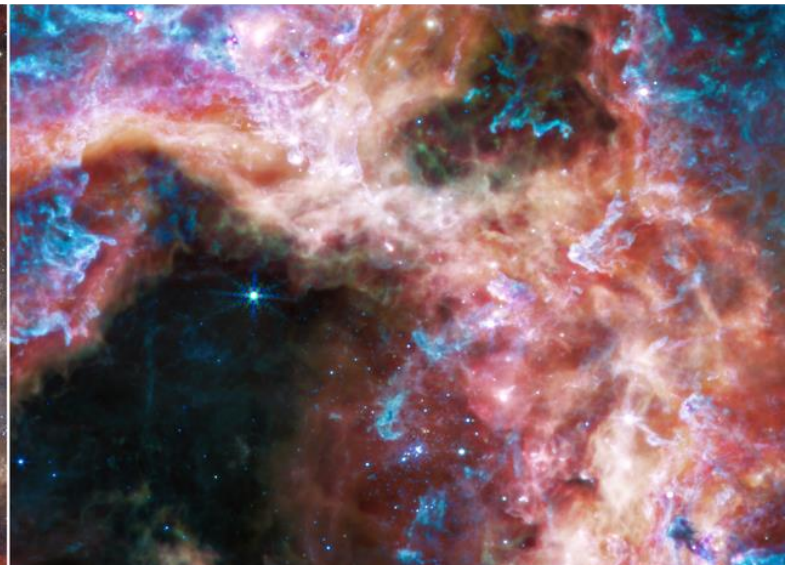

MIRI

The **Sweet-Parker magnetic reconnection model**

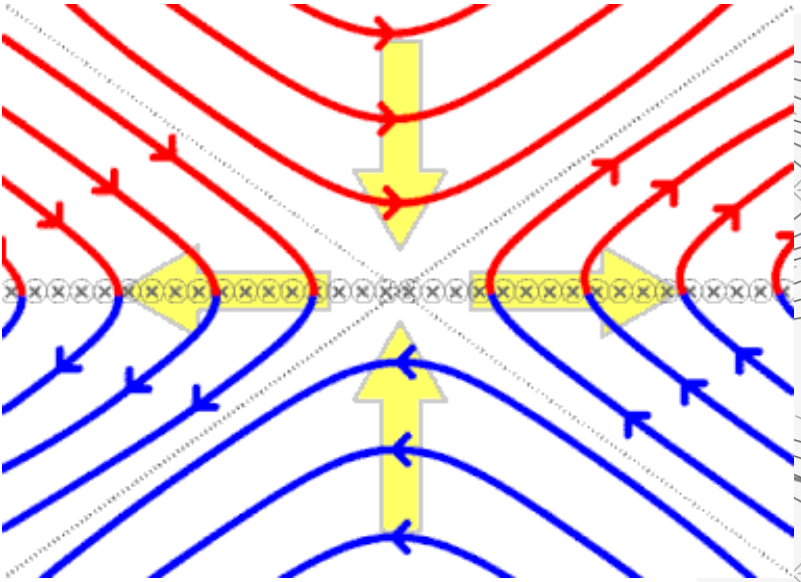

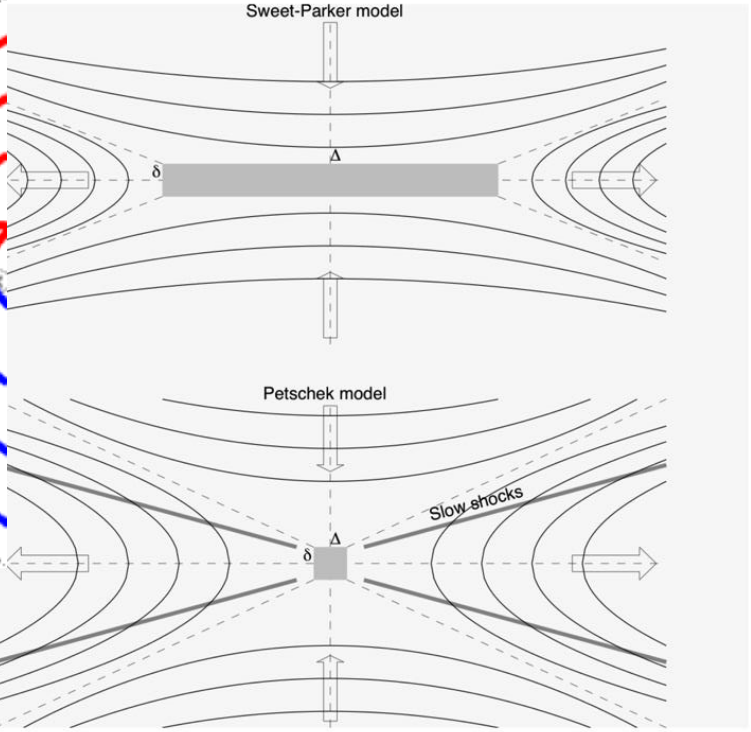

Geometry of the Sweet−Parker (top) and Petschek reconnection model (bottom). The geometry of the diffusion region (grey box) is a long thin sheet ($\Delta >> \delta$) in the Sweet−Parker model, but much more compact ($\Delta \approx \delta$) in the Petschek model. The Petschek model also considers slow-mode MHD shocks in the outflow region. [From Aschwanden (2020)]

The Sweet–Parker reconnection allows for reconnection rates much faster than global diffusion, (typical time-scales are of a few tens of days) but it is not able to explain the fast reconnection rates observed in solar flares. **However, it was the first basis for understanding solar flares**.

The individual links in the chain of solar MHD:

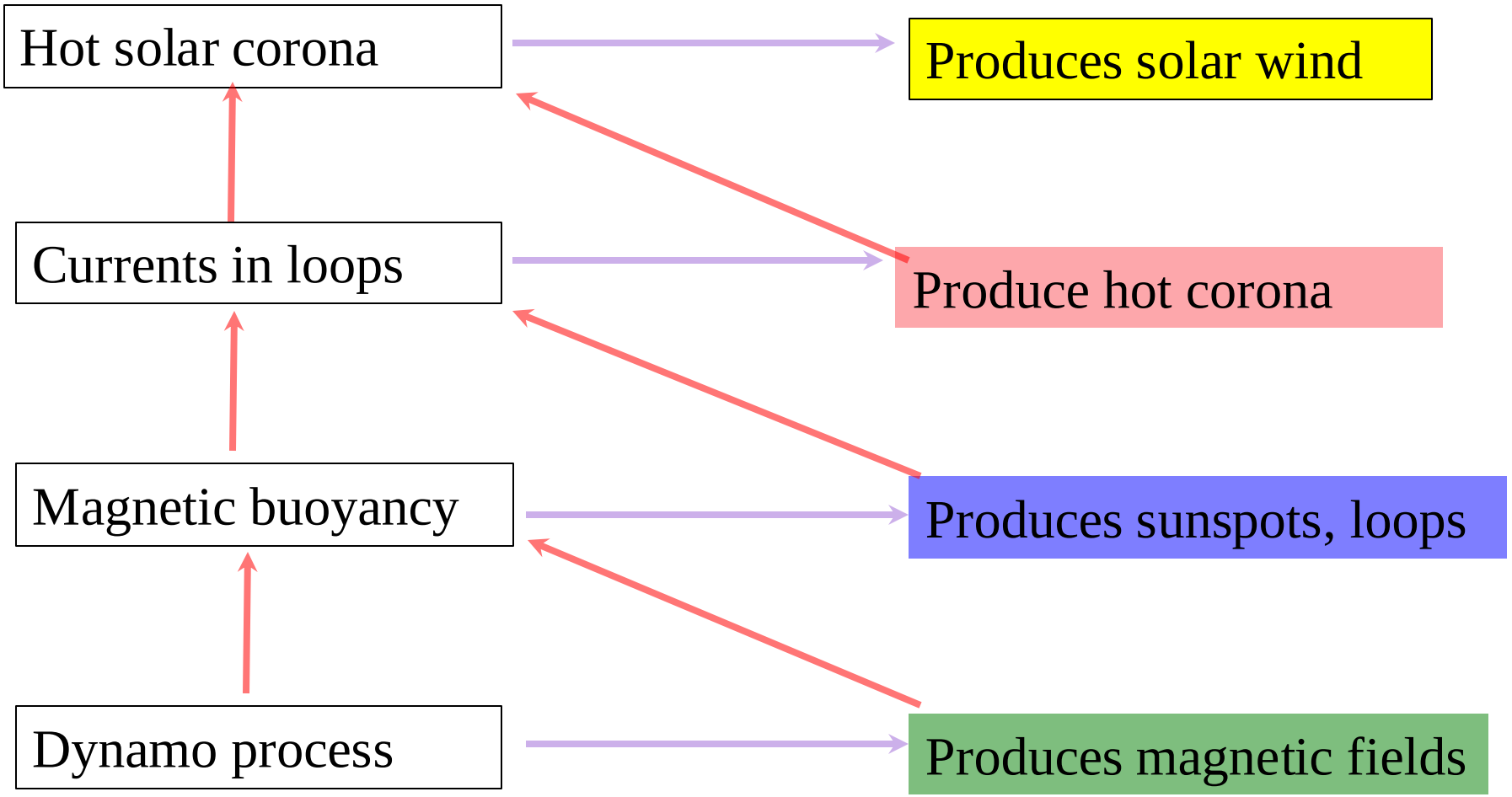

The majestic Solar Corona

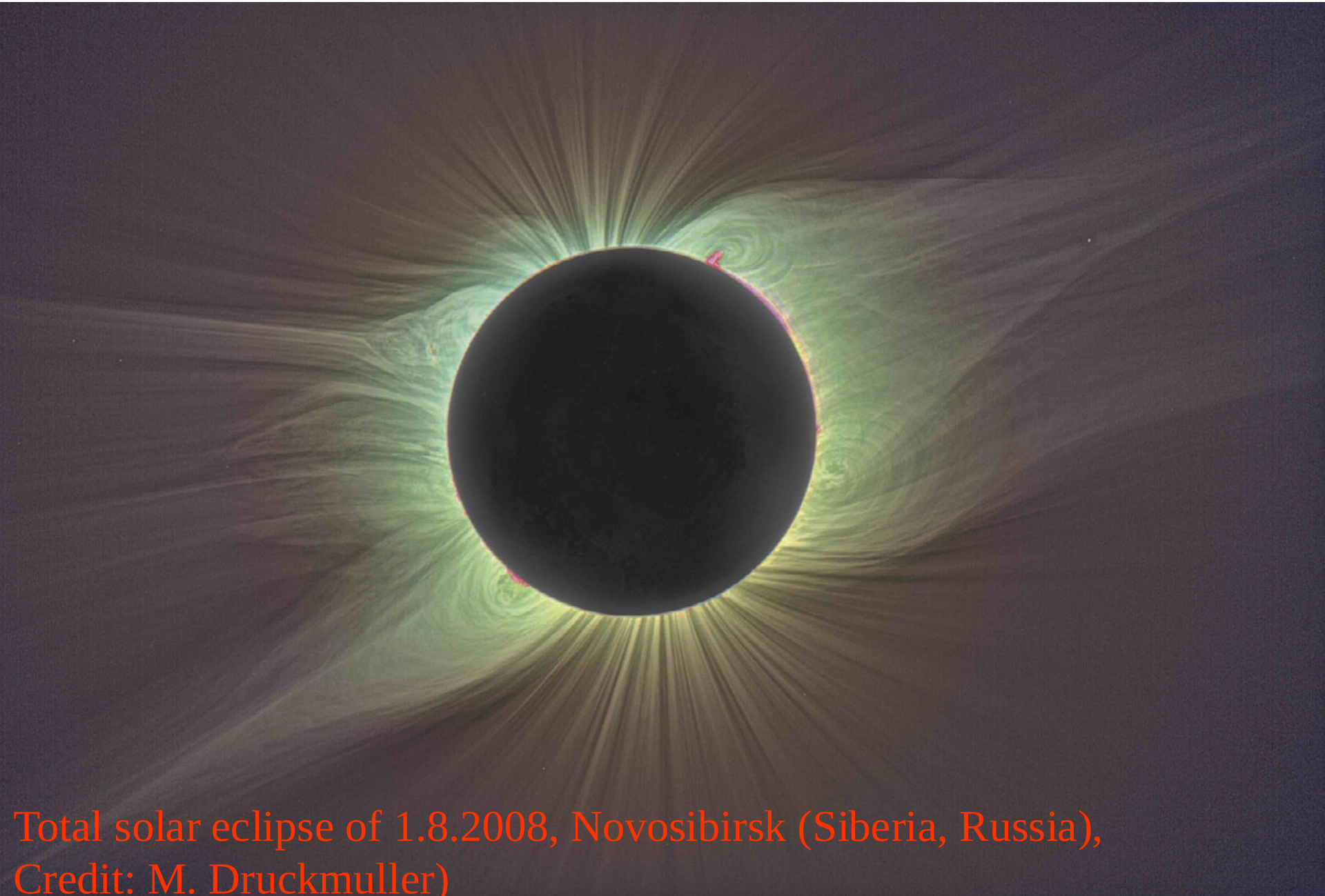

Total solar eclipse of 1.8.2008, Novosibirsk (Siberia, Russia), Credit: M. Druckmuller)

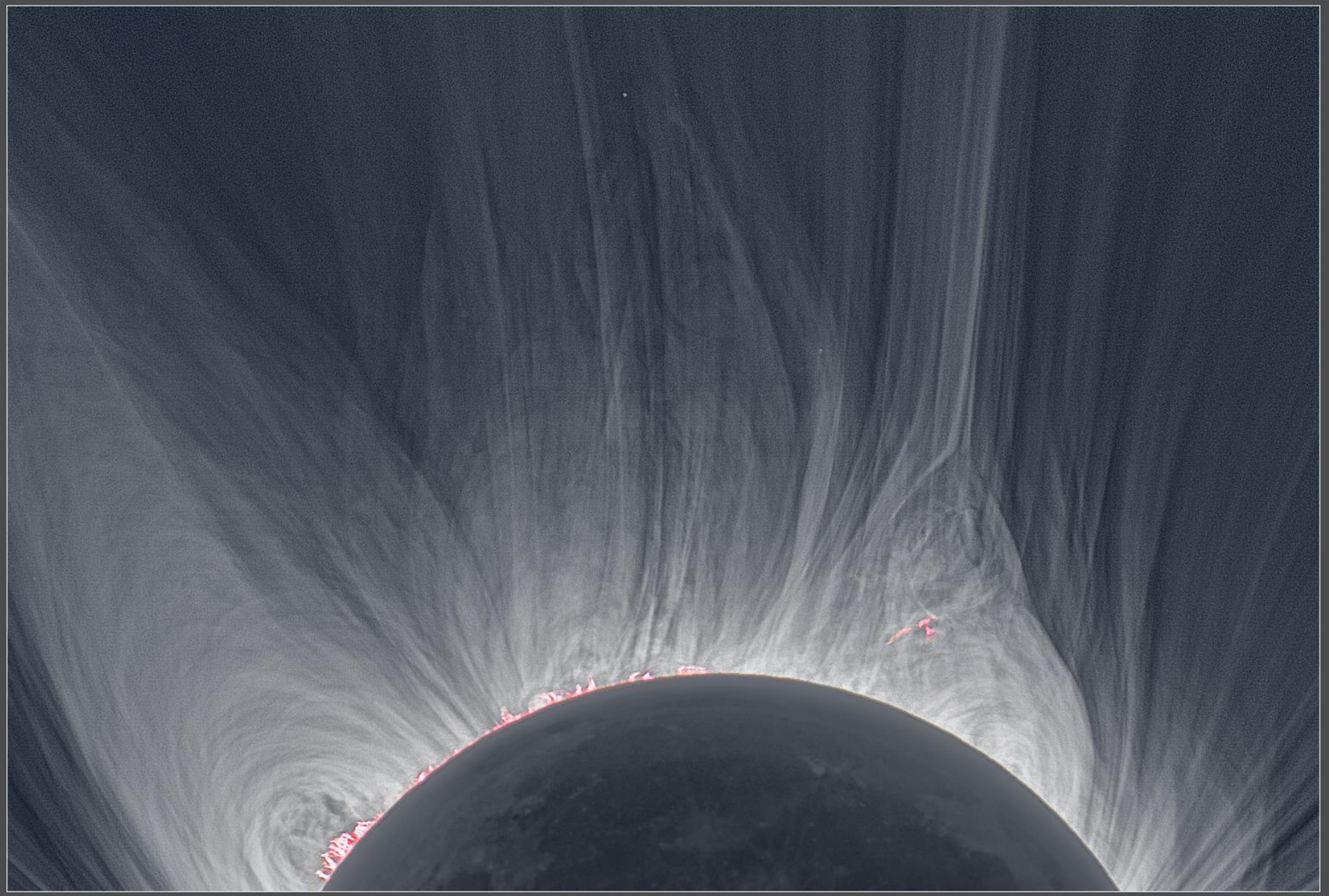

Total solar eclipse of 1.8.2008, Novosibirsk (Siberia, Russia) Credit: M. Druckmuller)

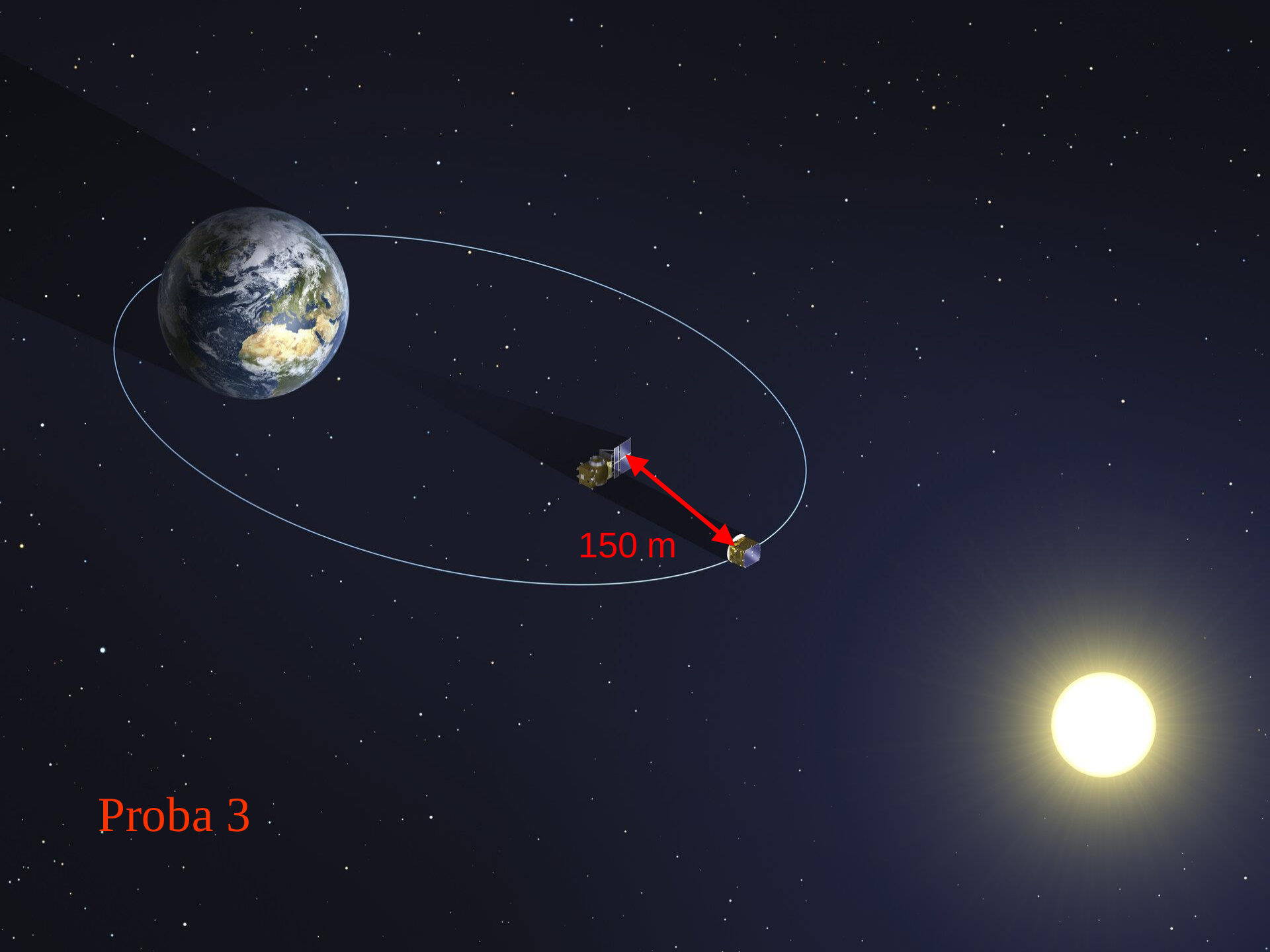
150 m
Proba 3

Parker's theorem for the nonequilibrium of nonsymmetric magnetic field topologies (1972)

THE ASTROPHYSICAL JOURNAL, 174:499–510, 1972 June 15

TOPOLOGICAL DISSIPATION AND THE SMALL-SCALE FIELDS IN TURBULENT GASES*

E. N. PARKER
Department of Physics, University of Chicago
Received 1971 December 8

ABSTRACT

It is shown that a large-scale magnetic field possesses a hydrostatic equilibrium only if the pattern of small-scale variations is uniform along the large-scale field. Thus equilibrium obtains only if the variations in the field consist of simple twisting of the lines, with the twists extending uniformly the full length of the field. Any more complicated topology, such as two or more flux tubes wrapped around each other to form a rope, or braided or knotted flux tubes, is without equilibrium, no matter what fluid pressures are applied along the individual lines of force. The result is rapid dissipation and field-line merging, which quickly reduces the topology to the simple equilibrium form. It follows from this general theorem that line merging has important consequences in turbulent fields. In spite of large magnetic Reynolds numbers of the individual eddies, the line merging reduces the small-scale fields in the turbulence below the value for equipartition with the turbulence. The effect has important astrophysical implications. It explains the absence of strong small-scale fields in the solar photosphere and in interstellar space in spite of the vigorous turbulence.

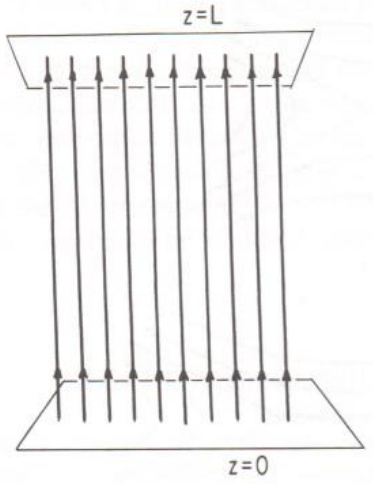

Coronal heating by many current sheets occurring in magnetic loops in the solar corona

THE ASTROPHYSICAL JOURNAL, 330:474–479, 1988 July 1

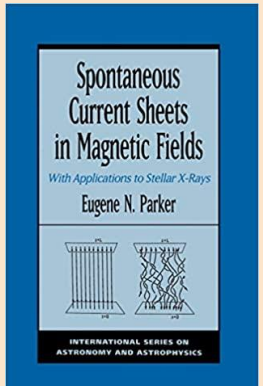

NANOFLARES AND THE SOLAR X-RAY CORONA[1]

E. N. PARKER
Enrico Fermi Institute and Departments of Physics and Astronomy, University of Chicago

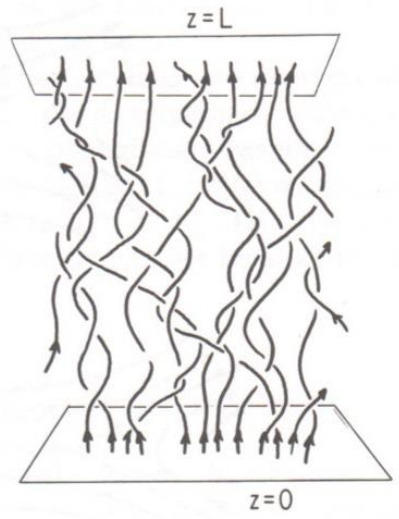

ABSTRACT

It is shown that when the magnetic field and the fluid motions in an ideal magnetofluid have a translational symmetry then, apart from isolated topologies, invariance along this principal direction of the fields is a necessary condition for magnetohydrodynamic equilibrium. In well-behaved field topologies lacking this invariance, nonequilibrium is the result. This theorem is analogous to the well-established Taylor-Proudman theorem in fluid dynamics and runs parallel to Parker's theorem for the necessary conditions for equilibrium in magnetostatics. It appears then that topological nonequilibrium may indeed be the basis for the continuous activity of the variable hydromagnetic fields in the universe.

Subject heading: hydromagnetics

I. INTRODUCTION

There are presently available two theorems on the necessary conditions for the steady ($\partial/\partial t \equiv 0$) equilibrium of velocity fields and magnetic fields. An equilibrium velocity field $\boldsymbol{v}$ in an ideal fluid of density ρ and pressure P satisfies Euler's equations,

$$\rho(\boldsymbol{v}\cdot\nabla)\boldsymbol{v} = -\nabla P + 2\rho\boldsymbol{v}\times\boldsymbol{\Omega}, \tag{1}$$

$$\nabla\cdot\boldsymbol{v} = 0, \tag{2}$$

in a frame of reference that is rotating with an angular velocity $\boldsymbol{\Omega}$. The Taylor-Proudman theorem (Proudman 1916;

The analysis and the results in the last two sections were carried under the assumption that there is no equipartition of energy between the magnetic and the velocity fields [Chandrasekhar 1956, and for an extension to incompressible fluids, $\rho = \rho(A)$, see Papers I, II],

$$\boldsymbol{v}(x,y,z) = \pm\frac{\boldsymbol{B}(x,y,z)}{(4\pi\rho)^{1/2}}. \tag{92}$$

Evidently the above solution satisfies identically the equations of motion, irrespective of any spatial dependence of the fields. Notice, however, that the case (92), wherein the centrifugal force arising from the fluid motions is exactly balanced everywhere by the tension of the lines of the magnetic force, is so far the only known solution of the MHD equations lacking any symmetry. It therefore seems to represent an isolated case.

The second assumption which enabled us to deduce the invariance requirement equation (56), is the analyticity condition, equations (18)–(21) or (63)–(66). Fields that are not analytic in the near neighborhood of a two-dimensional

Campfires’ are miniature solar flares discovered by ESA’s Solar Orbiter mission.

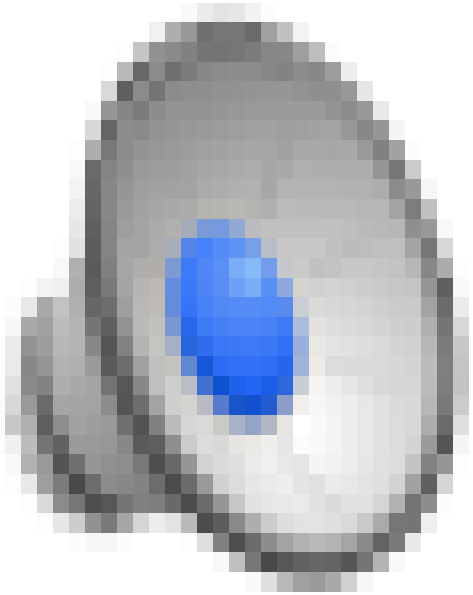

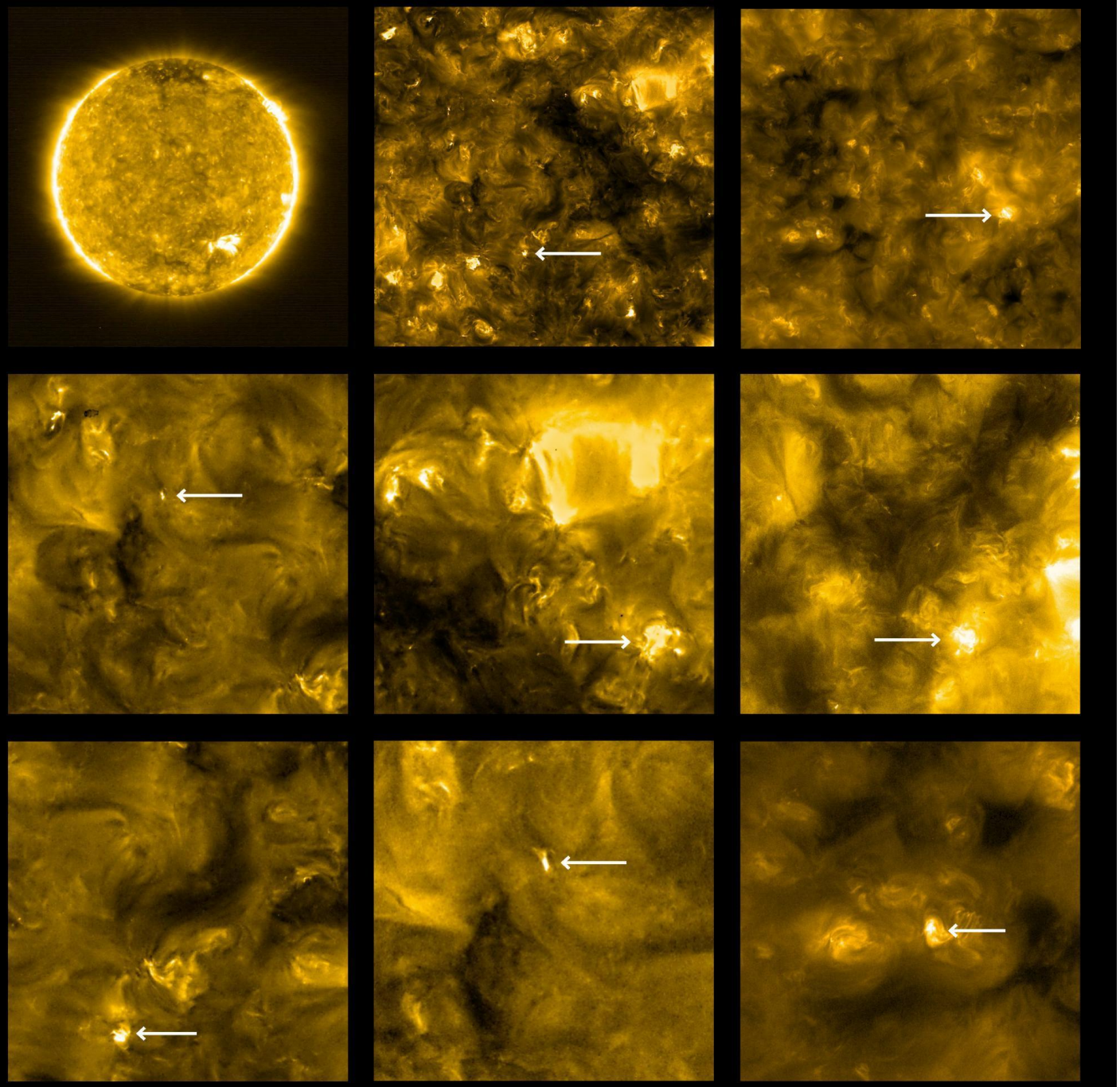

Magnetic switchbacks observed by the PSP

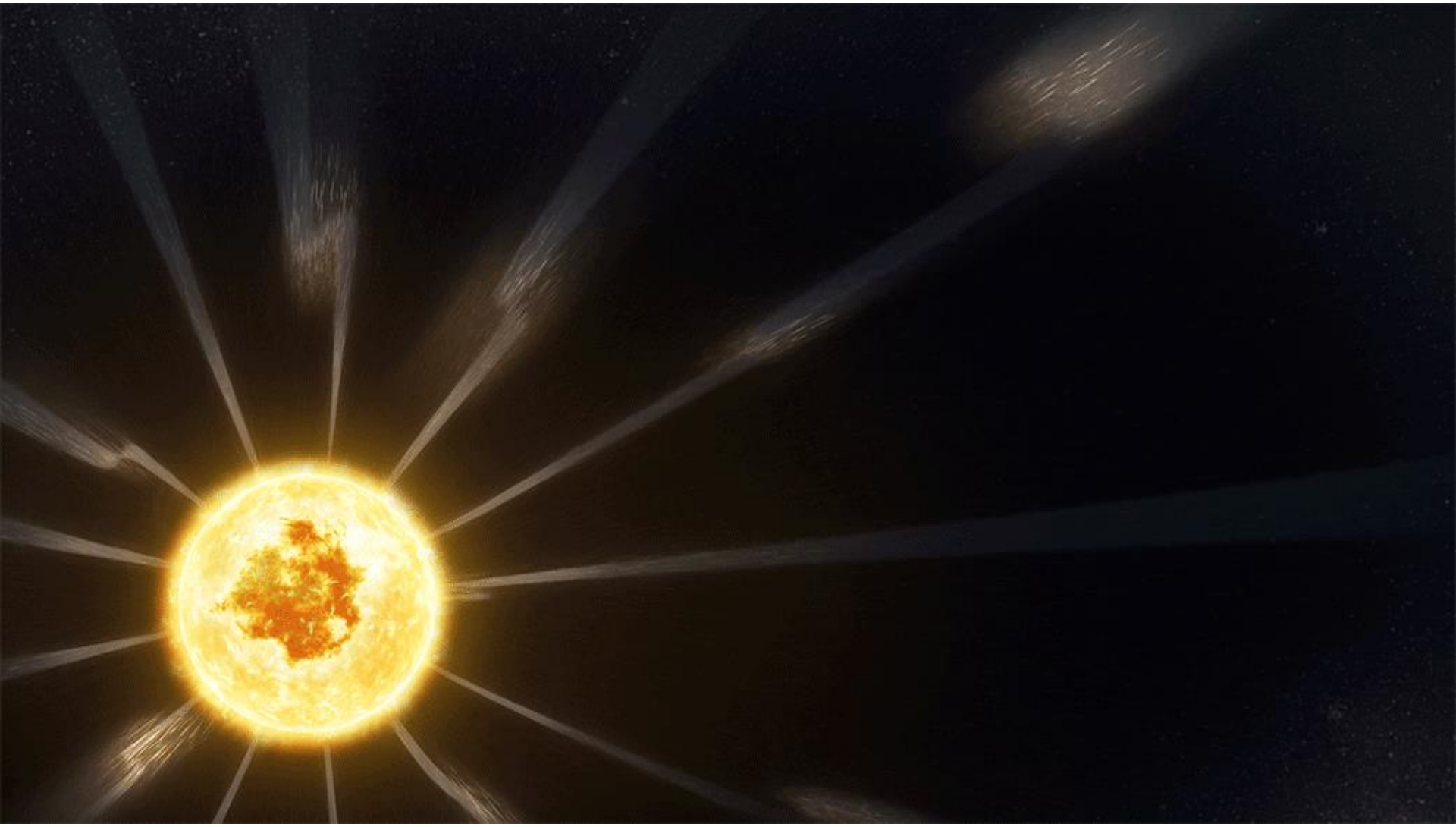

Parker Solar Probe observed switchbacks — traveling disturbances in the solar wind that caused the magnetic field to bend back on itself — an as-yet unexplained phenomenon.
Credits: NASA's GSFC/Conceptual Image Lab/Adriana Manrique Gutierrez

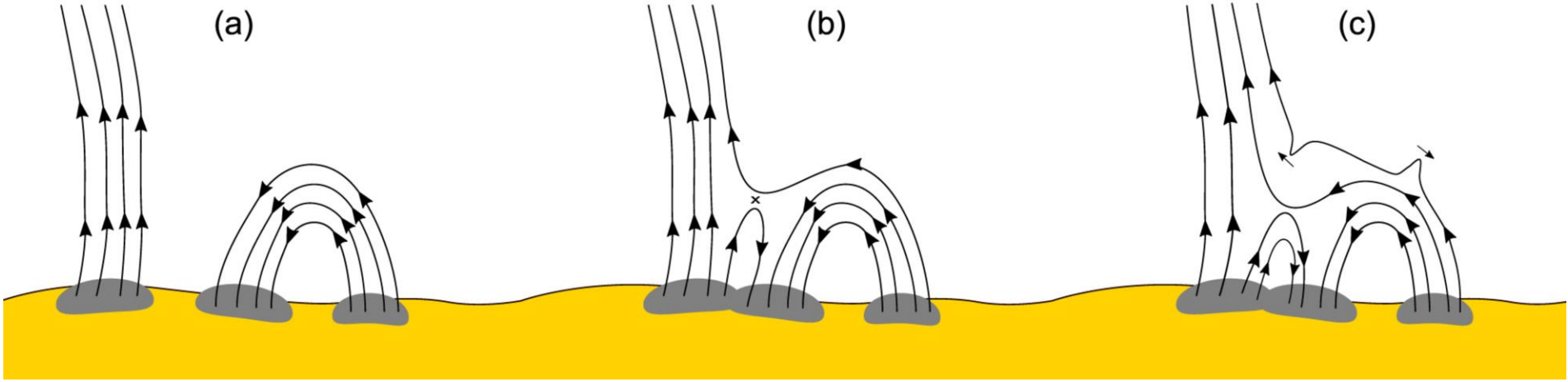

Illustration of the formation mechanism of magnetic switchbacks, observed originally (2018) by NASAs Parker Solar Probe spacecraft and followed by the ESA/NASA Solar Orbiter spacecraft (2022), wherein there is an interaction between a region of open field lines and a region of closed field lines. In this scenario an open magnetic field line is (a) dragged against a large coronal loop, by global circulation in the corona, (b) undergoes interchange reconnection, and (c) effectively jumps the approximate width of the originally closed loop, launching an S-shaped switchback in the magnetic field into the corona. Fisk & Kasper (2020), Telloni et al (2022). [Credit: ESA/NASA/GSFC].

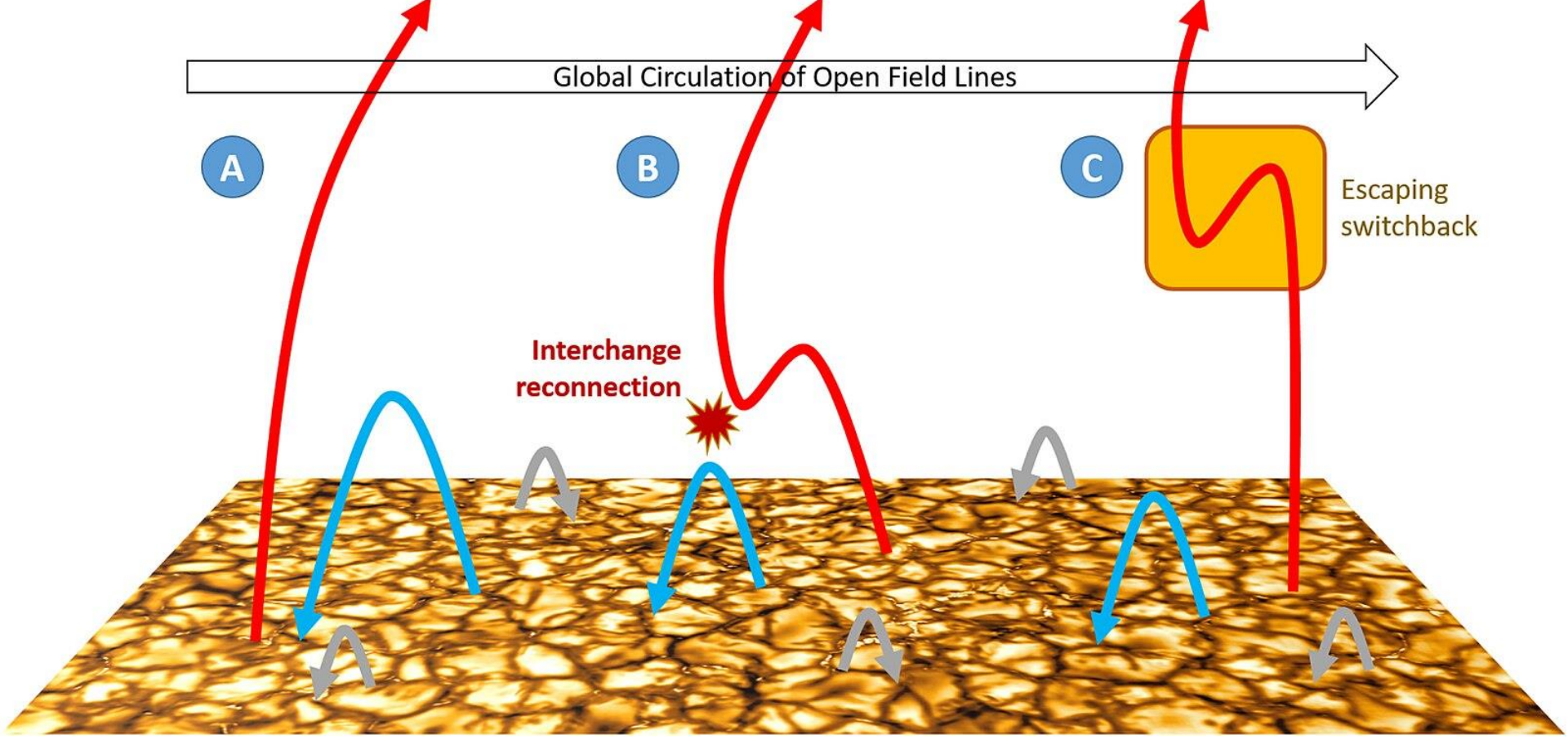

llustration of global magnetic field circulation enabled by interchange reconnection. In this scenario an open magnetic field line is (A) dragged against a large coronal loop, by global circulation in the corona, (B) undergoes interchange reconnection, and (C) effectively jumps the approximate width of the originally closed loop, launching an S-shaped switchback in the magnetic field into the corona. Fisk & Kasper (2020), Telloni et al (2022). [Credit: ESA/NASA/GSFC]

National Aeronautics and Space Administration

Where Do Switchbacks Come From?

Switchbacks are sudden reversals in the solar wind's magnetic field. They were a surprise discovery as NASA's Parker Solar Probe made its first close flyby of the Sun in November 2018.

How do switchbacks form? Here are the current theories competing to explain them.

(Not to scale)

www.nasa.gov

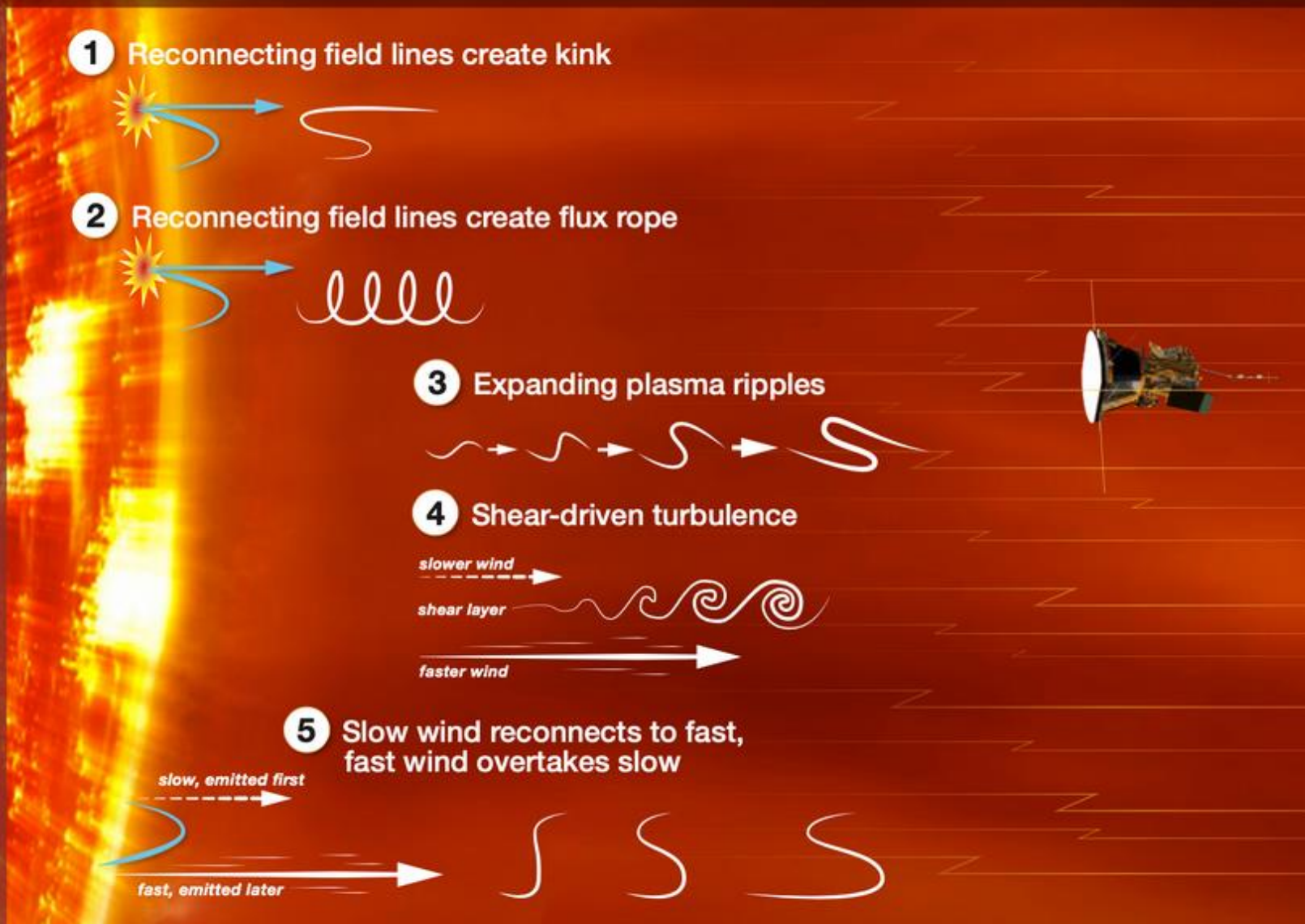

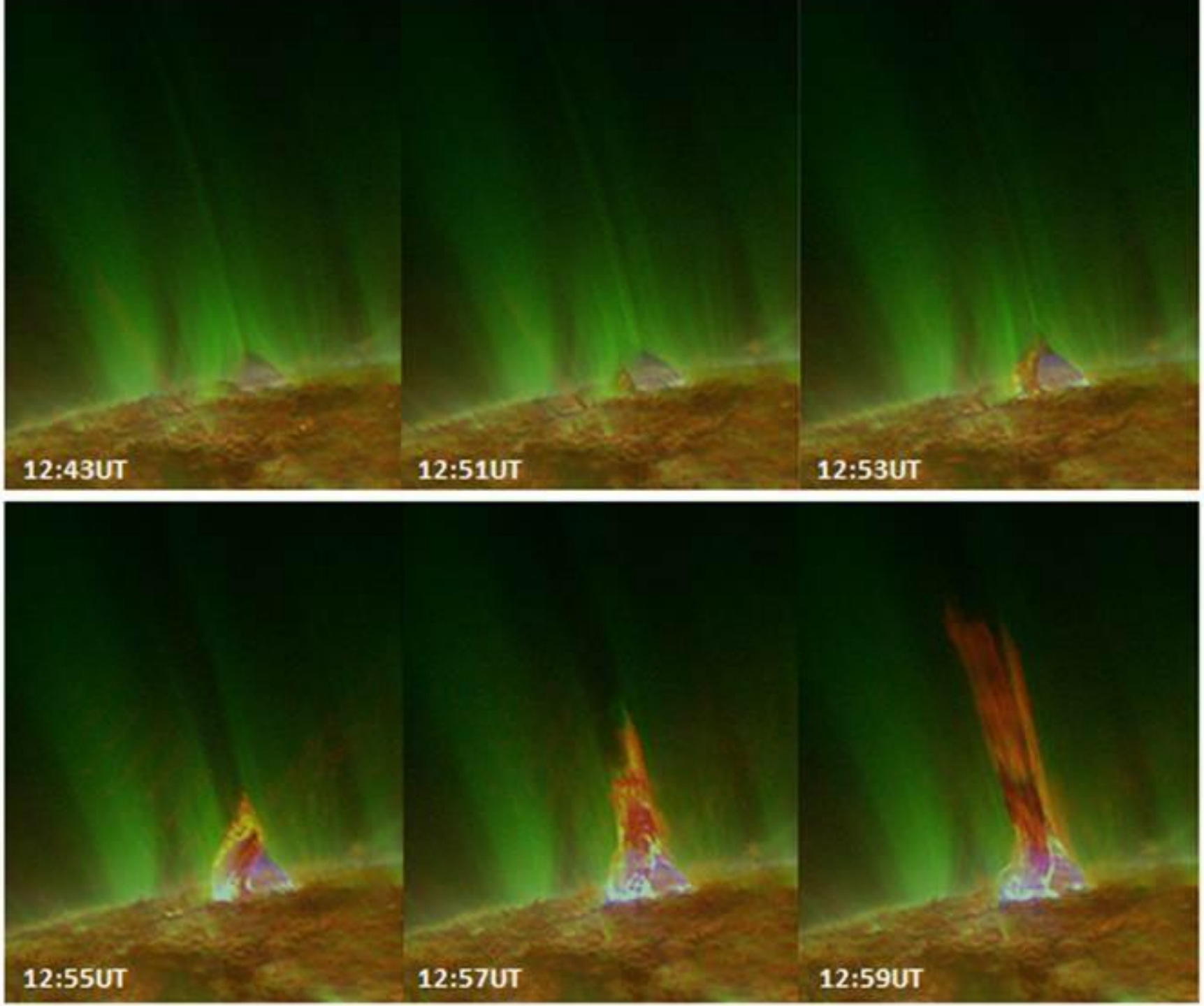
12:43UT
12:51UT
12:53UT
12:55UT
12:57UT
12:59UT

A&A 512, L2 (2010)
DOI: 10.1051/0004-6361/200913752

Astronomy & Astrophysics

LETTER TO THE EDITOR

Recurrent solar jets in active regions

V. Archontis[1], K. Tsinganos[2], and C. Gontikakis[3]

[1] School of Mathematics and Statistics. St. Andrews University, St. Andrews, KY16 9SS, UK
e-mail: vasilis@mcs.st-and.ac.uk
[2] Section of Astrophysics, Astronomy and Mechanics, Department of Physics, University of Athens, Panepistimiopolis, Zografos 157 84, Athens, Greece
[3] Research Center for Astronomy and Applied Mathematics, Academy of Athens, 4 Soranou Efessiou Str., Athens 11527, Greece

Received 27 November 2009 / Accepted 24 February 2010

ABSTRACT

Aims. We study the emergence of a toroidal flux tube into the solar atmosphere and its interaction with a pre-existing field of an active region. We investigate the emission of jets as a result of repeated reconnection events between colliding magnetic fields.
Methods. We perform 3D simulations by solving the time-dependent, resistive MHD equations in a highly stratified atmosphere.
Results. A small active region field is constructed by the emergence of a toroidal magnetic flux tube. A current structure is build up and reconnection sets in when new emerging flux comes into contact with the ambient field of the active region. The topology of the magnetic field around the current structure is drastically modified during reconnection. The modification results in a formation of new magnetic systems that eventually collide and reconnect. We find that reconnection jets are taking place in successive recurrent phases in directions perpendicular to each other, while in each phase they release magnetic energy and hot plasma into the solar atmosphere. After a series of recurrent appearance of jets, the system approaches an equilibrium where the efficiency of the reconnection is substantially reduced. We deduce that the emergence of new magnetic flux introduces a perturbation to the active region field, which in turn causes reconnection between neighboring magnetic fields and the release of the trapped energy in the form of jet-like emissions. This is the first time that self-consistent recurrency of jets in active regions is shown in a three-dimensional experiment of magnetic flux emergence.

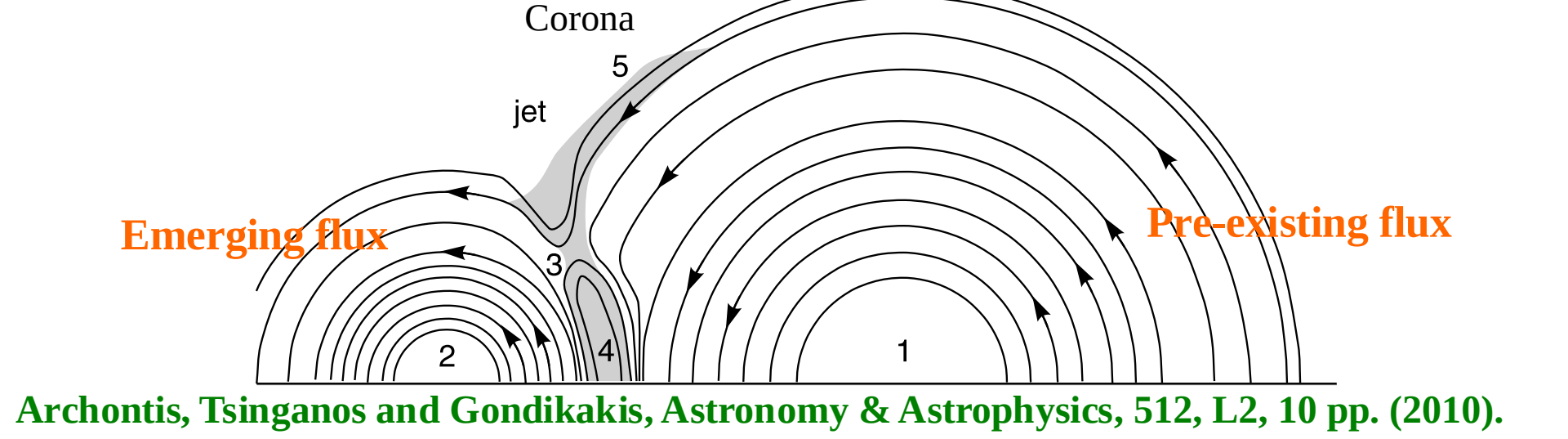

Archontis, Tsinganos and Gondikakis, Astronomy & Astrophysics, 512, L2, 10 pp. (2010).

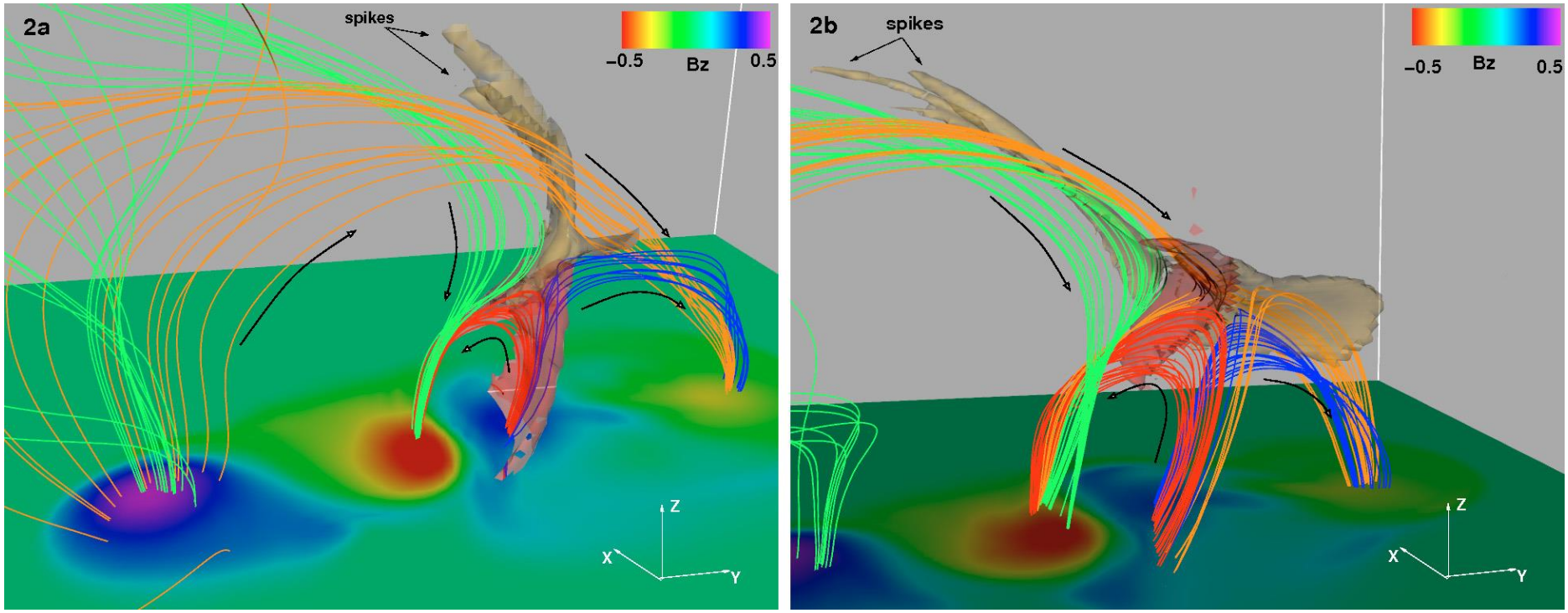

Fig. 2. 3d visualization of the jets (velocity isosurfaces, yellowish/grey) at $t = 144$ (*left*) and $t = 184$ (*right*). Side views are shown for the two snapshots. The current sheets (colored red) are visualized by calculating $\boldsymbol{J}/\boldsymbol{B}$. The horizontal slice is a *magnetogram* at $z = 2$. Note that the two upward elongated jets are emitted along similar directions (oblique-left). The arrows (black color) show the direction of the full magnetic field vector.

Angular momentum of e-m field:

S=c(**E**x**B**)/4π

d**p**/dV= **S**/c^2

d**L**/dV=**r**xd**p**/dV

L_z= eg/c = nℏ, n=1,2..

→ g = ne x 137

α = c^2/ℏc=1/137

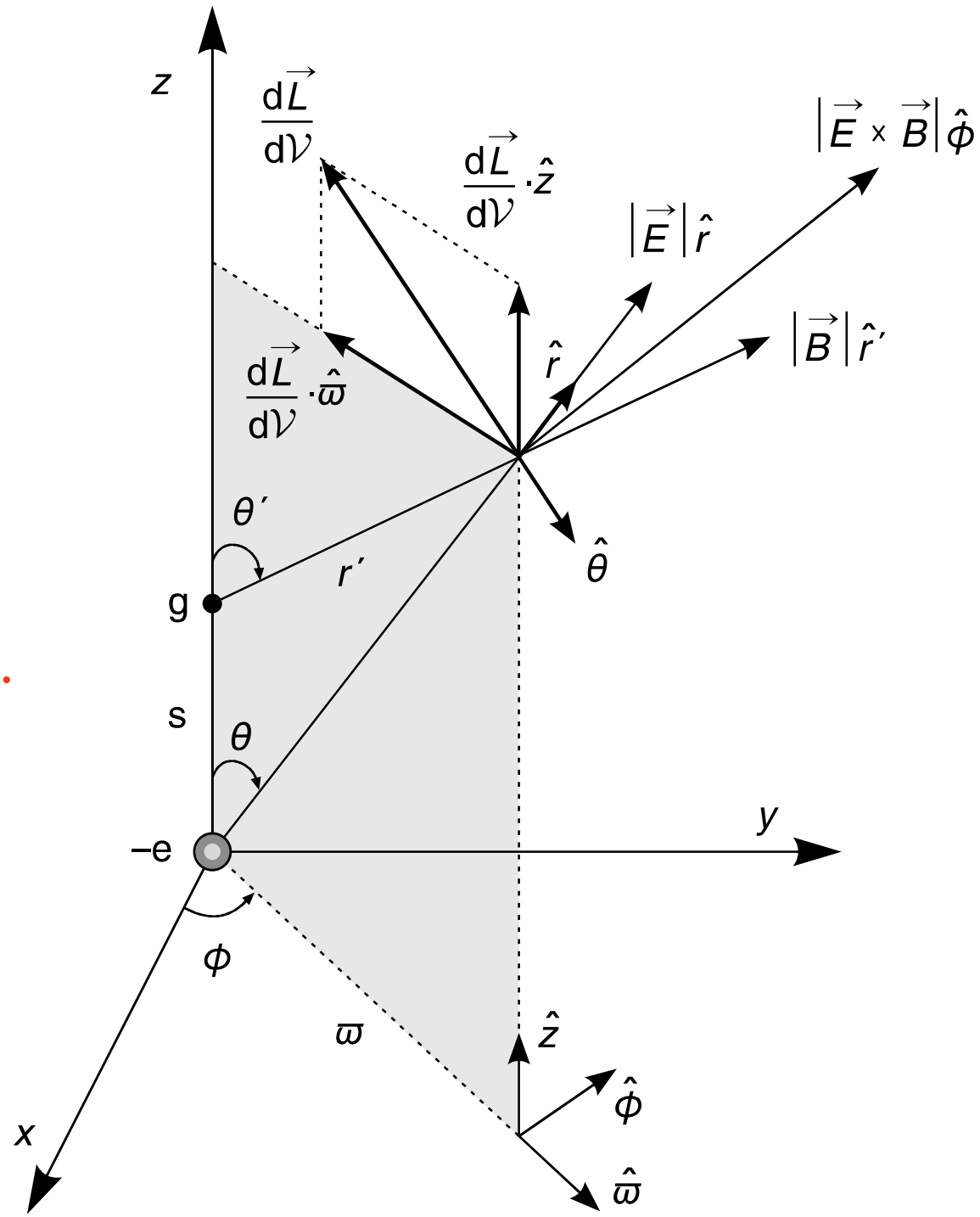

The **Parker limit** for magnetic monopoles (1982)

Magnetic monopoles and the survival of galactic magnetic fields

Show affiliations

Turner, Michael S. ; Parker, E. N. ; Bogdan, T. J.

The so-called Parker Bound, $F < 10^{-15}$ cm^{-2} s^{-1} sr^{-1} is obtained by requiring that magnetic monopoles do not short-circuit the galactic magnetic field faster than the dynamo mechanism can regenerate it.

Publication: Physical Review D (Particles and Fields), Volume 26, Issue 6, 15 September 1982, pp.1296-1305

Grand unified and Superstring theories, predict existence of MM

In his 1931 paper Dirac predicted the relation between the elementary electric charge e and the magnetic charge g:

$$g = ng_D = \frac{1}{2}\frac{\hbar c}{e}n \sim \frac{137}{2}en,$$

Where n=1,2,… and g_D is the unit of the magnetic charge

Mass of magnetic monopoles (MM):
Clasical: most recent searches are performed at the CERN LHC. The ATLAS experiment sought g_D MMs with masses of up to 2.5 TeV
Intermediate mass: 3÷7 TeV
Supermassive (GUT theories):
MM ≳ 10^{16}÷10^{17} GeV c^{-2} (1kg → MeV/c^2)

There are no definite theoretical predictions of the abundance of cosmic MMs. A bound largely used is the so-called Parker Bound, $F < 10^{-15}$ cm^{-2} s^{-1} sr^{-1} **obtained by requiring that MMs do not short-circuit the galactic magnetic field faster than the dynamo mechanism can regenerate it**. By taking into account typical coherence lengths ($\ell \sim 1$ kpc) of the galactic magnetic fields, the limit becomes $F < m_{17}\, 10^{-15}$ cm^{-2} s^{-1} sr^{-1}, for $m_{17} \geq 1$, with $m_{17} = mM/10^{17}$ GeV c^{-2}. Similar considerations applied to the survival of an early seed of the galactic magnetic field yield a more stringent bound, the 'Extended Parker Bound' (EPB):

Parker wind theory

Basic equations:

$$\frac{d}{dr}\left(\bar{\rho}Vr^2\right) = 0 \text{ (mass conservation)}$$

$$\bar{\rho}V\frac{dV}{dr} = -\frac{d\bar{P}}{dr} - \bar{\rho}\frac{GM}{r^2} \text{ (momentum conservation)}$$

$$\bar{P} = \bar{\rho}V_s^2 \;\; V_s = \sqrt{\frac{2kT_0}{m}} \text{ , (equation of state)}$$

3 (simple) equations

V_s is sound speed - most probable proton speed in a Maxwellian with temperature T_0.

$$R = \frac{r}{r_0}, M = \frac{V}{V_s}, \rho = \frac{\bar{\rho}}{\bar{\rho}_0}, \lambda = \frac{1}{2}\left(\frac{V_{esc}}{V_s}\right)^2 = \frac{GMm}{2r_0kT_0} \simeq 12 \text{ for } T_0 \simeq 10^6\,^\circ K, V_s = 131 \text{ km/s}$$

Two eqs for $\rho(R)$ and $M(R)$:

$$\frac{d}{dR}\left(\rho MR^2\right) = 0 \implies \rho MR^2 = \mu = \text{const.}$$

$$\rho M\frac{dM}{dR} + \frac{d\rho}{dR} + \lambda\frac{\rho}{R^2} = 0 \implies \boxed{\frac{1}{M^2}\frac{dM^2}{dR} = \frac{2}{R^2}\frac{2R-\lambda}{M^2-1}.}$$

$$\boxed{\ln M - \frac{M^2}{2} - \frac{\lambda}{R} + \ln R^2 = \ln B = \text{const.}, \text{(Bernoulli integral)}}$$

critical point $(R = Rc, M = 1)$: $\frac{dM^2}{dR} = \frac{0}{0}$, $R = R_c(1+\varepsilon)$, $M = M_c(1+\xi)$

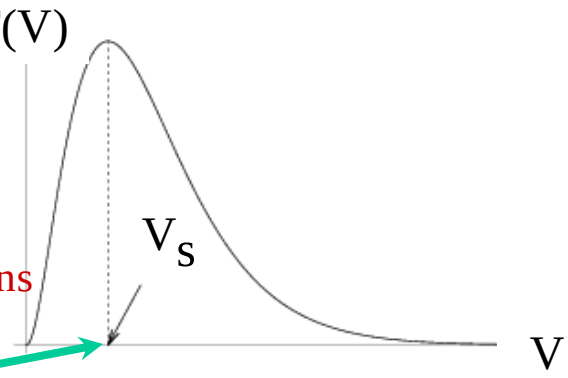

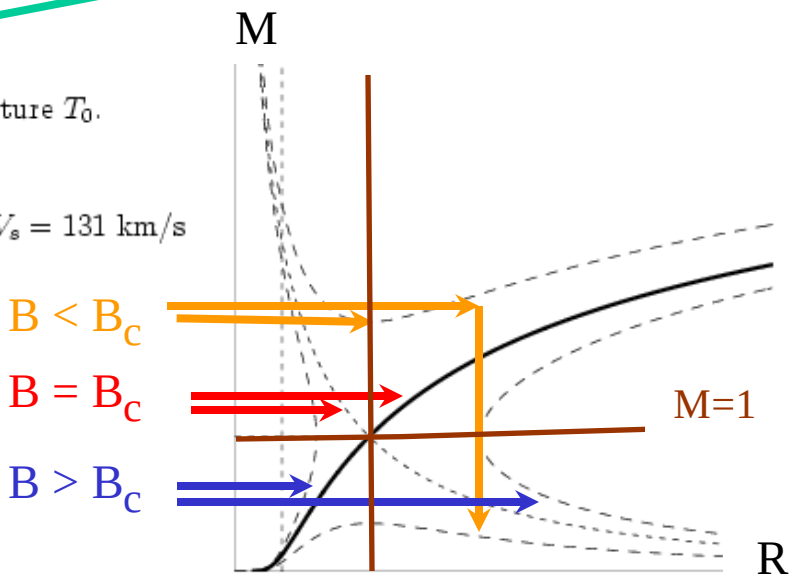

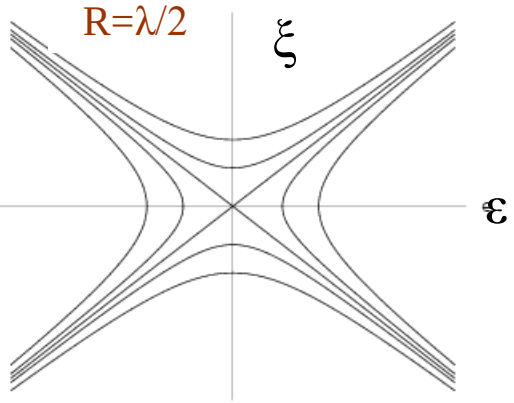

Ib) 1D-MHD: The Weber-Davis magnetized wind

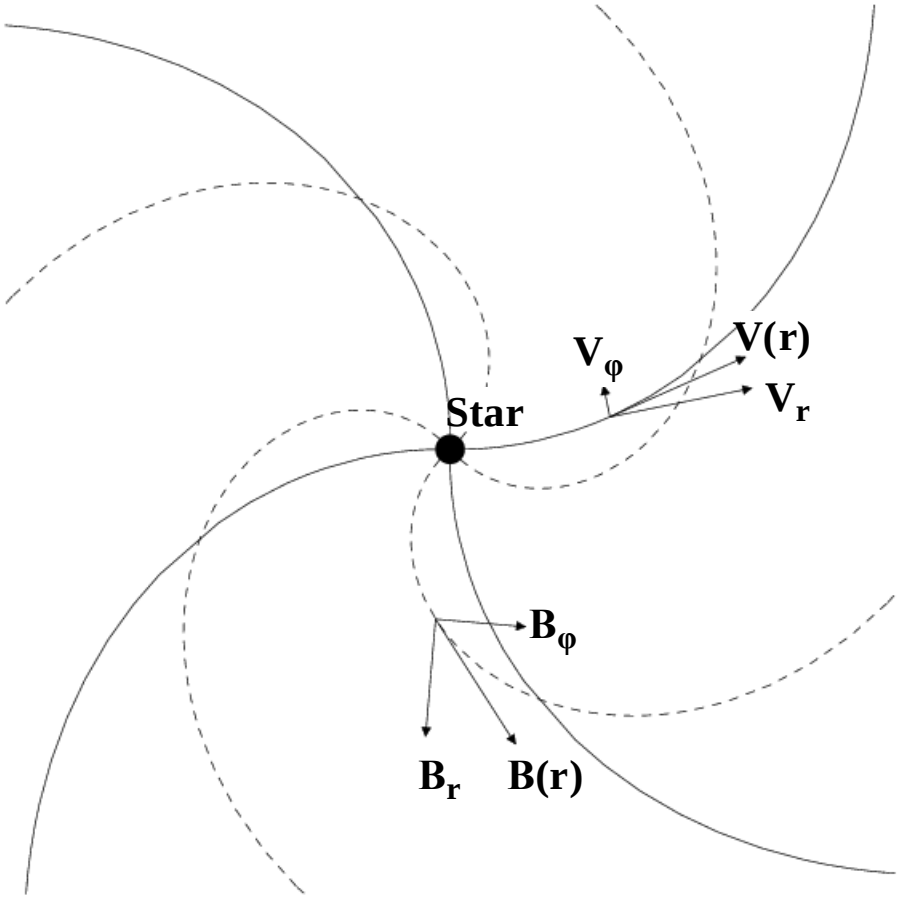

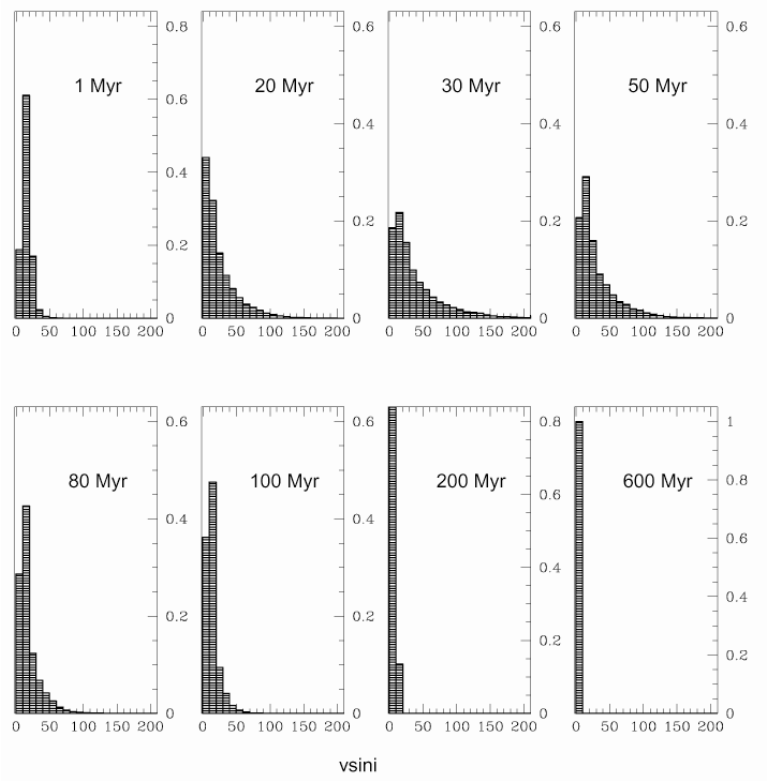

Distribution of Vsini for $1M_o$ stars of different ages
(Bouvier, Forestini & Alain 1997)

Parker vs. Weber/Davis Topologies of $V_r(R)$:

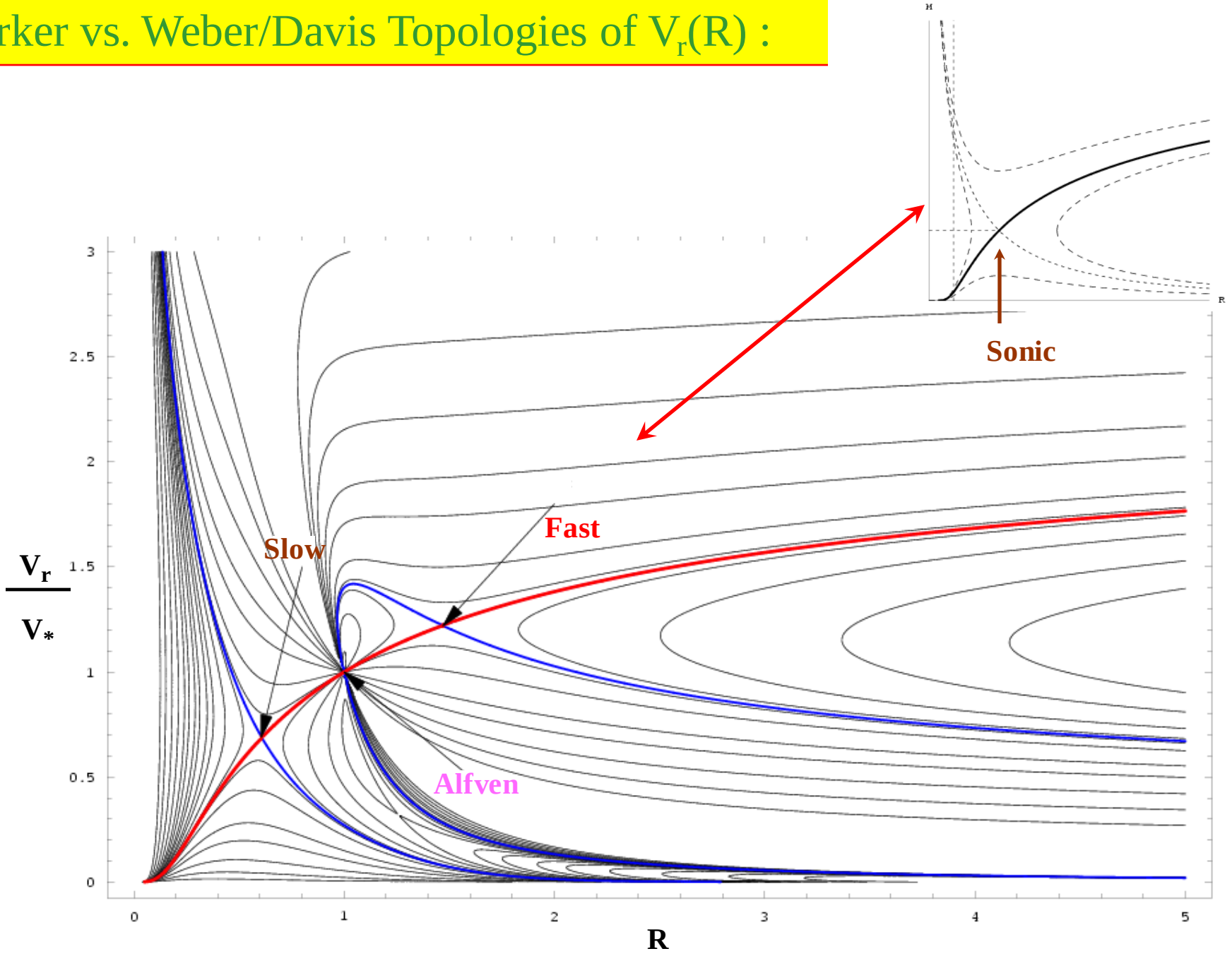

Slow and Fast magnetic rotators :

$$\mathcal{E} = \frac{1}{2}V^2 + h - \frac{GM}{r} - \frac{rB_\phi\Omega}{\Psi_A} = \underbrace{\frac{1}{2}V_o^2 + h_o - \frac{GM}{r_o}}_{\mathcal{E}_o} - \underbrace{\frac{r_o B_\phi^o \Omega}{\Psi_A}}_{\Omega L}, \quad \mathcal{E} \simeq \mathcal{E}_o + \Omega L\,,$$

where $\mathcal{E}_o$ is the energy of the thermally driven Parker wind and ΩL the Poynting energy of the magnetic rotator. Depending on which of these two terms dominates we have two possibilities:

1. $\mathcal{E}_o \gg \Omega L$: Slow magnetic rotator. In this case we have a thermally driven Parker wind
2. $\mathcal{E}_o \ll \Omega L$: Fast magnetic rotator. In this case we have a magnetorotationally driven wind

Slow magnetic rotator (our Sun)

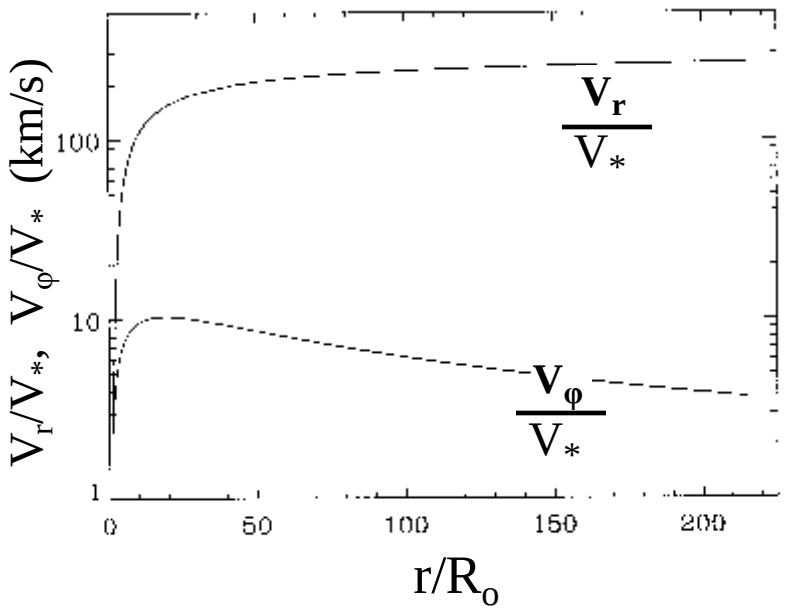

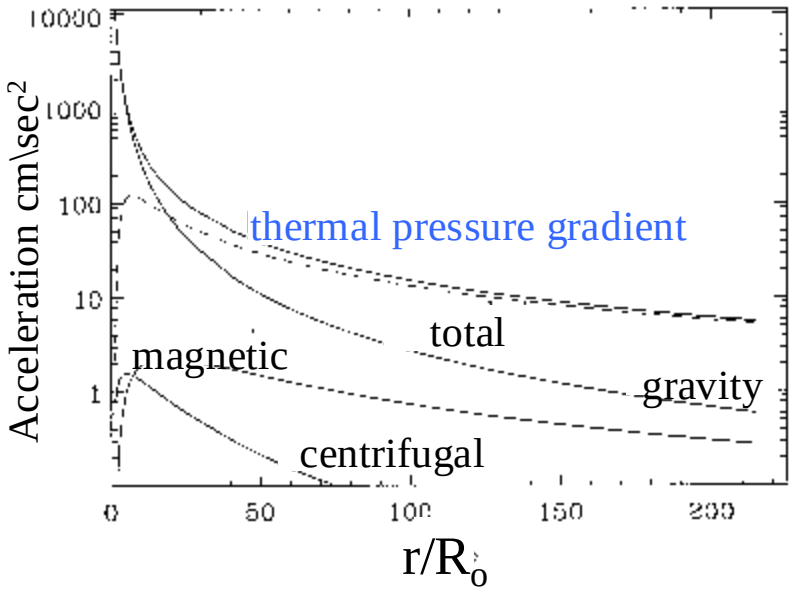

Fast magnetic rotator (YSO)

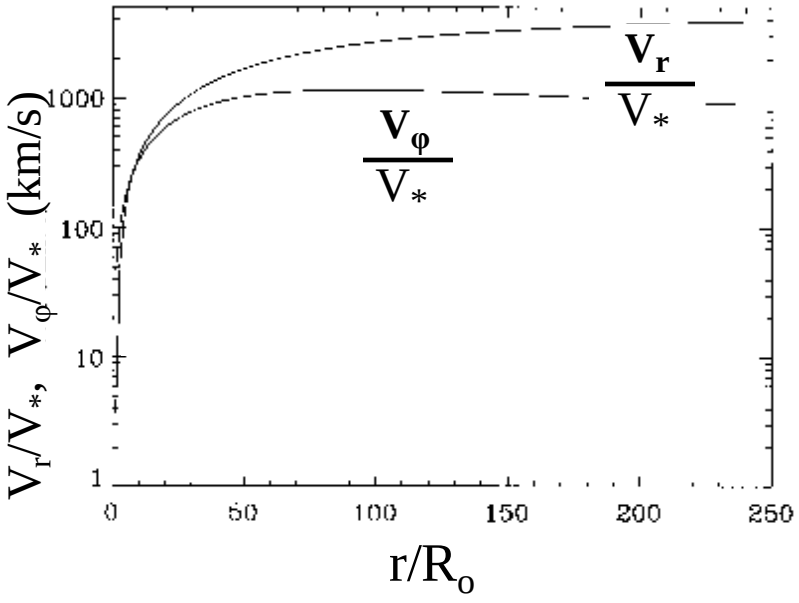

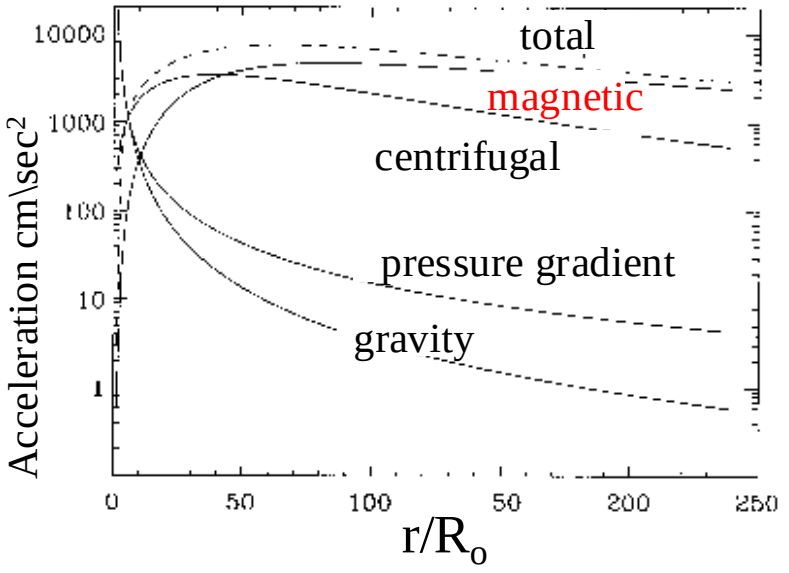

II. 2-D MHD plasma outflows: the issue of collimation

a) Time-independent (steady) outflows i) meridionally selfsimilar
ii) radially selfsimilar

b) Time-dependent plasma outflows

Single old Stars
(our Sun)

1 AU

HH 111
1994.9 UT
Green: Hα
Red: [S II]

Single Young Stars
(HH 111)

E F G H I J K L

1000 AU

Binary stars - microquasars
(SS 433)

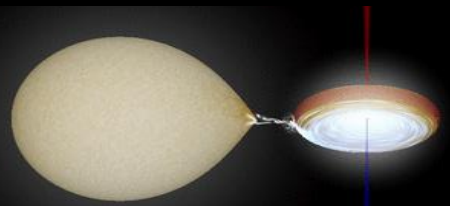

25000 AU
0.4 l.y.

Planetary neboulae
(Twin exhaust nebula)

1 l.y.

The Solar Wind as the prototype
of astrophysical MHD outflows

The case of collimated magnetized
astrophysical MHD outflows

Neutron Stars
(crab)

10 l.y.

M87 & its Black hole
(all scales)

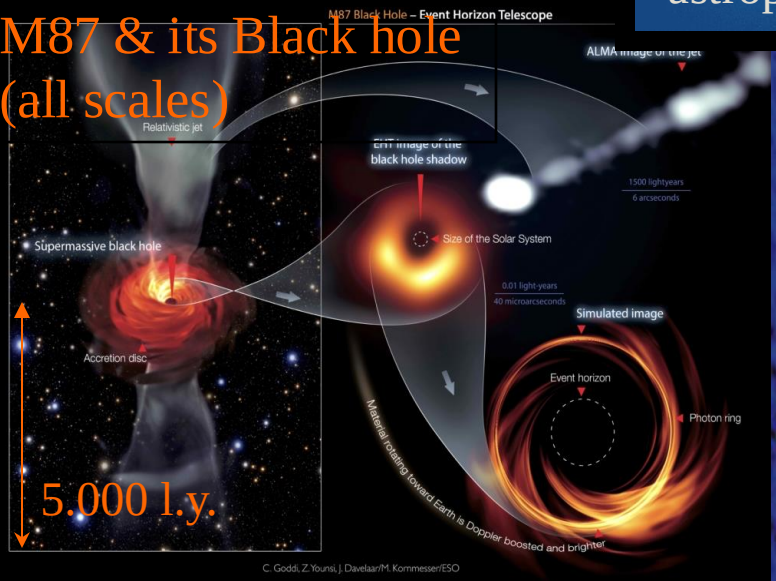

Radiogalaxies
(Cygnus)

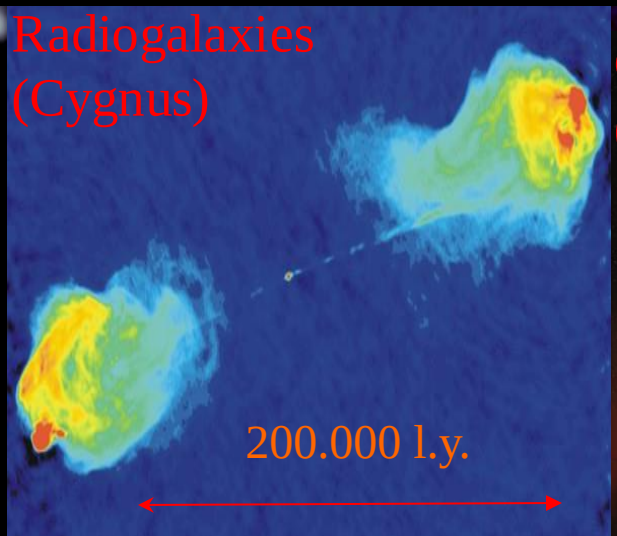

200.000 l.y.

GRB & Quasars
(Most distant quasar
P172+18, d=13×10^9 l.y.)

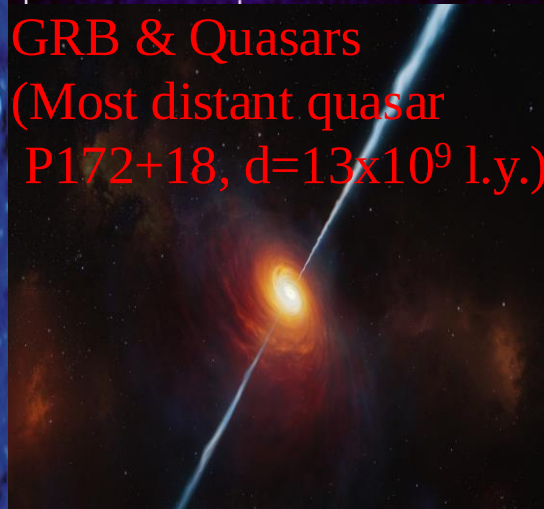

a) 2-D Time-independent (steady) studies - some general conclusions :

- Classes of analytical solutions via a nonlinear separation of the variables
- Critical points, characteristics and the problem of causality
- Classification of observed outflows in terms of efficiency of magnetic rotator
- Topological stability of collimated outflows
- etc, etc.

Analytical Solutions: Self-similarity

Quasar/radio galaxy

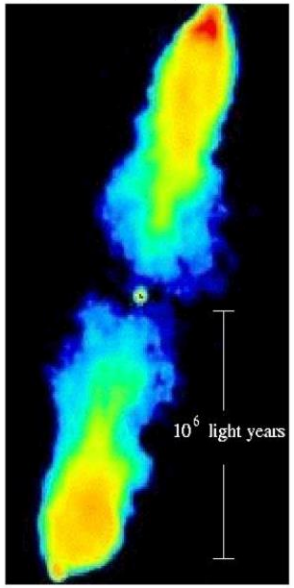

Microquasar 1E1740.7-2942

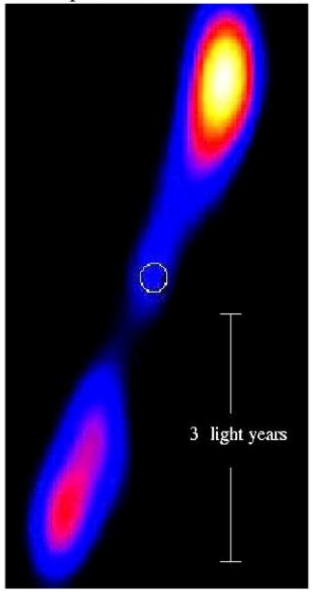

Protostellar jet HH 111

The issue of a systematic construction of exact models for astrophysical MHD plasma flows

Main assumptions for getting analytical solutions

1. *Ideal* MHD.

2. *Symmetric* outflow configurations, $\partial_3 = 0$, in system (x_1, x_2, x_3) *e.g.*, axisymmetric, or translationally symmetric.

3. *Natural* variables are poloidal Alfvén number and magnetic flux function $(M, A) \Longrightarrow$ switch from (x_1, x_2) to (M, A).

4. Consider Alfvén number $M(x_1, x_2)$ and cross-section of outflow tube $G(x_1, x_2)$ as functions of a single variable χ:

$$M = M(\chi),\ G = G(\chi)$$

I. In spherical coordinates $(x_1 = r\,, x_2 = \theta\,,)$ this unifying scheme contains two large groups of exact MHD outflow models:

(α) $\chi = \theta \longrightarrow$ *radially* self-similar models with *conical* critical surfaces. Prototype is the Blandford & Payne[1] (1982) model :

$$A(r, \theta) = g(\theta) r^x \text{ and } x = 3/4.$$

(β) $\chi = r \longrightarrow$ *meridionally* self-similar models with *spherical* critical surfaces. Prototype is the Sauty & Tsinganos[2] (1994) model :

$$A(r, \theta) = f(r) \sin^{2\epsilon}\theta \text{ and } \epsilon{=}1.$$

II. In orthogonal coordinates $(x_1 = x\,, x_2 = y\,,)$ this unifying scheme contains the group of *planarly* self-similar MHD models. Prototype is the Petrie et al[3] (2002) model :

$$A = G(x) e^{-z/H}$$

[†]Vlahakis & Tsinganos 1998, MNRAS, **298**, 777
[1]Blandford & Payne 1982, MNRAS, **199**, 883
[2]Sauty & Tsinganos 1994, A&A, **287**, 893
[3]Petrie, Vlahakis & Tsinganos 2001, A&A, **382**, 1081

The three classes of exact MHD wind/jet models

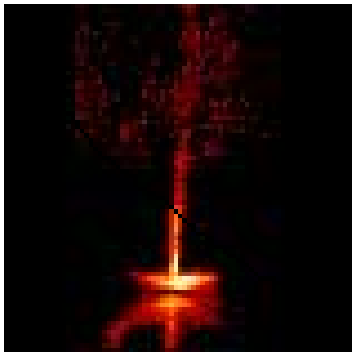

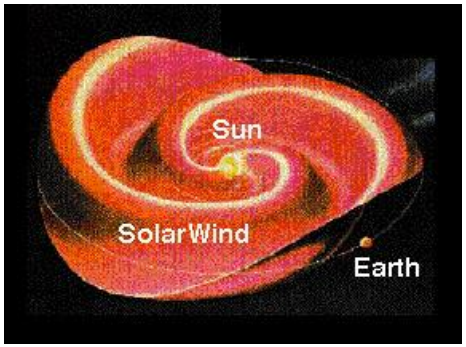

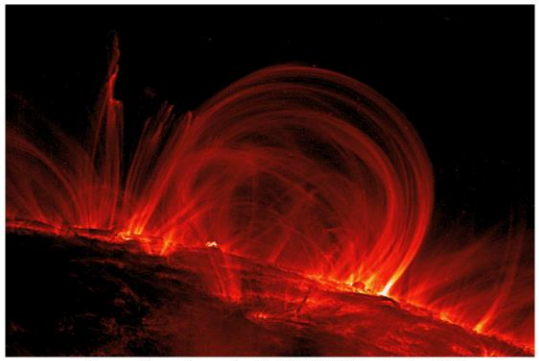

Coronal loop observed with TRACE 26 September 2000

$r=R\sin\theta$

$A(R,\theta)=g(\theta)R^x=F(\theta)\,r^x$

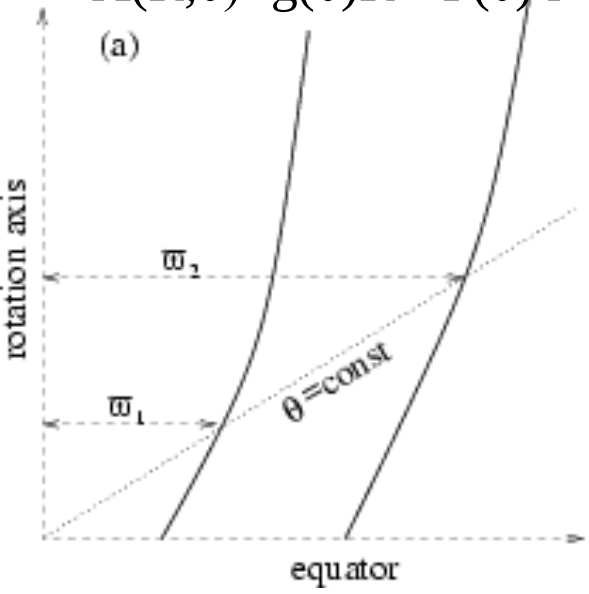

$A(R,\theta)=f(R)\sin^{2\varepsilon}\theta=G(R)r^2$

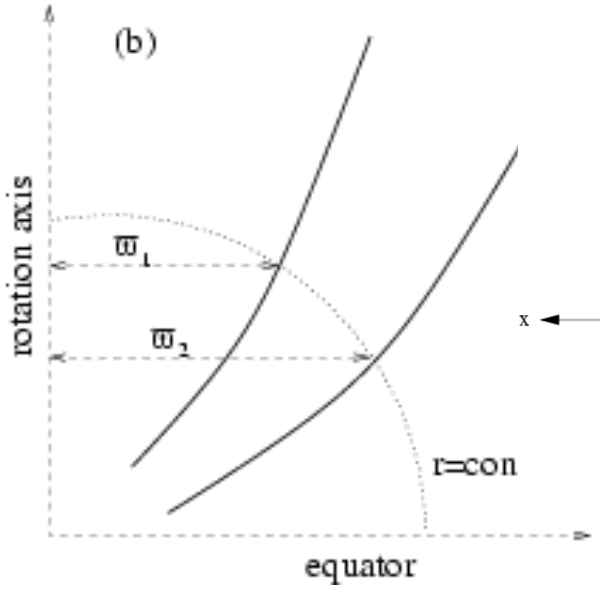

$A(x,z)=G(x)e^{-z}$

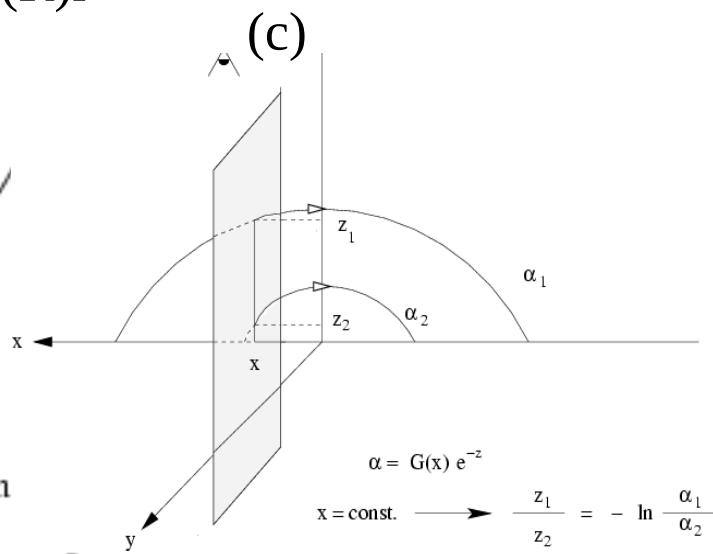

The issue of singularities/critical points :

(1) Equation for derivative of poloidal Alfvén number M_a:

$$\frac{\mathrm{d}M_a^2}{\mathrm{d}R} = \frac{N_M(R,F,M_a;\text{parameters})}{D(R,F,M;\text{parameters})},$$

(2) Equation for derivative of thermal pressure P_0:

$$\frac{dP_0}{dR} = \frac{N_P(R,F,M_a;\text{parameters})}{D(R,F,M;\text{parameters})},$$

(3) Equation for derivative of expansion function, or P_1 :

$$\frac{\mathrm{d}F}{\mathrm{d}R} = \frac{N_F(R,F,M_a;\text{parameters})}{D(R,F,M;\text{parameters})},$$

Difficulty: A physically accepted solution is determined by the requirement that it should pass through critical points which are not known *a priori* but are only determined simultaneously with the complete solution !

Singularities (Critical Points) : $N_M = N_F = N_P = D = 0.$

(a) Alfvén transition (star-type singularity): $M_a = 1$

imposes regularity condition $\Longleftrightarrow$ streamlines avoid kink.

(b) X-type MHD singularities selecting physical solution (a proxy for the imposition of physical b.c.'s at r_o and ∞).

$\Longrightarrow$ Obtain unique solution through critical points.

BUT

at which speeds are found these MHD saddle-type critical points ?

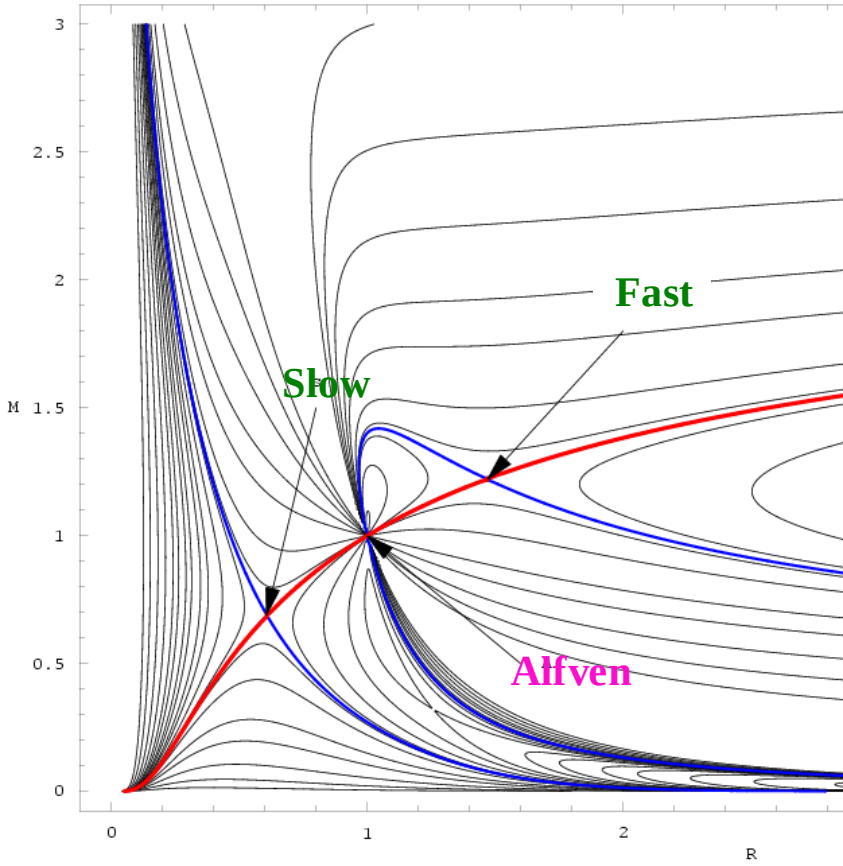

Nature of MHD PDE's & correct boundary conditions

1. *Elliptic* PDE's :

$$\left(\frac{\partial^2\Phi}{\partial x^2}+\frac{\partial^2\Phi}{\partial y^2}=0\right)$$

$\Longrightarrow$ *Dirichlet or Newmann* B.C.'s on a closed surface

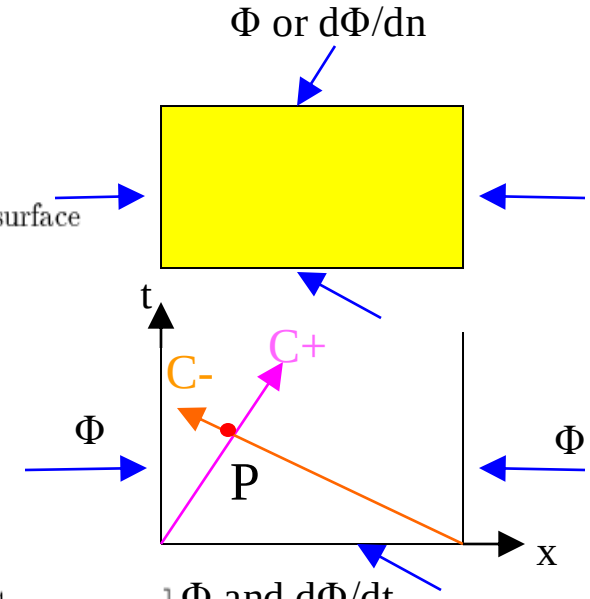

2. *Hyperbolic* PDE's :

$$\left(\frac{\partial^2\Phi}{\partial x^2}-\frac{1}{c^2}\frac{\partial^2\Phi}{\partial t^2}=0\right)$$

$\Longrightarrow$ *Cauchy* B.C.'s on an open surface.

3. *Mixed Elliptic/Hyperbolic* PDE's :

$$\left[\frac{1-M_a^2}{h_3^2}\right]\left[\nabla^2 A-\frac{\vec{\nabla}A\cdot\vec{\nabla}(\vec{\nabla}A)^2}{2(\vec{\nabla}A)^2}\frac{V_p^4}{V_p^4-V_p^2(C_s^2+V_a^2)+C_s^2V_{ap}^2}\right]=F_o$$

Elliptic in domains E_i, hyperbolic in domains H_i, i=1,2, ...

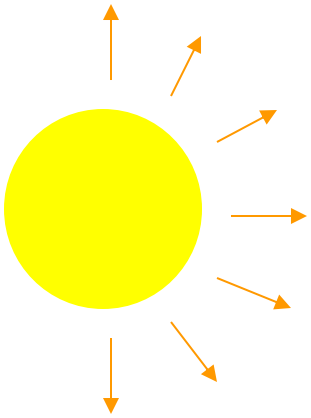

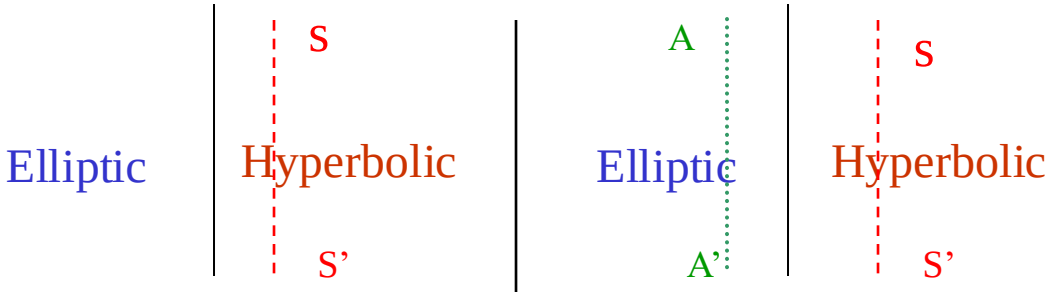

$\Longrightarrow$ B.C.'s on separatrices SS' in hyperbolic domains H_i.

But, these separatrices SS' in domains H_i are not known *a priori* but should be constructed simultaneously with solution.

The issue of causality and limiting characteristics:

The set of steady MHD equations are of mixed elliptic/hyperbolic character.

In hyperbolic regimes exist some separatrices which separate causally areas that cannot communicate with each other via an MHD signal.

[They are the analog of the limiting cycles in Van der Pol's nonlinear differential equation, or, the event horizon in relativity.]

The MHD critical points appear on these separatrices which do not coincide in general with the fast/slow MHD surfaces.

To construct a correct solution we need to know the limiting characteristics, but this requires an a priori knowledge of the solution we seek for !

Tsinganos et al, MNRAS, **283,** 811, 1996

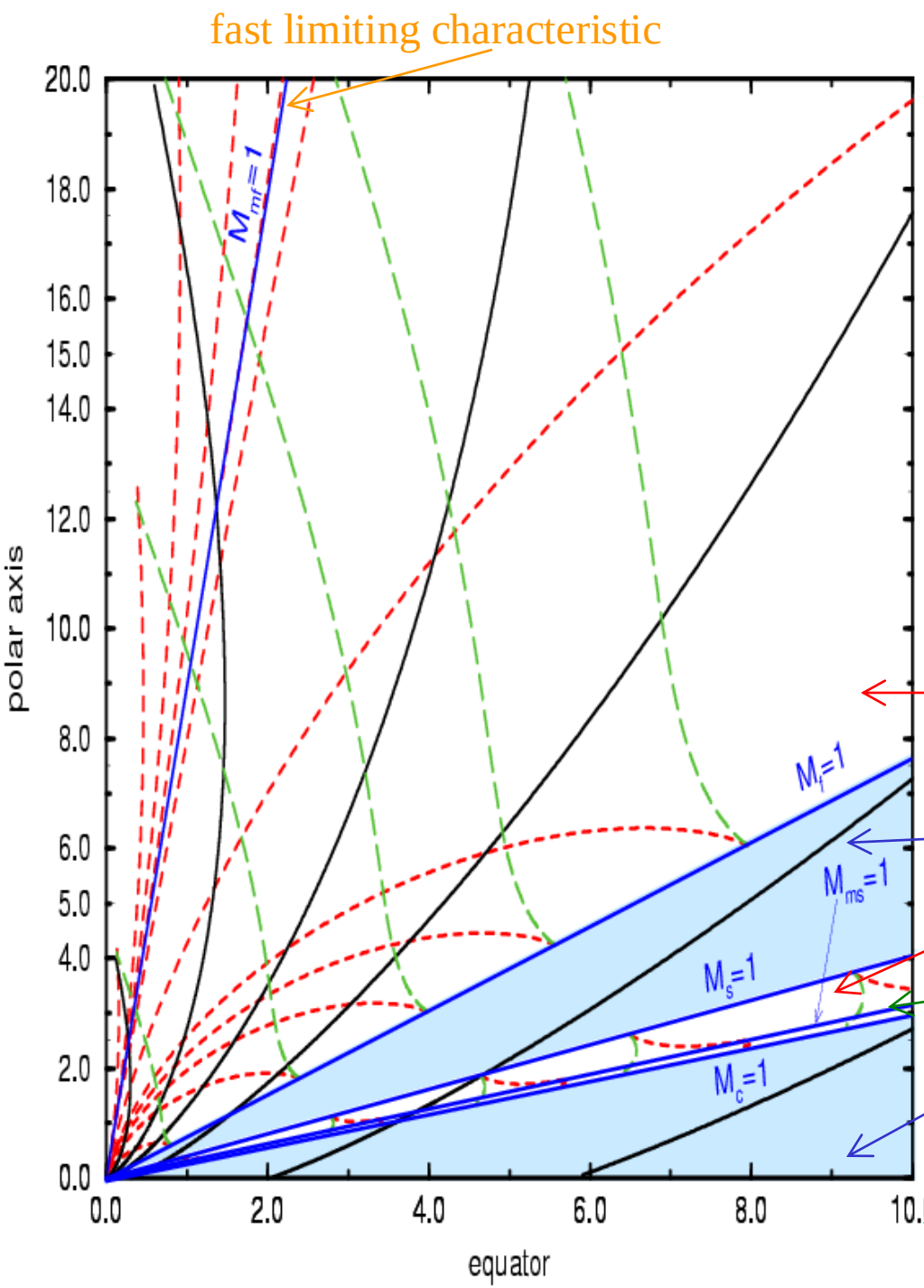

Plot of the characteristics in both hyperbolic regimes of a radially self-similar jet. In each of the two hyperbolic regimes (white domains) there are two families of characteristics.

Hyperbolic

Elliptic

slow limiting characteristic

Vlahakis et al, MNRAS, **318**, 417, 2000

Plot of the characteristics in the 2nd hyperbolic regime of a meridionally self-similar jet.

Dotted lines: poloidal magnetic field lines,
Solid lines (characteristics)
Thick-dotted line (cusp surface),
Dot-dashed line (slow-magnetosonic)

In hyperbolic regime there are two families of characteristics – one of them is tangent to the separatrix-limiting characteristic.
Dotted line (fast-magnetosonic)

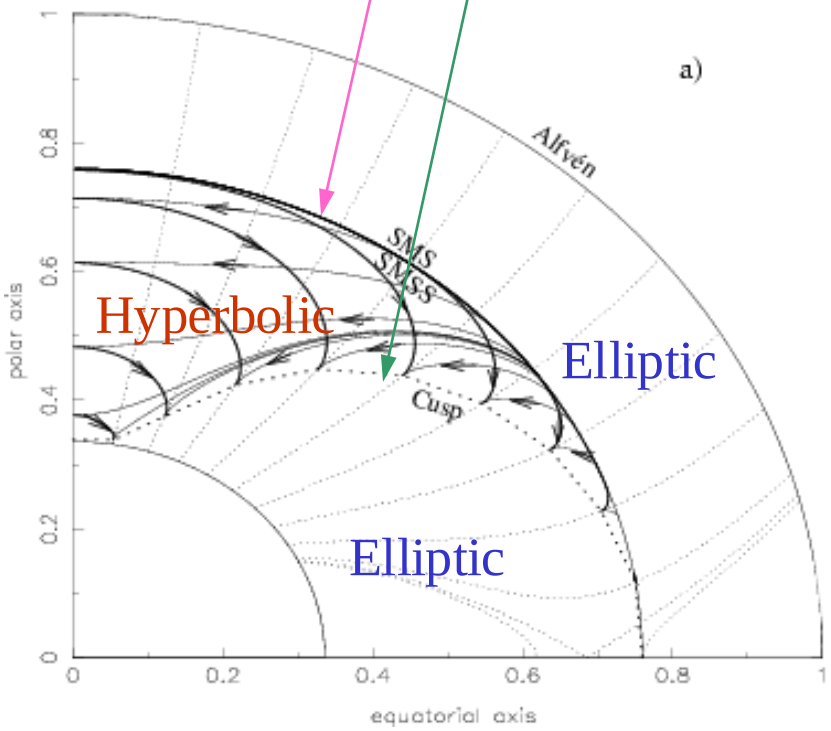

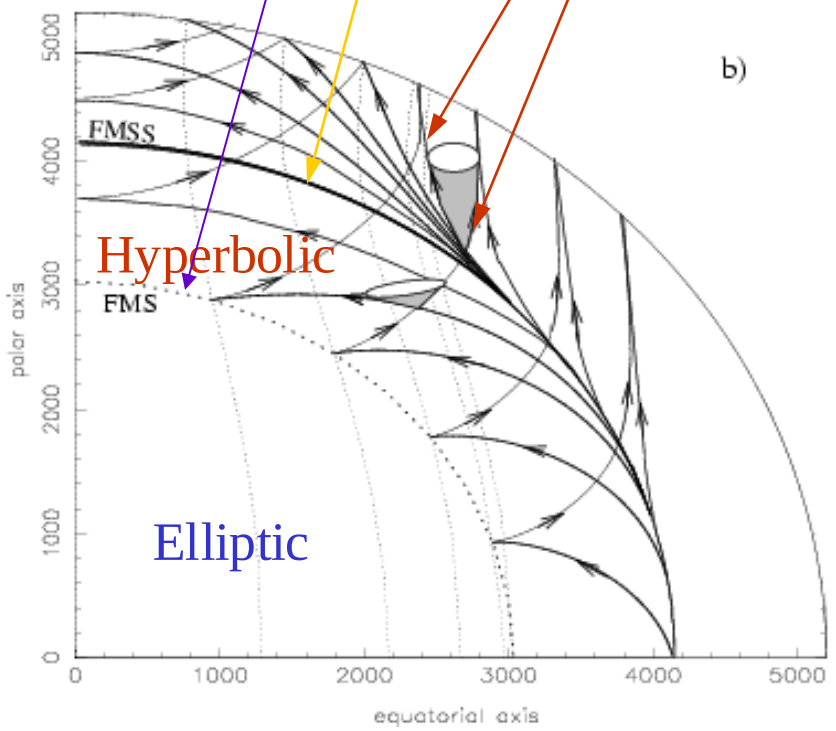

[see Sauty, Trussoni and Tsinganos AA, **421**, 797, 2004]

Basics of jet acceleration and collimation

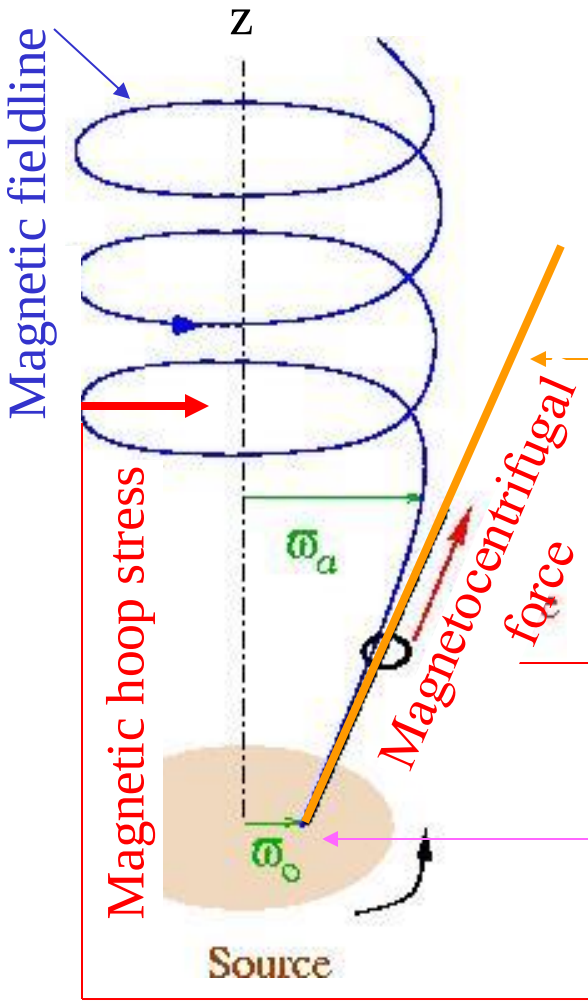

- On the disk, z=0, the rotational kinetic energy exceeds the magnetic enegy →Keplerian rotation of the B-field line rooted at r_o.
- Up to the Alfven distance, the B-field is strong enough → forces the plasma to follow the Keplerian rotation of the roots of the magnetic fieldline. In particular, when the inclination angle is less than 60^o, we have the "bead on a rotating wire" magnetocentrifugal acceleration.
- After the Alfven distance, the poloidal B-field energy is weaker than the poloidal kinetic motion → the B-field follows the plasma. The plasma inertia leaves it behind the rotating B-line → creation of strong B_φ
- The created strong B_φ collimates the magnetic field lines towards the z-axis and forms the jet.

Removal of disk angular momentum by magnetocentrifugal disk-winds:

A Keplerian disk (Ω_K) accreting at a rate $\dot{M}_a$ needs to get rid of angular momentum in a radius ϖ_o :

$$\dot{J}_a = \frac{1}{2}\Omega_K \varpi_o^2 \dot{M}_a$$

A disk-wind carries away angular momentum with a rate :

$$\dot{J}_w = \Omega_K \varpi_A^2 \dot{M}_w$$

If the disk-wind carries away a fraction f ($0 < f < 1$) of the angular momentum of the accreting matter, $\dot{J}_w = f\,\dot{J}_a$, then (e.g., f=0.5)

$$\frac{\dot{M}_w}{\dot{M}_a} = \frac{f}{2}\frac{\varpi_o^2}{\varpi_A^2}$$ = f/50 = 1/100

With a magnetic lever arm $\varpi \sim 5\varpi_o$, the disk-wind needs to carry away only a few percent of the accreting mass rate.

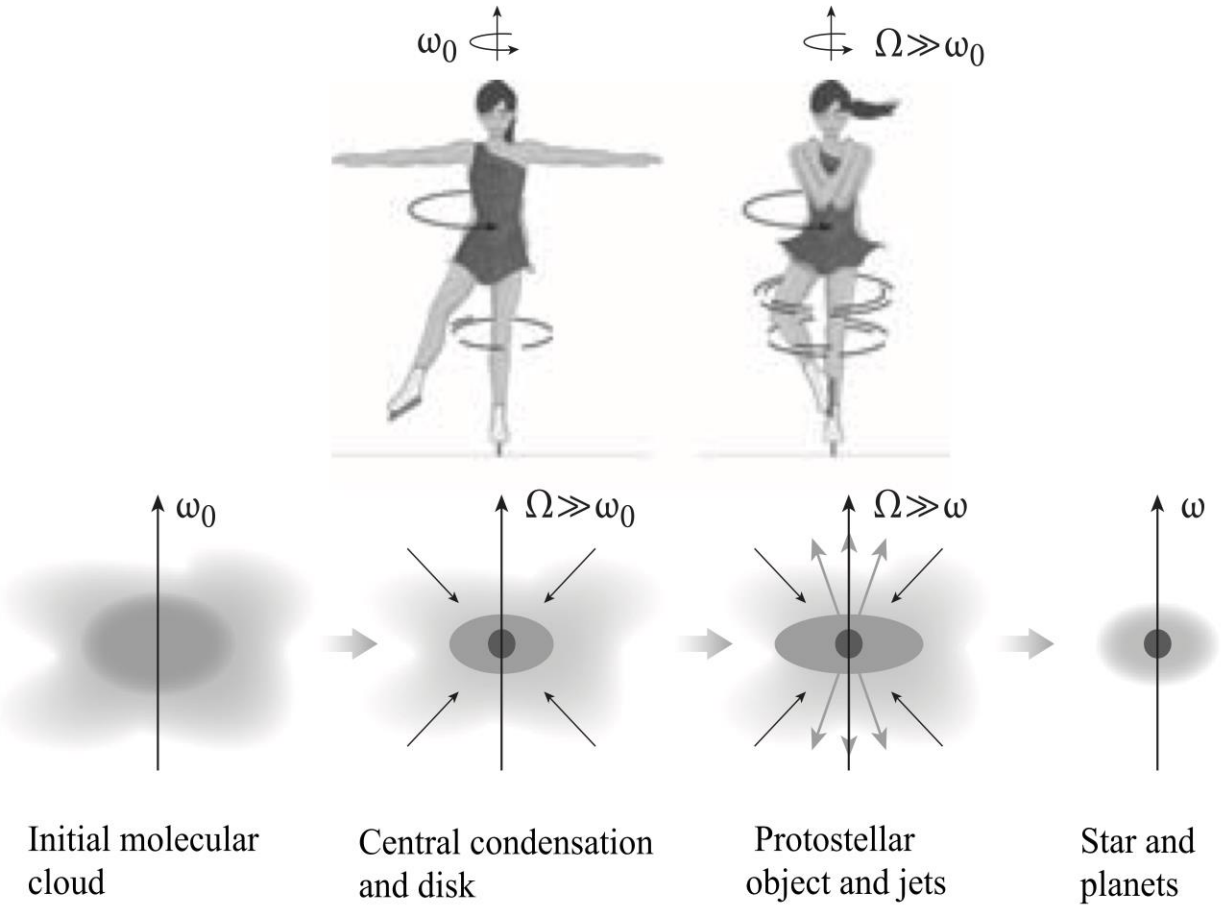
ω_0
$\Omega \gg \omega_0$
ω_0
$\Omega \gg \omega_0$
$\Omega \gg \omega$
ω
Initial molecular cloud
Central condensation and disk
Protostellar object and jets
Star and planets

Angular momentum conservation and how a protostar manages to overcome it.

Protostellar jets: they are the "ex machina Deus" in star formation...

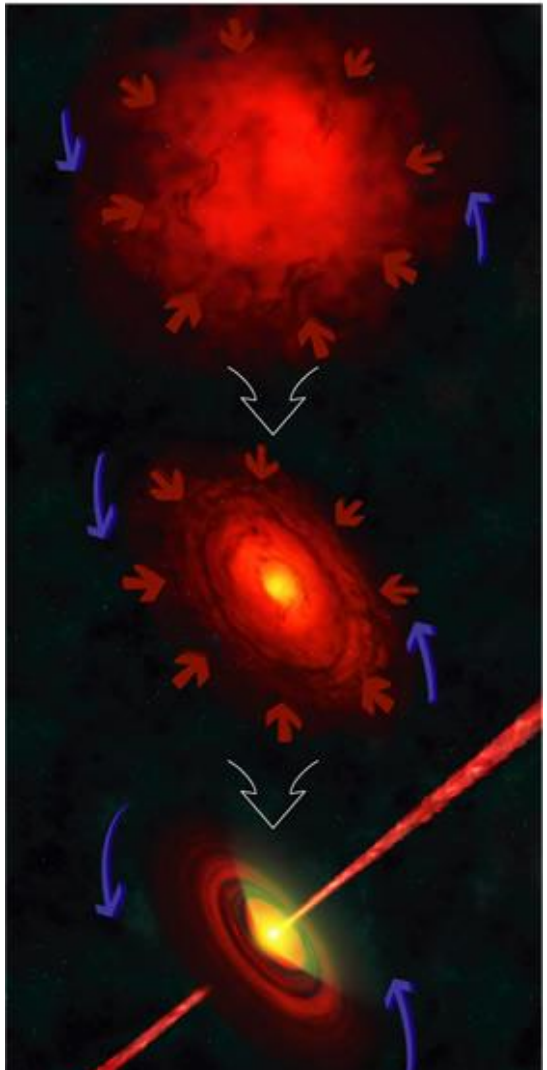

An energetic criterion for cylindrical collimation:

$$\varepsilon' = \frac{\Delta(\rho E)}{\rho L \Omega}$$

$\Delta f = f$(non polar streamline) - f(polar axis)

- $\varepsilon' < 0$ --> No collimation
- $\varepsilon' > 0$ --> Collimation

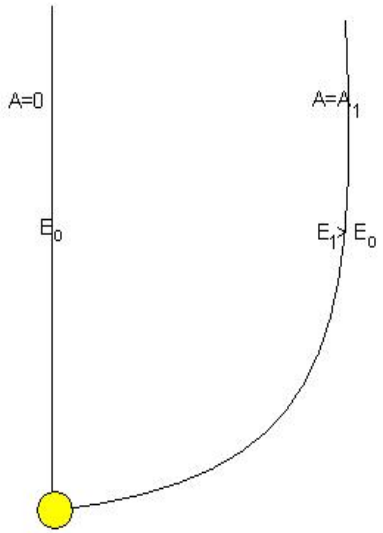

$$\varepsilon' = \mu + \varepsilon$$

Efficiency of Pressure Confinement

$$\mu \sim \frac{\Delta P}{P} = \kappa$$

Efficiency of the Magnetic Rotator

$$\varepsilon = \frac{L\Omega - E_{R,o} + \Delta E_G^*}{L\Omega} \quad \text{where} \quad \Delta E_G^* = -\frac{GM}{r_0}\left(\frac{-\Delta T}{T_0}\right)$$

- $\varepsilon > 0$ --> Efficient Magnetic Rotator (EMR)
- $\varepsilon < 0$ --> Inefficient Magnetic Rotator (IMR)

A classification of AGN jets :

Type 2 (Narrow Line) | **Type 1 (Broad Line)** | **Type 0 (Unusual)**

Radio Quiet

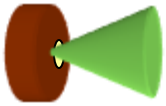

Seyfert 2
Narrow Emission Line Galaxies
IR Quasars ?

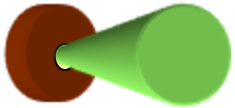

Seyfert 1
Quiet Quasars (QSO)

Broad **A**bsorption **L**ine QSO ?

BH spin ?
Environnement ?

ε, ε'

Narrow Line Radio Galaxies | **Broad Line Radio Galaxies** | **Blazars**

Radio Loud

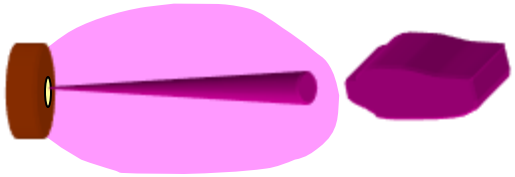

Fanaroff-**R**iley **I**
Rich environment?
Smaller torus opening angle?

?

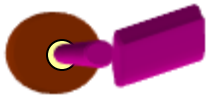

BL Lac Objects

Fanaroff-**R**iley **II**
Poor environment ?
Larger torus opening angle?

Steep **S**pectrum **R**adio **Q**uasars
?
→ **F**lat **S**pectrum **R**adio **Q**uasars

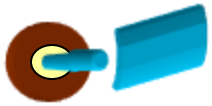

(**FSRQ**)

Decreasing Viewing Angle (Urry & Padovani 1994)

Extension of Parker's Solar Wind work to General Relativity by his students

Monthly Notices
of the Royal Astronomical Society

Issues ▾ Advance articles Submit ▾ Purchase Alerts About ▾ Mo

Volume 515, Issue 3
September 2022

< Previous Next >

JOURNAL ARTICLE

Double flows anchored in a Kerr black hole horizon – I. Meridionally self-similar MHD models with loading terms

Get access >

L Chantry ✉, V Cayatte, C Sauty, N Vlahakis, K Tsinganos

Monthly Notices of the Royal Astronomical Society, Volume 515 Issue 3, September 2022, Pages 3796–3817,
https://doi.org/10.1093/mnras/stac1990
Published: 27 July 2022 **Article history** ▾

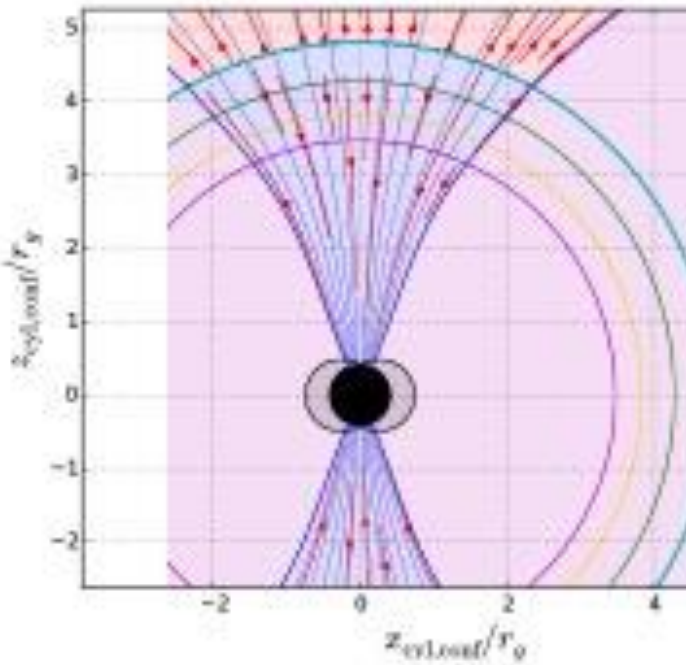

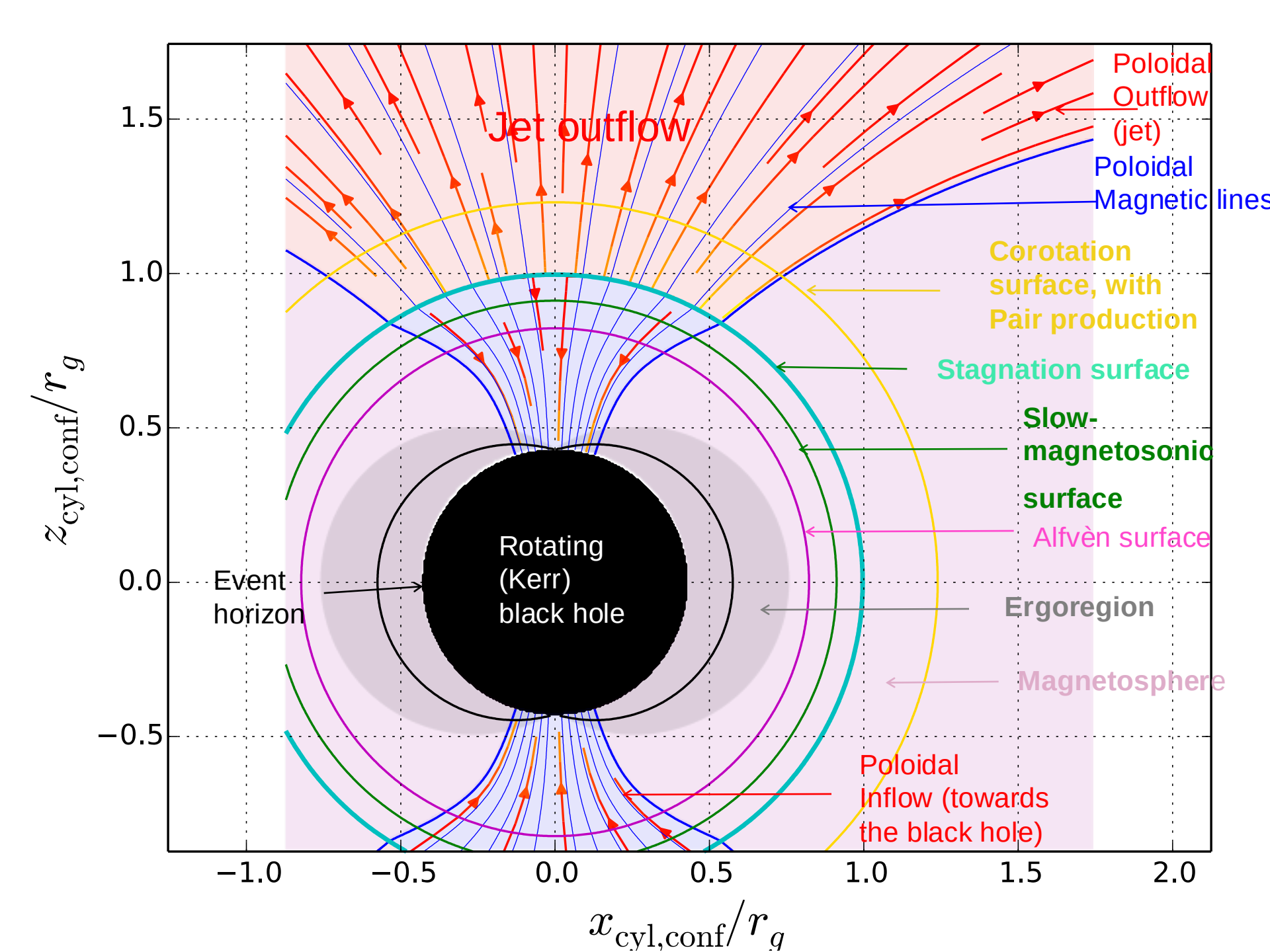
Jet outflow
Poloidal Outflow (jet)
Poloidal Magnetic lines
Corotation surface, with Pair production
Stagnation surface
Slow-magnetosonic surface
Alfvèn surface
Ergoregion
Magnetosphere
Poloidal Inflow (towards the black hole)
Rotating (Kerr) black hole
Event horizon
$z_{\mathrm{cyl,conf}}/r_g$
$x_{\mathrm{cyl,conf}}/r_g$
1.5
1.0
0.5
0.0
−0.5
−1.0
−0.5
0.0
0.5
1.0
1.5
2.0

Further Reading:

1. Αστροφυσική Πλάσματος, Κ. Τσίγκανος, σελ. **538**, Unibooks Publications, (2017)
2. Σύγχρονη Θεωρητική Μηχανική με 200 παραδείγματα και λυμένα προβλήματα, Κ. Τσίγκανος, σελ. 570, Unibooks Publications, (2022)
3. Protostellar Jets in Context (Astrophysics and Space Science Proceedings) 2009th Edition, by Kanaris Tsinganos, Tom Ray, Matthias Stute, Springer; 2009th edition (2009)
4. Solar and Astrophysical Magnetohydrodynamic Flows (Nato Science Series C:, 481) by Kanaris Tsinganos (1996), Springer; 1996th edition (1996)

[https://www.amazon.com/Books-Kanaris-Tsinganos/s?rh=n%3A283155%2Cp_27%3AKanaris+Tsinganos]

5. For a detailed list of publications in journals by the author, see the site:

http://users.uoa.gr/~tsingan/CV_2024.pdf

Εκδόσεις Unibooks, Αθήνα

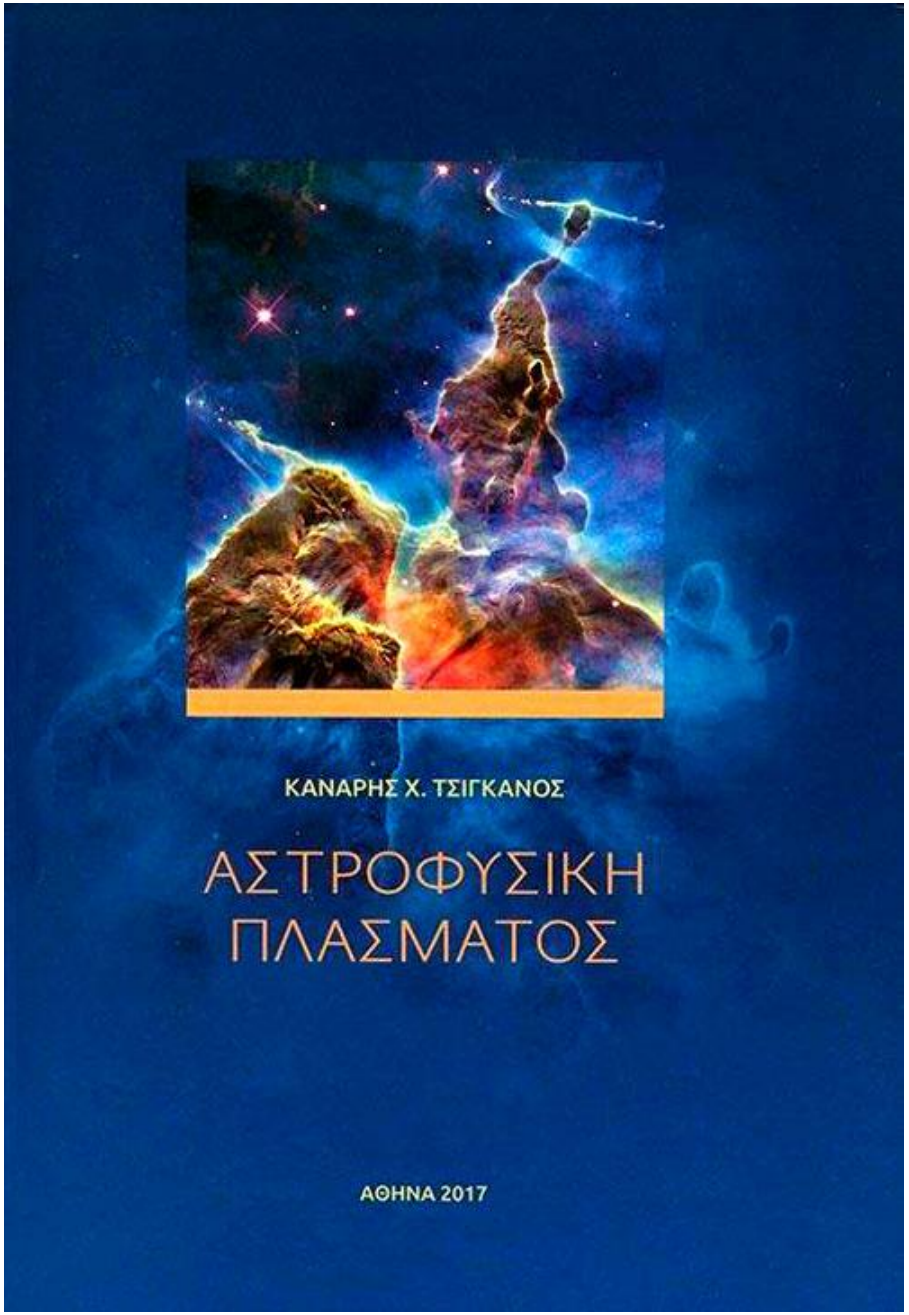

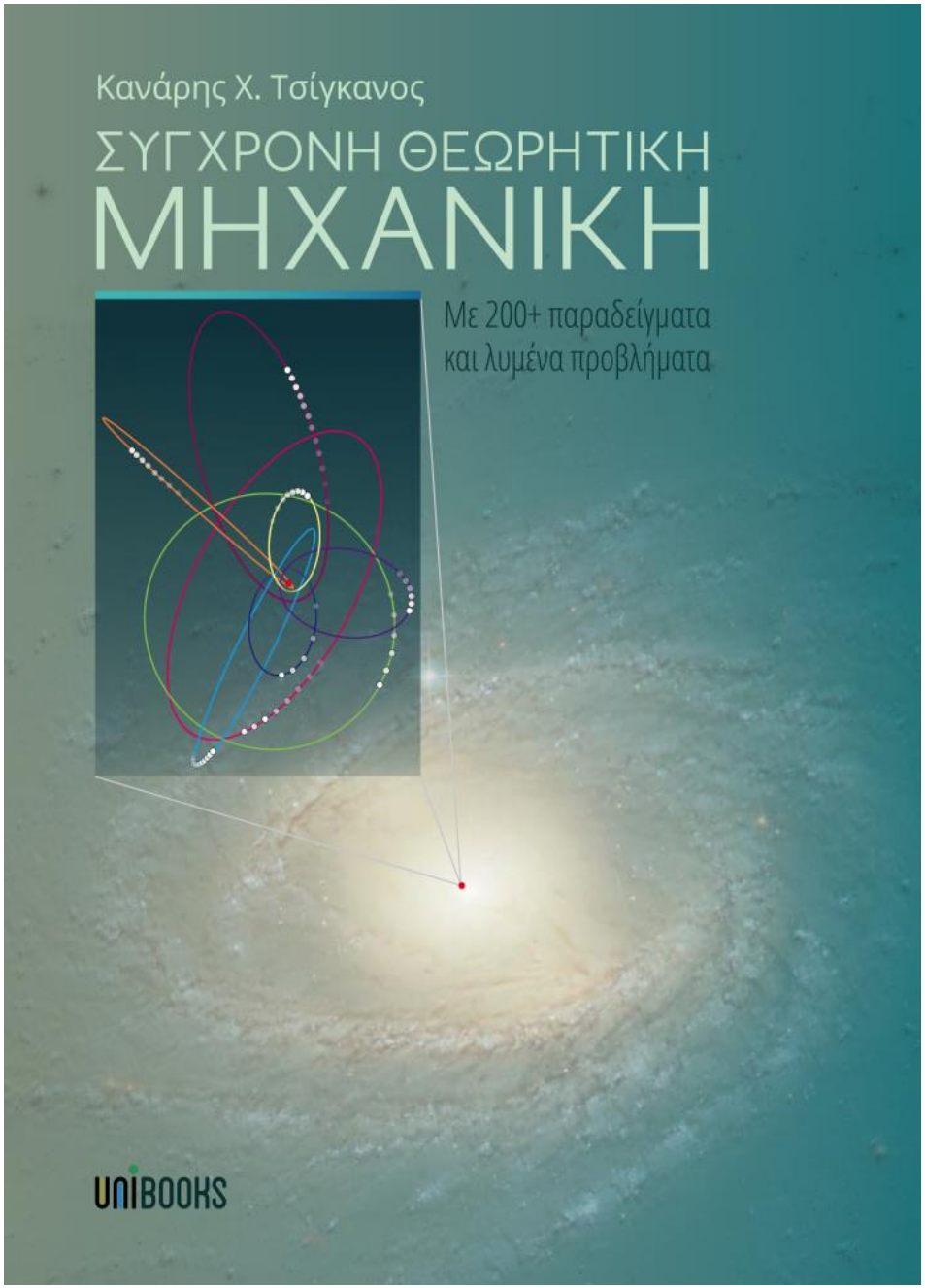

Εκδόσεις Ζήτη, Θεσσαλονίκη

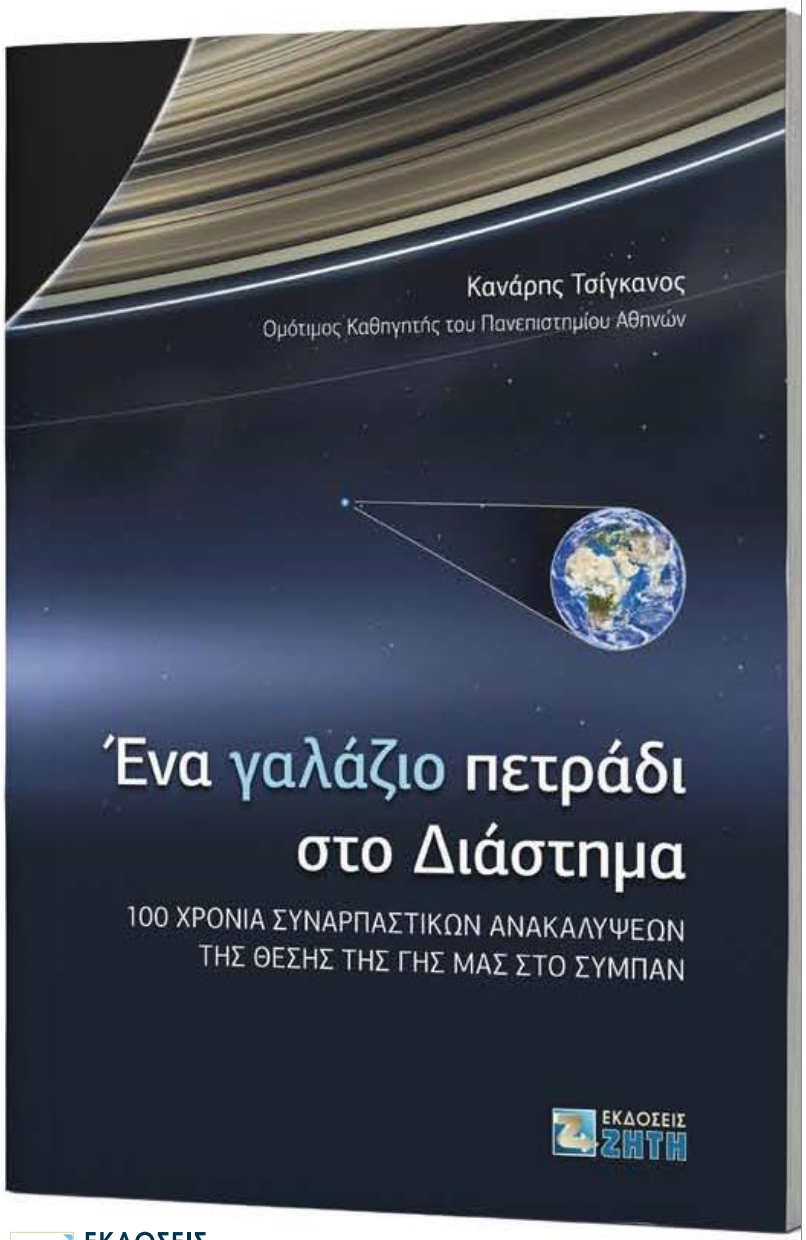

ΕΚΔΟΣΕΙΣ ΖΗΤΗ
Ζητήστε το κερδίζετε

ziti.gr

ΕΚΔΟΣΕΙΣ ΖΗΤΗ
Ζητήστε το κερδίζετε

ziti.gr